Design and Construction of a Guarded Hot Plate Apparatus to Evaluate the Thermal Resistance of Vacuum Insulated Panels using a New Accelerated Ageing Procedure

by

Alexander Hayes,

B.Eng., Carleton University 2013

A thesis submitted to the Faculty of Graduate and Postdoctoral Affairs in partial fulfillment of the requirements for the degree of

Master of Applied Science

in

Sustainable Energy Engineering and Policy

Carleton University
Ottawa, Ontario

Abstract

When bringing a structure up to current building standards, or voluntarily constructing to higher insulating levels, adjustments to the thickness of walls may be required. To meet the energy and space saving requirements of today's building market, builders are looking for new materials and practices to insulate their walls. Vacuum insulation panels (VIP) have shown potential to meet or exceed today's high insulating levels while keeping the thickness of the building envelope down. One of the problems facing owners and builders wanting to use VIPs, is their unknown service life. As such, recent research has focused on developing methods to accelerate ageing in order to determine the service life of VIPs. However, a disconnect exists between results obtained from accelerated ageing and real time degradation. The process outlined within this thesis presents a method to link the results obtained from accelerated ageing with real degradation. In addition, the thesis presents the design, construction and commissioning of a new guarded-hot-plate testing apparatus to evaluate the thermal resistance of the VIPs as they are artificially aged. The latter focuses on the moisture accumulation and thermal resistance of climate aged panels. The rate of moisture accumulation in the VIPs located in the climate chambers can be determined when comparing to climate profiles of VIP walls that were found in-situ. To study the effect of moisture on the thermal performance of VIPs, VIPs from two manufacturers were held in a climate chamber at 30°C and 90% RH for 30 days. The panels from the first manufacturer experienced a 0.2% mass increase from an initial mass of 840 g due to moisture and experienced a decrease of 5% in thermal resistance. The panels from the second manufacturer experienced a decrease of 6.5% in thermal resistance from a 0.05% gain in mass from an initial 246 g, proving that

that even a small amount of moisture can negatively affect the thermal resistance of the panel. The accelerated ageing method described in this thesis builds on these findings and aims to determine the service life of panels in different climate zones.

Acknowledgements

I would like to thank my supervisor, Dr. Cynthia Cruickshank, for her unwavering confidence in me, her support of my continued learning and for our friendship through my time at Carleton University.

I would like to thank all my colleagues within the Solar Energy Systems Laboratory including Chris Baldwin, Brock Conley, Nina Dmytrenko and Tyler Ulmer for their friendship, guidance and assistance through my Master's. I would like to thank Jordan McNally for his help in the construction process of the supply piping for the guarded hot plate apparatus.

I would like to acknowledge Alex Proctor, Ian Lloy and Kevin Sangster in the machine shop at Carleton University for their help in the construction of the guarded hot plate. A special thanks to Kevin Sangster for taking the time to work with me and explain all the steps needed to make the project a reality.

I would like to thank StyroRail for the financial support, material and continued interest through the project.

I would like acknowledge Dylan Bardy and Josh Russell for their constant friendship, support, drive for a sustainable future and desire to push limits in and out of academic endeavors.

Lastly, I would like to thank my family for their continued support and encouragement in my pursuit of continued education.

Table of Contents

List of Tables

List of Figures

Nomenclature

Symbol	Description	Units
VIP	Vacuum insulation panel	
GHP	Guarded hot plate	
GHB	Guarded hot box	
EPS	Expanded polystyrene	
XPS	Extruded polystyrene	
ASTM	American Section of the International Association for Testing Materials	
q_x	Rate of thermal energy	W
k	Thermal conductivity	W/m·K
A	Cross sectional area	m^2
L	Thickness	m
h	Thickness	mm
T	Temperature	℃, K
ΔT	Difference in temperature	℃, K
RH	Relative humidity	%
y	Cold plate temperature	℃
z	Set point number	
p_w	Water vapour partial pressure	Pa
p_{ws}	Saturation pressure	Pa
ϕ	Relative humidity	
t	Time	Hour

t_{d}	Dew-point temperature	℃
$t_{\mathrm{v,P}}$	Confidence interval	
R_{SI}	Thermal resistance	m^2·K/W
u_{Comb}	Combination of individual uncertainties	
θ	Sensitivity index	
u	Uncertainty	
S_{x}	Standard deviation	
$S_{\bar{\mathrm{x}}}$	Standard deviation of the means	
N	Sample Size	
x	Sample	g
$\bar{x}$	Sample mean	g
v	Degrees of freedom	
v	Poisson's Ratio	
W	Deflection	mm
E	Young's Modulus	Pa
M	Moment	N
σ	Tensile strength	N/m^2
F	Force	N

Subscript

Req	Required Temperature	℃
SI		
Comb	Combined Uncertainties	

T_{Hot}	Temperature hot	
T_{Cold}	Temperature cold	
s	Systematic	
r	Random	
M	Mass	g
max	Maximum	

1 Chapter: Introduction

1.1 Background

Canada's residential sector consumed approximately 1500 PJ in 2015 and of that approximately 960 PJ or 62% went into space heating [1]. Building codes in Canada are being emended in order to reduce the amount of energy being consumed within residential and commercial buildings. The national and provincial building codes are putting a larger emphasis on energy efficiency and insulation standards for buildings [2]. In addition to the minimum standards there are an increasing number of voluntary building standards such as R2000 homes [3], Energy star [4] and Passive House [5] standards which aim to improve building performance. With both mandatory and voluntarily standards aiming to reduce the amount of energy used in the conditioning of the space within a structure, a higher insulated building envelope is required. As a result, builders and owners are required to design thicker envelopes to meet the ever increasing insulation requirements, with the thickness of walls either decreasing internal living space or increasing the overall footprint of the building.

If additional insulation is to be added to the outside of a home, the ability to access behind the façade must be considered as well as the increased thickness of the wall. In some cases the added insulation can increase a wall's thickness by an additional 10 cm in order to bring it up to the required level. Increasing the wall thickness can be a real challenge for existing homes that may be spaced closely together or along property lines. When building or renovating a structure, there are rules and regulations governing how close the building can be to the property lines or other buildings which are referred to as property setbacks. Setbacks ensure clear access is maintained around the structure and

increases building safety by decreasing the likelihood for fire to propagate between structures. An example from the city Ottawa bylaws is that any detached houses must be setback 1 m from the property line on the interior side lots [6]. If more insulation was added to the exterior of the home already built to the setback the home would then be in violation of the building code. Ensuring that the new exterior dimensions of the structure do not violate any zoning laws must be considered when looking to improve the insulating capacity of a home. If adding additional insulation to the outside of a building is not an option due to maintaining a façade, or due to property setbacks, insulation can be added to the interior of the home. However, work done to the interior of a home can cause a disruption to current living arrangements and can reduce the amount of livable floor space. In some cases the premium for internal floor space can be so great that the minimum insulation level allowable will be chosen just to keep the thickness of the walls down. In either case, builders and owners are looking for ways to increase the insulating level of their building envelopes internally or externally while keeping the overall wall thickness down. A way to achieve this is by selecting materials that have lower thermal conductivity, as they will have a greater thermal resistance compared to a product of the same thickness. Insulating products that have a lower thermal conductivity can achieve a target insulating level with a thinner profile than a product with a higher thermal conductivity.

To meet the energy and space saving requirements of today's building code, builders are looking for new materials and practices to insulate their walls. Vacuum insulation panels (VIPs) have shown potential to meet or exceed today's high insulating levels while keeping the thickness of the building envelope down. VIPs are of interest to builders as they have a low profile and a low thermal conductivity giving them a high

thermal resistance for their thickness, allowing them to effectively insulate to high levels in areas where space is a premium.

1.2 Vacuum Insulated Panels in Building Envelopes

The potential for energy and space saving is a major driver to integrate thin materials, such as VIPs, in building envelopes. However as of yet there has not been a widespread adoption of VIPs within building envelopes as there are a number of barriers preventing their acceptance. These barriers include how to integrate the panels into the building envelope assembly, their unknown lifespan, how they affect moisture transport through a wall, their low durability when being handled and their ageing characteristics over time. Without knowing the service life of the VIPs, builders are reluctant to use the panels in their projects for fear that the panels may fail or cause premature degradation to the structure. Despite this some builders, owners and researchers have been willing to incorporate panels into existing and new construction projects to gain experience in construction and understanding on how VIPs behave over time in building envelopes. There are currently a number of demonstration projects that have incorporated VIPs into their envelopes with examples in Switzerland and Germany [7], however few projects have incorporated sensors for ongoing monitoring of the panels' performance. Having few cases where sensors are installed in walls has resulted in very little information on how panels perform on a long-term basis. As such, the mechanisms that lead to the degradation of panel performance is becoming a more widely studied topic.

The desire to understand how the thermal performance of VIPs behave over time has led research groups to develop and conduct accelerated ageing testing, in order to make up for the lack of long-term data on VIP degradation. Degradation of VIPs is observed

through a decrease in insulating performance due to moisture accumulation and or loss of vacuum over time. However, as of yet, there is no recognized standard for the procedure to perform accelerated ageing tests on VIPs [8]. As there is no standard procedure to accelerate the ageing of VIPs, many different attempts have been made to degrade panels in a manner that can be used to predict degradation in real life. Despite the number of laboratories around the world working to predict the service life of VIPs, developing an accelerated ageing test that can successfully link the results to real time degradation has been an area of great study in recent years. The International Energy Agency's Energy Conservation in Buildings and Community Systems program (IEA/ECBCS) HiPTI - High Performance Thermal Insulation Annex 39, recognizes that data from real life ageing of panels is needed to validate predictions made from artificial ageing [9]. As such, the work conducted in this thesis focuses on characterizing the relationship between accelerated ageing predictions and the degradation of panels under normal operation.

1.3 Vacuum Insulation Panels

In conventional fibrous insulating materials such as batt insulation, heat transfer by convection is significant within the spaces of the material. Insulation manufacturers have found that by decreasing the space between fibers, the amount of convection that occurs within the material decreases (but is not eliminated), and as such the amount of energy that is transported through the material decreases. In order to eliminate or significantly minimize convective currents from occurring within a space, a vacuum must be created within the space, as they are free of gases and liquids that can form convective currents. Although a smaller component then convection, conduction in gases is also a mode of heat transfer that can be reduced by implementation of a vacuum within a space. Conduction

in gases within a space is eliminated by the removal of molecules. Vacuum makes an ideal insulator as it can significantly reduce or eliminate convection and significantly reduce conduction. VIPs eliminate convection and conduction through air as means of heat transfer by maintaining a vacuum within a sealed bag. The sealed bag is filled with a porous insulating material that provides stiffness and rigidity to a VIP so that it does not collapse due to the vacuum [10]. Figure 1-1 shows a cross sectional representation of a VIP, showing the core material and the protective foil cover, which is usually comprised of several plastic and aluminum layers laminated together. VIPs obtain their high insulating values through the elimination of convection within a space by creating a vacuum within the core. Typically VIPs are manufactured with an internal pressure of approximately 1 mbar and a thermal conductivity around $4x10^{-3}$ W/m·K [11]. Fumed silica sheets and powdered silica (SiO_2) have proven to be an effective core materials for VIPs where the silica core prevents the panels from collapsing in on themselves while allowing air to be extracted from within the porous core material [12, 13]. Another reason fumed silica sheets are chosen is that the voids formed in the sheet are smaller than the mean free path of the molecules that make up atmospheric gases [11]. The mean free path is defined as the average distance that a molecule travels before a collision between other molecules in a fluid or gas occurs [14]. Having the pore size smaller than the mean free path of air greatly reduces the amount of gaseous heat transfer by trapping any of the remaining air molecules within the pores of the material and unable to collide with other particles and transfer energy by convection. The remaining paths for energy to travel through a panel is left to solid conduction through the core material and thermal radiation [11]. Having a

small mean free path helps reduce the convection within a VIP even when a complete loss of vacuum is experienced compared to conventional fibrous insulation.

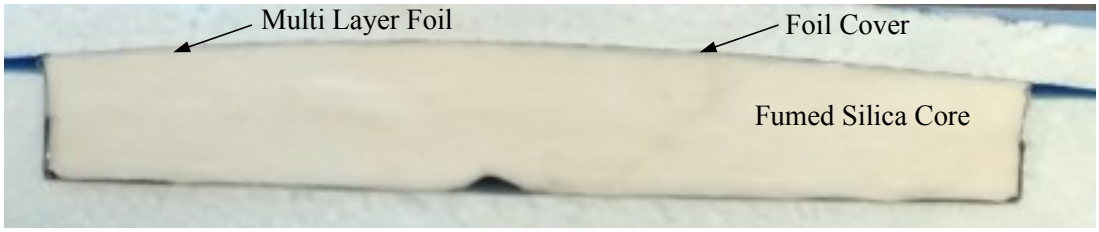

Figure 1-1: Cross section of VIP

1.4 Research Objectives

The research objective of this thesis was to develop a method to accelerate the ageing of vacuum insulation panels and then evaluate the performance of these panels as they are being aged. To meet this objective, the following subtasks were conducted and are presented in this thesis.

- Research ageing mechanisms of vacuum insulation panels to determine which factors contribute the most to degradation of thermal resistance
- Research methods previously used to accelerate ageing and methods used to measure thermal resistance
- Based on what accelerated ageing methods exist, propose a test method to accelerate the ageing of vacuum insulation panels
- Design, construct and commission a guarded hot plate in order to evaluate the thermal resistance of insulating material
- Validate the performance of the guarded hot plate based on known materials
- Evaluate the thermal resistance of VIPs before and after time spent in clime chambers to determine if moisture degrades panel performance

The work completed in this thesis will contribute to the on-going efforts to determine the effective service life of VIPs and further develop an approach to characterize the relationship between the accelerated ageing of vacuum insulation panels and their degradation in real time.

1.5 Contributions to Research

This work includes the:

1. design of a guarded hot plate apparatus to evaluate the thermal resistance of insulating samples.
2. construction, instrumentation and verification of the guarded hot plate used to evaluate the thermal resistance of insulating samples
3. evaluation of the thermal resistance of vacuum insulation panels to obtain a baseline performance before accelerated ageing
4. development of a new procedure to characterize the accelerated ageing of vacuum insulation panels
5. installation of VIPs within a wall along with instrumentation to determine how panels degrade over time.

1.6 Organization of Research

The information presented in this thesis is a summary of the work conducted over the last two years and is presented in the following chapters.

Chapter 1 – Introduction: An introduction to VIPs, their use in walls and the motivation behind the study.

Chapter 2 – Literature Review: A review of previous works conducted on VIPs to determine the mechanisms of ageing and accelerated ageing tests performed.

Chapter 3 – Experimental Procedure: An outline of the procedure used to evaluate the thermal resistance of material using the guarded hot plate and the proposed accelerated ageing procedure.

Chapter 4 – Experimental Setup: A detailed description of the guarded hot plate and its components.

Chapter 5 – Results and Discussion: A summary of the results obtained during the commissioning of the guarded hot plate and from accelerated ageing process.

Chapter 6 – Conclusions and Future Work: A summary of the conclusions from this thesis and an outline of future work.

2 Chapter: Literature Review

Chapter 2 contains an overview of the current state of research pertaining to the ageing of VIPs which includes examining the current definitions of service life of VIPs to determine how industry classifies effective end of life for VIPs. A detailed review has been conducted on the ageing mechanisms for VIPs, to determine what causes panels to degrade and how they degrade. A summary of the current accelerated ageing methods as well as the accelerated ageing testing that has been conducted on VIPs will also be presented.

Despite the number of buildings with VIPs increasing and the number of laboratories around the world working to predict the service life of panels, there are still recognized challenges in the industry. One recognized challenge is to link accelerated ageing results of panels to real life degradation in order to predict the service life of the panels [9]. As VIPs rely on their internal vacuum to maintain their superior insulating characteristics, any transport of atmospheric gases across the foil would decrease the insulating capacity of the panel. The desire to understand how the thermal performance of VIPs behave over time has led research groups to develop and conduct testing on VIPs in order to develop an accelerated ageing procedure. However as of yet, there is no recognized standard for the procedure to perform accelerated ageing tests on VIPs [8]. Many studies have been attempting to link the results of accelerated ageing studies to real time degradation [15-20]. In this review, a summary of the ageing mechanisms of panels, the tests that have been conducted to accelerate the ageing of panels, as well as various methods that exist which define the service life of VIPs, will be presented.

2.1 Performance of Vacuum Insulation Panels

The following section presents various methods or definitions that have been used to define the service life of VIPs, as well as the ageing mechanisms that lead to the degradation of panels performance.

2.1.1 Definition of Service Life

A number of studies have been conducted to define the service life of VIPs, however, to date there is no agreed upon standard as to what the effective service life for a VIP is. A definitive end of life criteria for VIPs however, would be when the vacuum inside the panel is completely lost, whereas a more conservative definition would be when the panel reaches some fraction of its manufactured internal pressure or thermal performance. In a study done by Kunivc [19], the definition used for the service life of a VIP was the time taken to achieve double the initial thermal conductivity of the VIP. The level to which a user defines this upper thermal conductivity can be unique to their application or objective. In the report, their panels started with a thermal conductivity of approximately $4x10^{-3}$ W/m·K with a thickness of 0.01 m. By doubling the thermal conductivity of their panels, this would be the equivalent to having 0.05 m of Expanded Polystyrene (EPS) on the wall which they were comparing against. However, this paper has shown that the end of life criteria should be based on when the thermal conductivity increases to a predetermined value, which is either absolute or relative to the starting thermal conductivity. A paper by Baetens et al. [21] gives two definitions for service life of panels, the first being "the time elapsed from the moment of manufacturing until the moment the effective thermal conductivity of the panel has exceeded a certain limiting value". The second definitions given in the paper was "the time elapsed from the moment

of manufacturing until the moment the time-averaged effective thermal conductivity of the vacuum insulation panel equals a critical value". The difference between the two definitions is the allowable amount of time that the VIPs can stay at a specific thermal resistance. An illustration of these two definitions can be seen in Figure 2-1 where there are two points on the plot representing the two definitions. For example, panels may have an initial thermal conductivity of $4x10^{-3}$ W/m·K and using the first definition, once the panels reach a specified limit such as three times the initial thermal conductivity, the panels effective service life would be met. Comparing the first point to the second point at $24x10^{-3}$ W/m·K where the thermal conductivity is six times the initial thermal conductivity but the averaged thermal conductivity up to that time has just met the service life definition.

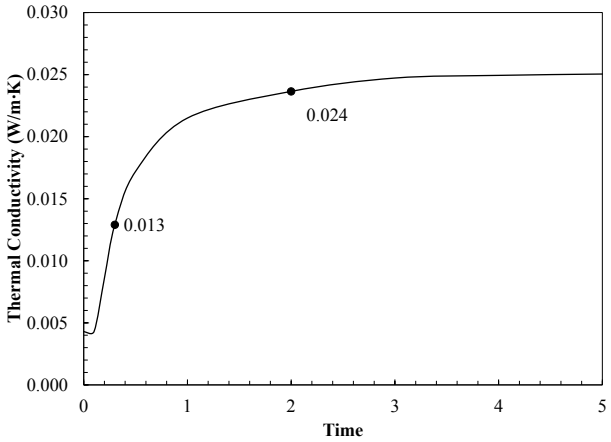

Figure 2-1: Plot of Baetens et al. [21] service life definitions

In the first definition, the moment that a VIP's thermal conductivity exceeds a defined value, the panel is considered defective, whereas, for the second definition, the panel's performance throughout its service period is considered. The second definition takes into consideration that a panel may perform exceptionally for a time period before its performance decrease however, its average performance for a period of time may be better than a defined value.

The performance of panels can also be defined by a rate at which the internal pressure changes as defined by Brunner and Simmler [11]. In this method a maximum allowable internal pressure is defined as well as a target time that the panels must remain under this pressure. With both a target pressure and timeframe, an annual pressure gain could be defined. With this target rate a comparison can be made to observed degradation in panels and it can be seen if panels were degrading at a faster or slower rate compared to their maximum allowable rate. Defining panel degradation in this manner allowed for the observation of a panel's rate of degradation throughout its life and make notes if panels experienced different rates of degradation throughout testing and service. From literature, it can be seen that there are multiple definitions as to what the end of service life for VIPs is and is dependent on the application and the user's acceptable level of degradation of the product.

2.1.2 Ageing Mechanisms in VIPs

Excluding an instantaneous failure of a panel due to a puncture of the foil cover, atmospheric gases such as N_2, O_2 and H_2O can permeate the foil of VIPs through diffusion. Diffusion is the transport of molecules from a higher concentration to one of lower concentrations and in the case of atmospheric gases and the foils of VIPs this occurs at small pores in the VIPs foil, where moisture and dry gases transport across the foil to areas of low concentration within the panel core [15, 16]. A large contribution to the diffusion of moisture into a VIP is caused by convective mass transfer across the panel foil. Before reaching the foil layer of the VIPs within a wall, any moisture would have to transfer through the exterior building envelope. Research has been conducted to determining which gases transport the fastest across the foil and under which conditions do the greatest

amounts of gas diffuse into the panels. Through researching what factors lead to a decrease in panel performance, several areas of focus were identified including, what environmental conditions cause the greatest transport of atmospheric gases across the foil, do different gases transfer across the foil at different rates, do different gases affect the thermal performance of the panel differently and does the type of foil that the panel is manufactured with affect the transfer rates of gases into the panel.

Schwab et al. [15, 16] sought to determine which environmental conditions affect the internal pressure of panels and if the internal pressure of a panel could be altered through exposure to temperature and humidity variations and if size and foil material had any effect on the rate that gases diffuse into the panels. In the testing, two styles of foils, Laminated Aluminum Foil (AF) and aluminium coated Multilayer Metallized Film (MF), were tested for two sizes of panels. The panels were stored in climate controlled boxes with different temperature and relative humidity. In total six climate chambers were used to condition the panels with three chambers were held at fixed temperatures of 25°C, 45°C and 65°C with a humidity level of 75% RH. The other three chambers, were held at the fixed temperatures of 25°C, 45°C and 65°C, with partial water vapour pressure allowed to remain constant with the surrounding lab. Panels from all six chambers had their moisture content and internal pressure measured routinely throughout a period of approximately one year, to determine if the mass or level of vacuum within the panels was changing.

It was found that the rate of moisture and pressure gain in the panels were greater for panels kept at elevated temperature and humidity levels compared to panels kept at lower temperatures and humidity levels. The types of foils used in the testing showed different rate of permeation depending on the composition of the foil and the temperature

and humidity of the surrounding environment. The conclusions drawn from the tests was that the climate around a panel does affect the amount of moisture transport into the panel, with warmer/humid conditions seeing higher rates of moisture gain than cooler dryer conditions. The type of foil also played a role in limiting the amount of pressure and moisture increase observed, where panels with thicker foils had the least amount of pressure and moisture gain through testing. Based on the defined end of service life criteria for thermal performance it was concluded that the rate at which the internal pressure changed within the panels was low enough for use in building envelopes. However, the rate at which moisture increased within the core gave cause for further testing to determine the effect that moisture within the panel core had on thermal resistance. The challenge here was that no link was made to kinetics of the degradation process and as such leaves the question as to how it was concluded that the panels met the required service life.

Building on their findings that moisture transport across a panels foil cannot be ignored, Schwab et al. [22] conducted a study to determine the effects that moisture content had on a panel's thermal resistance. VIPs with specific moisture contents within their core were manufactured to evaluate the thermal resistance of panels of known moisture content. The panels were tested with a mean panel temperature of 10℃ using a guarded hot plate apparatus. It was observed that the thermal conductivity increased significantly as the moisture content of the panel increased, with the results being larger than expected for amount of moisture that transported into the panels. It was suggested that thermal transport through liquid water was occurring through the panel in addition to gaseous thermal conductivity. The conclusion from the study was that moisture accumulation within a panel causes a greater increase in the thermal conductivity of a VIP than dry gases.

Simmler and Brunner [11] conducted similar testing to those performed by Schwab et al. [15, 16], to determine how the climate surrounding a panel could affect a panel's internal pressure and moisture content. Panels of two foil types were held at different temperatures and humidity levels to determine if the internal pressure of a panel changed due to these conditions and which if either, had the greatest effect on the moisture transfer into the panel. Results from this study showed a range of pressure and moisture increase rates for the panels held under different conditions of 30°C, 90% RH to 80°C, 80% RH. It was concluded that the higher temperature conditions caused the higher rates of moisture gains and that water vapour pressure is a strong driver in panel degradation. A second conclusion was made that the type of foil used affects how a panel resists moisture and pressure gains where the thicker AF panel resisted moisture and pressure gains better than the MFs. It was noted though that a downside to using AF panels compared to MF panels is that the edge heat flow or thermal bridging around the panel can be much larger than the heat flow though the core of the panel itself and compared to the MF panels, due to the thermal conductivity of the aluminum compared to that of the core. The study went on to test if the surface area of panels had an effect on the rate at which moisture or pressure is gained through the foil. In this test panels of two sizes were tested under elevated temperature and humidity levels. The results led to the conclusion that rate of water increase is greater in the smaller panels compared to the larger panels due to the edge to surface ratio being greater for the smaller panels. The results showed that most of the transport was occurring through the seams of the panels.

A brief summary of the reports presented above that have looked at ageing mechanisms in VIPs can be found below in Table 2-1. Through research it can be seen

that moisture content of a panel can be altered by high temperature and humidity environments and that there is a decrease in insulating potential of panels as moisture content increases.

Table 2-1: Summary of mechanisms that cause panel degradation

Author	Purpose of Test	Test Performed	Conclusions
Schwab et al. [15]	· To determine how ambient temperature and humidity levels effect internal pressure and moisture content	· Held three different foil type panels in climate chambers under a range of temperature and humidity levels	· Humidity and temperature environments effect moisture and pressure gains · Foil types have an effect on the permeation rates.
Schwab et al. [16]	· Combining a combination of previous papers to predict service life of panels	· Developed an equation to estimate combine panel degradation based on observed climate aged rates	· Humidity and temperature environments affect moisture and pressure gains · Foil types have an effect on the permeation rates.
Schwab et al. [22]	· To determine the effects of moisture content on thermal conductivity	· Evaluated the thermal resistance of panels manufactured with known moisture content	· Moisture content affects the thermal conductivity of panels at a level of 0.5×10^{-3} W/m·K per mass %
Brunner, Simmler [11]	· To study the pressure and moisture increase within a panel due to climate conditions around the panels	· Held three different foil type panels in climate chambers under a range of temperature and humidity levels	· Foil types have an effect on the permeation rates. · Humidity and temperature environments affect moisture and pressure gains · Internal pressure gain is mainly caused by water vapour

2.2 Accelerated Ageing

The reason to perform the accelerated ageing tests is to understand the factors that lead or contribute to the degradation of a product and then replicate these conditions in a laboratory setting under a shorter time period. Accelerated ageing is used when a faster rate of degradation is required to determine how long a product will last. Many industries use accelerated ageing to test their products for a variety of reasons including product safety, customer satisfaction, or to meet certification standards. A challenge in developing any accelerated ageing test is determining which environmental conditions are most important to mimic and then designing a method to replicate the conditions [20]. It is important that when conducting accelerated testing, that only conditions that would take place under normal service are initiated on a product, thus a link can be established between accelerated time and time under normal operation [20]. When conducting accelerated ageing, the test performed must be adjusted to simulate normal operating conditions as much as possible so as not to cause excessive damage or failure on the product which would not have be seen under normal operating conditions [19].

2.2.1 Current Accelerated Ageing Standards and Techniques

There are many industries that make use of accelerated ageing for consumer safety and satisfaction. As an example, in the automotive industry tires are tested for parameters such as total kilometers until failure so that a recommendation as to the safe number of kilometers that can be put on the tires can be made. In this example, accelerated testing is used to prevent putting a driver in harm's way by having them drive until the tires fail, and to keep testing consistent. In the accelerated test, a tire is held in contact with a large spinning disk that has its surface coated in asphalt. As the sizes of both the tire and the

wheel are known and with the number of rotations of both the large and small wheels recorded, the resulting distance the tire traveled can be determined [23].

An example of an accelerated ageing test that is used to test materials and components intended for use in the building envelopes is the Nordtest Method, NT Build 495 [24]. NT Build 495 is used to determine how materials react to sun exposure, wetting from rain as well as thermal cycling from freeze and thaw cycles. The test method is intended to simulate natural climate strains and concentrate the individual climate factors on the sample in an effort to accelerate the ageing of the product [24]. Products tested through this method are repeatedly exposed to cycles of the four climate conditions above for a minimum of one hour under each condition. The Nordtest Method was developed to test materials that are held in the vertical position in the building envelope under conditions seen through the products life [24]. The Nordtest Method has been implemented in testing sample wall sections to determine how a wall would function in a real life application. Jelle [20] performed a test on a wall assembly, where a full mock-up of a composite wall was tested using the Nordtest method to determine how a particular exterior plaster would resist the elements if a worker was to accidentally chip or crack the plaster during installation on a home.

2.2.2 Accelerated Ageing Tests Performed on VIPs

In a report presented by Wegger et al. [25], the Nordtest Method was used to test two different scenarios for VIPs at a construction site. The test was conducted to determine if VIPs left exposed to the elements on construction sites would experience greater degradation than panels protected from the elements. In the setup, one VIP was left exposed to the elements and the second was covered as if shielded from direct exposure to

the elements. The two panel configurations where then subjected to a repeated four-hour cycle for approximately 175 days in which both the thermal conductivity and physical condition of the panels were recorded at intervals throughout. During the testing it was observed that the exposed panel bowed and was permanently deformed towards the elements whereas the protected one did not. During testing, the thermal conductivity of the panels increased by approximately 2% and 6% for the protected and exposed panels, respectively. The results from this testing suggests that panels left exposed on a construction site will degrade faster than if they were protected. The results from this testing can help determine the level of degradation panels may experience if left exposed to the elements on a construction site before being installed into a wall. However, using the results to predict the rate at which panels degrade once they are integrated into a wall section may be misleading as the conditions experience in the accelerated testing may not be indicative of conditions seen by panels encased in a wall especially exposed to direct rain and sun. A second difficulty in this testing is relating the procedure to time. In this procedure it is not clear how one complete cycle of testing relates to time under normal operating conditions.

Wegger et al. [25] also tested panels in high temperature and humidity conditions where panels were stored at 30-day intervals. The panels were held in sealed bags containing a container of water, then placed in the heating cabinets held at 70°C. After each 30-day period, the panels were evaluated for thermal performance. The panels in this test saw a large decrease in thermal performance, where the panels' starting thermal conductivity of 4.4×10^{-3} W/m·K increased to 17.9×10^{-3} W/m·K over 60 days. It was concluded that the panels experienced a loss of vacuum which was caused by exposure to

excessively high temperature and moisture conditions, which suggests that only conditions that are found under normal operation should be tested in accelerated ageing testing. However, before the loss of vacuum, the testing procedure was determined successful for altering the moisture content and thermal resistance of the panels.

In an accelerated ageing test performed by Kunivc [19], an attempt was made to age VIPs by exposing the panels to elevated temperatures. The idea behind the testing was that in order for a material to degrade, a reaction in the material has to occur and for this to happen a minimum activation energy in the material must be reached. However, because the foils around a VIP are usually made of a few laminated layers, an activation energy for the combined material needed to be calculated. The activation energy for the panels foil was calculated by comparing the time it took to degrade panels to a specific level using the Arrhenius equation. Panels were held for a set number of days at a constant temperature and after the heating process the panel's thermal conductivity was recorded. The lab then took new panels and degraded them at higher temperatures compared to the first tests. The panels held at higher temperatures had their thermal conductivity measured throughout their heating process and when the thermal conductivity matched that of a panel aged under lower temperatures the time taken to age the panel was recorded. Upon collecting several sets of panels that had been aged to the same thermal conductivity under different temperatures and times an average activation energy for the material could be calculated. By finding the activation energy of the foil being tested, the lab could make predictions as to the performance of the panels when exposed to different temperatures. For example, Kunivc [17] predicted that if the panels were exposed to a mean temperatures of 23℃, that they would be able to withstand 30 years before the internal thermal conductivity of a panel

was doubled. The conclusion for a 30 year lifespan was made through extrapolating the calculated data and is an estimate on how the panels will perform under a fixed temperature condition. The drawback of this process is that it is not possible to capture the natural temperature fluctuations that occur during the year. It is important to note that the panels were also not subject to any humidity during testing. If the panels are to last only 30 years under ideal dry and stable conditions, one is left to wonder how VIPs will perform under humid and fluctuating temperature environments.

As VIPs rely on a foil cover to maintain their level of thermal resistance, any gas or moisture transport across the protective foil will lead to an increase in their thermal conductivity. Using this understanding, a test procedure was developed by Kumaran et al. [26] to expose panels to an increase in pressure around a panel to determine if the rate at which atmospheric gases penetrate the panels could be altered by increased ambient pressure. The aim of the test was to alter the internal pressure of the panel, and testing saw panels exposed to 3 – 5 bar overpressure. The increased pressure around the panel caused the panels to shrink by approximately 6% in all dimensions. Thermal performance testing was done before and after the exposure to the high pressure and the panels tested showed an average decrease in thermal resistance of 45%. An investigation into how and why the panels shrunk showed that the porous of the core material had collapsed and it was speculated that more solid conduction was occurring through the core material. The test concluded that pressure around a panel does affect the thermal resistance of a panel, however it was not determined if any additional gases entered the panel. The previous test was discounted for use in this study as only conditions found within the

intended use should be replicated in accelerated ageing testing and there would not be a condition where a home would experience these pressures.

A similar test was conducted by Wegger et al. [25] where VIPs were tested under overpressure conditions in an attempt to increase gas and moisture transport through the foil covers. During the test, panels were held at 8 bar overpressure for up to 33 days and in a similar way like Kumaran et al. [26] the panels experienced a reduction in overall dimensions of between 10 – 15% with an average decrease in thermal resistance of 35%. Both the testing performed by Wegger et al. [25] and Kumaran et al. [26] showed that high external pressure around panels can lead to a decrease in thermal performance of a panel, however both tests were not able to link their findings to time spent under normal operating conditions or how long the panels should last in the built environment as the pressure around the panels would not be found under normal operating conditions.

In a recent study done by Kim et al. [18] the ageing performance of vacuum insulation panels was evaluated. The internal pressure and the thermal conductivity of panels were evaluated from VIPs that had been subjected to thermal cycles between -15℃ and 80℃. The pressure increase values were turned into a permeation rates for gases across the foil. By combining this permeation rate with the internal pressure that meets the end of life criteria for panels, the study was able to extrapolate a lifecycle for the panel of 25 years. In this case, the panels were not exposed to moisture, which likely would have decreased the service life.

In a study conducted by Mukhopadhyaya et al. [8] a remark was made that there are so many variables that can affect the thermal performance of a VIP including, size, foil, core material and whether a desiccant is used or not to absorb water, all of which can make

it difficult to create a standard method to predict the service life of panels. An accelerated ageing study was conducted on panels that where cycled from a warm and dry environment to a cooler and humid one holding the panels in each condition for a week. The cycling process would continue through an 8 month period where the panel's thermal performance was tested after every cycle. It was found that all the panels aged at different rates with some of the panels even losing their vacuum during testing. It was noted that the thermal resistance of the panels was higher after the warm and dry conditions compared to the cooler and damp conditions which suggest that moisture contributes in a greater capacity to the thermal degradation of panels compared to heat alone. Also noted was that panels from the same manufacturing batch had a range of thermal resistance values between panels at initial testing, and that the rate that panels degrade could be just as important as the initial thermal resistance of the panels from the factory.

There have been many different approaches taken to age VIPs, many of which have shown that thermal performance drops when moisture content and the internal pressure increases. How these tests go about accelerating the ageing of the panels varies and the techniques used have been examined. The desired outcome for the ageing of panels is to be able to relate the testing done to number of years of service the panel should expect. Not only is important when conducting accelerated testing, to maintain conditions that would take place under normal service be initiated on a product but the link be made to conditions seen under normal operation to establish a time that panels would last under normal operation. A brief summary of the reports discussed on accelerated ageing of VIPs is included in Table 2-2.

Table 2-2: Summary of accelerated ageing testing

Author	Purpose of Test	Testing Performed	Conclusions
Wegger et al. [25]	· To determine the effectiveness of different accelerated ageing tests on thermal resistance of VIPs	· Nordtest Method · Moisture and temperature ageing · Pressure testing	· Cosmetic and damage to some panels · A wide range of results found · Temperature and moisture testing provided most promising results
Kunivc et al. [19]	· To link accelerated ageing and service life through Arrhenius law	· Exposing panels to elevated temperatures for a period of time to link exposure time and temperature to thermal degradation	· Related panel temperature and service life · 30 year life of the panels held at 23℃ before doubled thermal conductivity
Kumaran et al. [26]	· Testing to determine if external pressure can increase the rate that dry gases transport across the foil	· Exposing the panels to an elevated pressure environment	· Increased external pressure caused a drop in performance due to crushed core material
Kim et al. [18]	· To determine if exposing panels to temperature cycling will affect thermal performance	· 12 hour cycles between -15℃ and 80℃ for two periods of eight days	· Concluded a 25 year service life for their panels
Mukhopadhyaya et al. [8]	· To determine how cycling temperature and humidity affects panel performance	· Panels from a number of manufacturers are held under hot and dry then cool and damp conditions each for a week over the course of a month	· Study suggests that the panel performance decreases with moisture content and overall cycling of ambient conditions

Wegger et al. [25] studied how pressure and moisture of panels change over time. Their results indicated that moisture accumulates at a faster rate compared to gases within a panel. Schwab et al. [15, 16] studied how the thermal conductivity of panels changes due to pressure and moisture gains. Their results indicated that a 4% change in internal pressure of a VIP does very little to the overall thermal performance due to the mean free path of the fumed silica whereas a 4% change in mass of a panel could increase the thermal conductivity of a VIP by up to 50%. Through understanding the ageing mechanisms and interpreting the results from conducted accelerated testing, the decision to focus on the moisture content of the VIPs as the ageing mechanism in this thesis was made.

2.3 In-Situ Testing of Panels

To gain an understanding of how a product will age, manufacturers sometimes employ a technique called in-situ testing. In-situ testing or "in position" testing is any test where the product is tested under real life conditions. In some cases, a mock-up will be created to expose the product to natural conditions that the product would see under regular use. Testing using a mock-up would be preferred if a product's ageing characteristics are unknown and there is a risk that installation of the product into a real application could cause premature damage to the end application. VIPs are an example of a product that is being monitored for degradation through in-situ testing in order to gain a better understanding of their service life under normal application. As the rate of degradation for products being tested in-situ is in real time, testing periods can be over several years or more if the product does not degrade quickly. Despite in-situ testing potentially taking a long amount of time compared to accelerated ageing, in-situ testing of a product is the only true way to determine how a product performs under actual application. Real world testing

provides understanding on how a product interacts with its surroundings and the conditions surrounding the product. In the case of walls with integrated VIPs, real world testing can show how moisture transfers through the wall and provide data on the surface relative humidities of the different layers within the wall. In-situ testing can also be used to provide the necessary means to calibrating and validating predictive testing. Future work will obtain results from in-situ testing started in this thesis to validate the predictive modeling conducted. As in-situ testing will be used in this thesis a summary of in-situ tests performed on VIPs will be presented.

An in-situ test was performed by Brunner and Simmler [27] where VIPs were installed within a roof with instrumentation to record the temperature and humidity levels on the inside and outside surfaces of the panels. The panels were placed in the roof, and environmental conditions were recorded that would later serve to provide a comparison between panels (and how they degrade) and the predicted values. Data was recorded over a period of three years and during this time, the panels were removed from the roof at specific time intervals and weighed to see if any moisture had permeated the protective foil of the panels. During the testing, panels experienced outer surface temperatures between -10°C and 60°C which would be equivalent to center of panel temperatures of 5°C and 40°C, respectively. The center of panel temperatures of 5°C and 40°C would be obtained if the internal room temperature was maintained at 20°C throughout the year. The relative humidity sensors indicated that the panels were exposed to almost continuous saturation throughout the duration of the test. The moisture that was present in the sealed space around the VIP was suspected to have originated from rain during installation and through permeation of the water barrier of the roof during testing. The moisture that was present

around the panels lead to a moisture increase of around 0.1 – 0.15 mass%/annum. Using the rate of internal pressure gain and rate of increased moisture content, the calculated rate for the annual increase in thermal conductivity became $0.12x10^{-3}$ W/m·K.

As VIP are compact, light and provide a high insulating capacity for their thickness, their use in remote communities is being explored as shipping costs for conventional insulating material can be quite high. Mukhopadhyaya et al. [28] led an investigation to determine the economics and thermal performance of VIPs constructed into a wall in Yukon as part of a retrofit project to increase the thermal resistance of a building, bringing the wall back up to building code. In addition to the economic investigation, a better understanding of how panels perform long-term in a Canadian subarctic climate was sought. Instrumentation was placed throughout the wall in order to evaluate the conditions around the VIPs and to evaluate the thermal resistance of the panels over time. The aim of the evaluation was to gain a better understanding of how VIPs perform in the subarctic environment. After three years of monitoring the wall, they concluded that VIP use in the Canadian subarctic climate showed promise and that the panels showed no significant signs of ageing.

Despite the need for accelerated ageing, in-situ testing must still be conducted to validate and calibrate predictive models for ageing of VIPs. As this is the case, in-situ testing has been incorporated for the proposed accelerated ageing of VIP within this report. More information will be presented on how in-situ testing will be incorporated into the proposed accelerated ageing procedure in the Experimental Procedure section of this thesis.

2.4 Thermal Resistance Testing

In this section, a summary of a few of the methods that could be used to evaluate the insulating capacity of building materials will be presented. There are several ways in which the performance of a panel can be defined, however in this thesis the thermal resistance of the material will be used to quantify a material's insulating capacity as opposed to recording the thermal conductivity of the material. There are many ways to evaluate the thermal resistance of an insulating material, all of which require a heat source, a means of measuring or evaluating the energy flowing through the sample and a temperature difference across the sample. The four methods that will be discussed in this section are in-situ testing, the heat flow method, the hot box method and the hot plate method.

In-situ testing or in-position testing is testing of material under conditions found in regular use of the product. In the case of VIPs within a wall, in-situ testing for thermal resistance makes use of heat flux plates to measure the energy transfer through the panel and the natural temperature differences between the indoor and outdoor conditions as the driver of energy. A benefit to in-situ testing is that data on how a panel performs under normal operation can be obtained, however due to using natural temperature differences across the wall there is no repeatability in the testing. Having no repeatability in testing conditions makes it a challenging method to use for comparing products at different times and as such more repeatable testing methods such as the heat flow meter, the hot box method and the hot plate method are often explored.

One approach to test the thermal performance of building materials is using a heat flow meter apparatus as outlined in ASTM C518 [29]. In the heat flow meter approach,

heat flux sensors are used to measure the amount of energy flowing through a specimen of known thickness while a constant temperature of the hot and cold surfaces is maintained. The heat flux method is considered a secondary or comparative method of evaluating the thermal performance of an insulating material as materials of known resistance are required to calibrate the apparatus. The calibration of the heat flow apparatus requires materials of similar thermal performance as well as thickness of the material that will be evaluated. Finding materials of similar thermal performance as well as thickness poses a challenge when the thermal resistance of a material may not be known and when testing VIPs of high insulating capacity for their thickness. The heat flow meter apparatus is often used when comparing multiple samples of the same material to one another in applications such as quality control where samples are drawn from a batch and compared to a sample of an agreed upon level of performance. The decision not to use a heat flow apparatus in this study was made as the ability to test many different materials of thermal resistance and thickness was desired.

Another means of testing the thermal performance of building materials comes in the form of a hot box apparatus where materials are tested with a thermal gradient across the sample as outlined in ASTM C1363 - 11 [30]. The hot box method was developed to test composite assemblies of materials under steady-state conditions to determine an average thermal resistance of the assembly. In the hot box method, the ambient conditions on both the warm and cold side of the sample are maintained as opposed to surface temperatures. An advantage of the hot box method is that full mock-ups of walls can be evaluated for thermal performance and an understanding of how all the components of a wall interact together can be obtained. Conley and Cruickshank [31] used a hot box to

study how thermal bridging occurs when using VIPs in a wall assembly to quantify the effects that thermal bridging has on the overall thermal performance. Even though the hot box method can be used to evaluate the thermal performance of individual materials with convection on both sides, this study will examine the use of VIPs in building envelopes where conduction would occur on both surfaces. As such a test method where the surface temperatures could be maintained as opposed to the ambient temperature was sought and as such the guarded hot plate (GHP) apparatus as defined by ASTM C177 [32] was then explored in more detail.

The GHP apparatus is considered a primary method for evaluating the insulating capacity of material as it can be used to test samples of different thermal resistance and thickness [31]. As outlined in ASTM standards the thermal performance of a range of materials can be evaluated using the GHP and the design and accuracy of the GHP can be adapted to meet the requirements of the material being tested. The GHP method has been used to evaluate the thermal performance of VIPs in a number of studies with a notable test performed by Mukhopadhyaya et al. [10] where different materials were explored for use as core material in an effort to find alternative materials that could withstand the force of the vacuum and deliver an acceptable level of thermal resistance to use as VIP cores. GHPs have also been successfully used to test the thermal resistance of panels after accelerated ageing tests to identify how pressure and moisture content within the panels affects the overall thermal performance of the aged panels [25, 19]. As the GHP method can evaluate materials of different thermal resistance and thickness and because it has been used to evaluate the thermal performance of VIPs in other accelerated ageing tests, the GHP method was selected to evaluate the thermal performance of the VIP within this study. A

full explanation as to how the GHP apparatus is used and how it was constructed can be found in the Experimental Procedure sections of the thesis, respectively.

2.4.1 Thermal Resistance of Material as a Function of Mean Temperature

A challenge in this study was determining what mean temperatures to test the panels under and what temperatures to set the plates to in order to reach these mean temperatures. As thermal conductivity is temperature dependent, the average or mean temperature of a sample being tested would make a difference on the evaluated thermal resistance [14, 33]. Holman [33] describes that as a material heats up, more energy is able to be transported through lattice vibration and by free electrons in the solid, resulting in an increase in energy transport with temperature. Understanding that temperature can affect thermal resistance values in materials, ASTM standards were consulted to determine how to select testing temperatures in order to properly report material properties.

ASTM C578 standard specification for rigid, cellular polystyrene thermal insulation, outlines the manufacturing standards and industry standards for reporting thermal property of both expanded polystyrene (EPS) and extruded polystyrene (XPS) [34]. The standard practice for reporting the thermal resistance of EPS and XPS is at a mean temperature of 24±1°C tested with a temperature difference of 22±1°C. In addition to the standard reporting temperatures ASTM recommends that materials be evaluated through a range of temperatures based on the application of the product and to test the product with a temperature difference suitable for the application of the product [35].

In addition to ASTM standards, a report by Lorenzati et al. [36] outlined a procedure they used to determine what mean temperatures they used to report their thermal

resistance values of their VIP. Two tests were conducted with the first exploring how the thermal conductivity of VIPs behave as the average temperature is varied. The results from the first test showed that like EPS, a VIP's thermal conductivity increases with a rise in average temperature, however the increase is non-linear with the thermal conductivity increasing faster as temperature increases. The information gained from this testing shows that in different situations the panels would perform differently such as between winter and summer, with the panels performing better in a cooler setting. It was also determined that when testing the thermal resistance of VIPs under a variety of mean sample temperatures that the relation of thermal conductivity to temperature was non-linear. The fact that the relations of thermal conductivity to temperature was non-linear was noteworthy as most building materials follow a linear relation for thermal conductivity and temperature.

The second test was to understand how the thermal conductivity of a VIP would behave with the average temperature of the panel being maintained and the temperature difference across the sample changing. Results from the second test showed that as the temperature difference across the sample increased the uncertainty in the measured thermal conductivity decreased and the results became closer to one another. When high performing insulating materials, such as VIPs, are testing with a low temperature difference across the sample, the uncertainty in the calculated thermal conductivity increases. The conclusions drawn from the testing determined that with a temperature differences equal to or greater than 36℃ the uncertainty in the thermal conductivity values calculated were less than 2% and the testing was found to be more repeatable and have less variation in results between testing. The conclusions gained from their second test will be used in the

testing of the thermal resistance of the VIP panels in this study, with more information on the testing procedure to come in the Experimental Procedure section of this thesis.

2.5 Gaps in Current Literature

This section provides a summary of the findings in literature and makes suggestions as to how these findings may be linked together in order to expand the knowledge within the field. Through a review of the literature, an overwhelming number of studies point to moisture accumulation within a panel as being the single greatest contributor to the degradation of thermal resistance of a VIP. In the presented reports, panels were tested in climate chambers at fixed temperature and moisture conditions, with testing conditions that would be considered at opposite sides of climate conditions found in walls such as cold and dry or warm and moist. Testing how VIPs perform to the opposing climate conditions provides a clear indication as to which conditions affect panels the most between cold and dry or warm and moist however, from these tests, only estimations can be made as to how panels may perform at climate conditions in-between those tested. Currently, there is a lack of testing over the complete range of conditions VIPs will experience in actual applications. As such, there is a research gap connecting specific climatic or surface conditions of the VIPs to actual rates of moisture gain. For example, does the rate of moisture gain increase evenly as temperature and moisture increases or does the rate of moisture gain increase faster as temperature and moisture increase. It is already known to watch for high temperature and humidity conditions next to VIPs in walls, but is there a moisture content within the air that at lower moisture levels there is little concern yet for higher levels of moisture content the concern for the panel's degradation is greatly heightened? Having data points on the extremes of the climate conditions is limiting the

ability to predict the degradation of panels as average climate conditions are used or assumptions as to panel behaviour under different conditions are made. The test method proposed in this thesis aims to address these gaps through additional testing over the complete range of conditions the panels would expect to experience in Ottawa.

For accelerated ageing tests, VIPs are usually held in climate chambers until some service life condition is met. Currently, a link to real degradation is being attempted by using averaged climate conditions surrounding VIPs within a building envelope or by taking the averaged time that specific conditions were experienced. However, past work that has been conducted on the link between degradation experienced through accelerated ageing and time in the real word is an area that can be expanded on [8]. A possible solution to improve predictions to real world degradation may be to breaking the environmental conditions seen beside VIPs tested in-situ down into smaller groups. The time the VIPs were exposed to each of the environmental conditions could then be compared to more rigorous climate chamber testing of the VIP to improve the link between time spent in accelerated climate ageing and normal operations.

Finally, in current literature, most thermal resistance evaluations are conducted at singular mean sample temperature values where literature shows that thermal resistance is dependent on temperature. Thermal resistance evaluations of VIPs could be conducted over a range of mean temperatures to determine how VIP performance varies, helping designers and builders determine where in a buildings envelope VIPs should be placed to optimize the performance of the wall. For example in a heating dominated climate, VIPs may be placed closer to the exterior of the wall in order to keep the panels cooler and the thermal resistance higher, and as such keep more heat within the structure. Evaluating the

performance of aged VIPs at different temperatures and humidities will help determine how moisture affects the panels over time. Specifically, moisture may cause more energy transport under warmer conditions through evaporation and condensation between the warm and cold surfaces of the structure or testing equipment.

This thesis will address these gaps in literature using a new testing procedure for accelerated ageing and by thermal resistance evaluation of both dry and aged panels in a GHP apparatus.

3 Chapter: Experimental Procedure

The desire to understand how the thermal performance of VIPs change over time has led research groups to develop new methods to study the ageing of VIPs. To date, there is no recognized standard or procedure to perform accelerated ageing testing on VIPs [8]. Chapter 3 outlines a new testing procedure that was developed, based on previous research, to study the ageing of VIPs. The developed method aims to make a better link between results obtained from accelerated ageing to normal degradation through studying the rates moisture accumulates within VIPs under different environmental conditions and how thermal resistance of VIPs are effected by changing moisture content.

Research shows that moisture accumulation within a VIP core contributes to a drop in insulating capacity, where the level of degradation caused by moisture can be greater than that caused by air infiltration. In reports by Schwab et al. [17] and Brunner and Simmler [27], moisture accumulation within panels under normal operation is observed and is credited with degradation of panel performance. With the understanding that moisture accumulation within VIPs is causing degradation to panel performance the focus of this developed accelerated ageing process is on the moisture accumulation within VIPs and how the thermal performance is impacted.

Understanding that all panels are constructed differently and that there are many factors that can cause a difference in the rate at which moisture transports across a panel's foil, developing a procedure that is able to test the ageing characteristics of multiple panel types is developed. Preliminary testing under the developed methodology was conducted and is reported on in the Results and Discussion Section 5 of this thesis, however this

methodology forms the base of a larger project on predicting the service life of VIPs for any given location or application.

3.1 Proposed Test Procedure to Characterize Service Life of VIPs

This section of the thesis discusses the five steps that are involved in the proposed new method of accelerated age testing of VIPs.

- Baseline thermal resistance testing of the VIPs before accelerated ageing
- Determining how the thermal resistance of panels changes with respect to moisture content
- Evaluating the rate that moisture transports across the panels foil through climate ageing of VIPs
- Monitoring temperature and humidity levels next to VIPs within a sample wall section to gain results from real time panels degradation
- Validating the predictive model based on results from in-situ testing

3.1.1 First Step – Baseline performance Testing

Prior to ageing the panels, it is important to obtain the baseline thermal resistance of the panels that are to be tested, in order to give a reference value (of their starting thermal resistance) for subsequent testing. In the baseline testing unaged or dry panels will be tested across a range of mean sample temperatures as the thermal resistance of materials are a function of mean temperature as introduced in Section 2.4.1. Obtaining thermal resistance values for a panel across a range of temperatures will indicate the upper and lower thermal resistance values for the panels. Figure 3-1 shows an example of what the thermal resistance for a panel with 0% moisture content might look like. Before climate

ageing the panels, the dry or initial mass of the panels will be recorded to be used as a baseline mass.

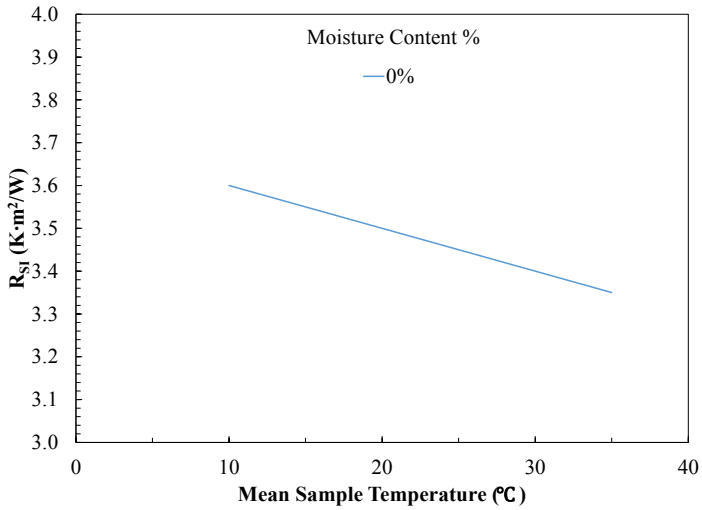

Figure 3-1: Baseline thermal resistance of a VIP as a function of mean sample temperature

3.1.2 Second Step – Moisture Permeation and Thermal Resistance

The next step in the procedure is to confirm that the moisture content of panels can be altered and that an increase in moisture content of a panel will decrease the thermal resistance of the panel. In order to complete this step, a climate chamber can be used to drive moisture into the VIPs by creating a warm and humid climate and as such, a large gradient in moisture content across the foil of a VIP. With the difference in moisture concentration and temperature across the foil of the VIP, convective mass transfer of moisture will occur causing moisture to diffuse into the panels. The panels will be held in the climate chamber for a period of time before being removed, weighed and the thermal resistance evaluated. The thermal resistance of the panels will be recorded as the moisture content of the core increases to a maximum saturation level. In this stage of testing, recording the time at which the moisture enters the panel is not as critical as understanding how the thermal resistance changes with moisture. Recording the rate at which moisture enters the VIPs will be the focus of the third stage. As discussed in the Literature Review,

the thermal resistance of a material is dependent on temperature, and when a VIP is subject to an increase in temperature, its insulating properties decrease. Figure 3-2 shows a representation of the second procedure and indicates the possible relationship between thermal resistance results and temperature. Each of the lines in Figure 3-2 represent a different percentage moisture content from dry panels to a saturation point where dry panels thermal performance will be greater than that of the wet or aged VIP.

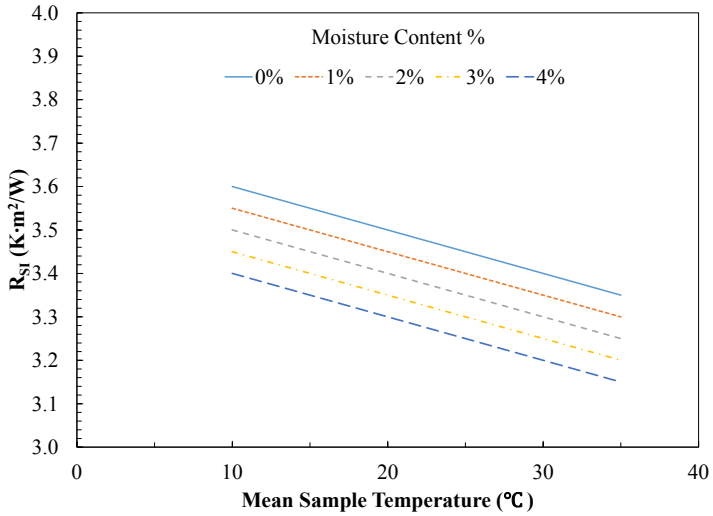

Figure 3-2: Thermal resistance of a VIP as a function of mean sample temperature and moisture content

3.1.3 Third Step – Moisture Gain at Different Climate Conditions

The third step in the procedure is to characterize how panels experience different rates of moisture gain based on temperature and humidity levels. The goal of this step is to determine the rate that moisture accumulates within a panel under the different temperature and humidity conditions found in walls. The testing in the third step will use the climate chambers to increase the moisture content of the panels while recording the time it takes the moisture to accumulate within the panels by weighing the panels at specific intervals. The results will be used to determine the rate of moisture gain within panels based on temperature and humidity levels around the panels. Figure 3-3 and Figure 3-4

show an illustration of the hypothesized results for the third part of the procedure. In both figures, increasing rates of moisture gain are expected to be seen as the RH around the panels increases. In order to develop the curves, a fixed temperature and humidity level will be set in one climate chamber and two dry panels will have their mass recorded until they reach a saturation point. A saturation point will be reached once the VIPs stop taking on water. Upon completing this test, the humidity level in the climate chamber will be increased while the temperature is held constant. New dry panels will then be aged at the new humidity level until they reach the saturation level. The process will continue at this temperature set point until a determined number of humidity levels have been tested, upon which the temperature will be changed and the process of testing at the different humidity levels will begin again. An increase in the climate chamber temperature is hypothesized to drive more moisture across the foil of a VIP compared to lower temperatures and is illustrated in Figure 3-3 and Figure 3-4. At this point, the results from the first step, thermal performance versus moisture content testing can be overlaid with the second step. The connection will link thermal resistance to the rate at which moisture accumulates within a panel. As an example, one could determine the level of thermal resistance of a VIP that had been left in a 30°C, 45% RH room for a year by using the information from steps 1 and 2. The process would start by finding the 30°C table and on it the 45% RH line, where the moisture content for the one year period could be obtained. Once the moisture content is known, Figure 3-2 would be used to know the thermal resistance of the panels at that percentage moisture content. The process could also be used in reverse having a minimum acceptable thermal resistance of the panel in mind one could look up at which percentage moisture content this would occur at and then using the information from the

second step determine how long it would take to reach the minimum level under different climate conditions. The fourth step of the procedure is to develop a mathematical equation that can be used to solve for the lifespan of a panel based on climate conditions found in walls.

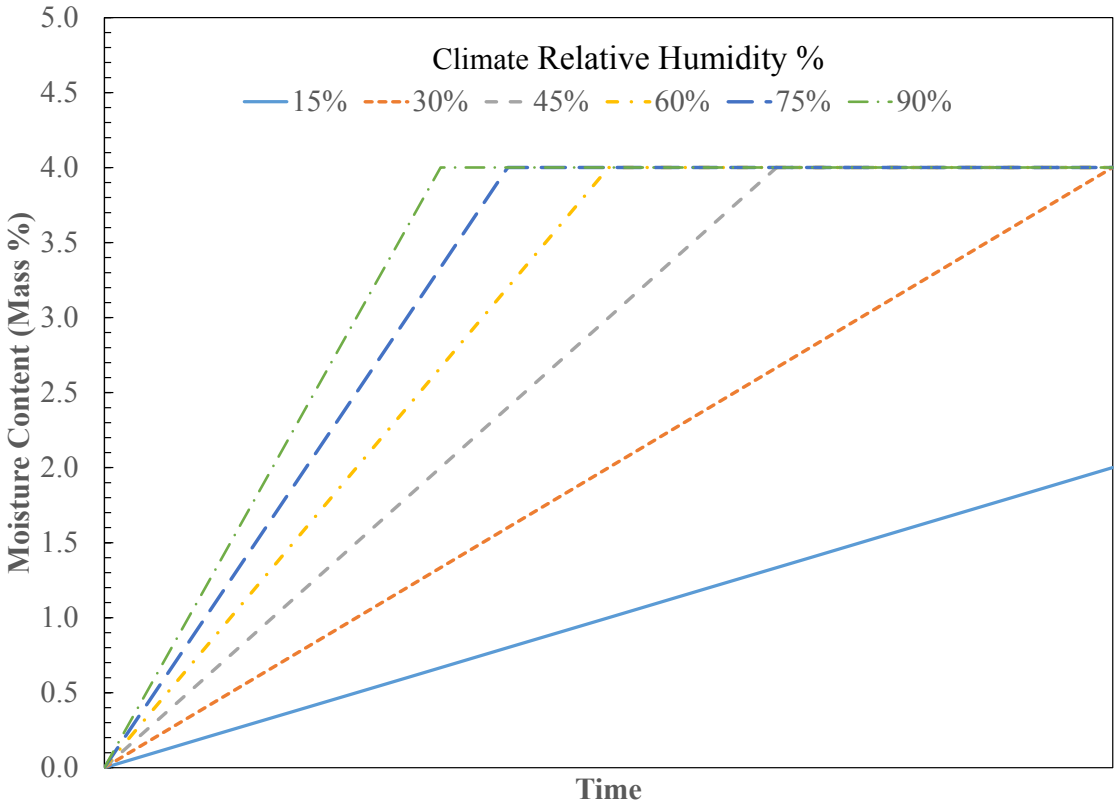

Figure 3-3: Moisture gain at different humidity levels for panels held at lower temperature

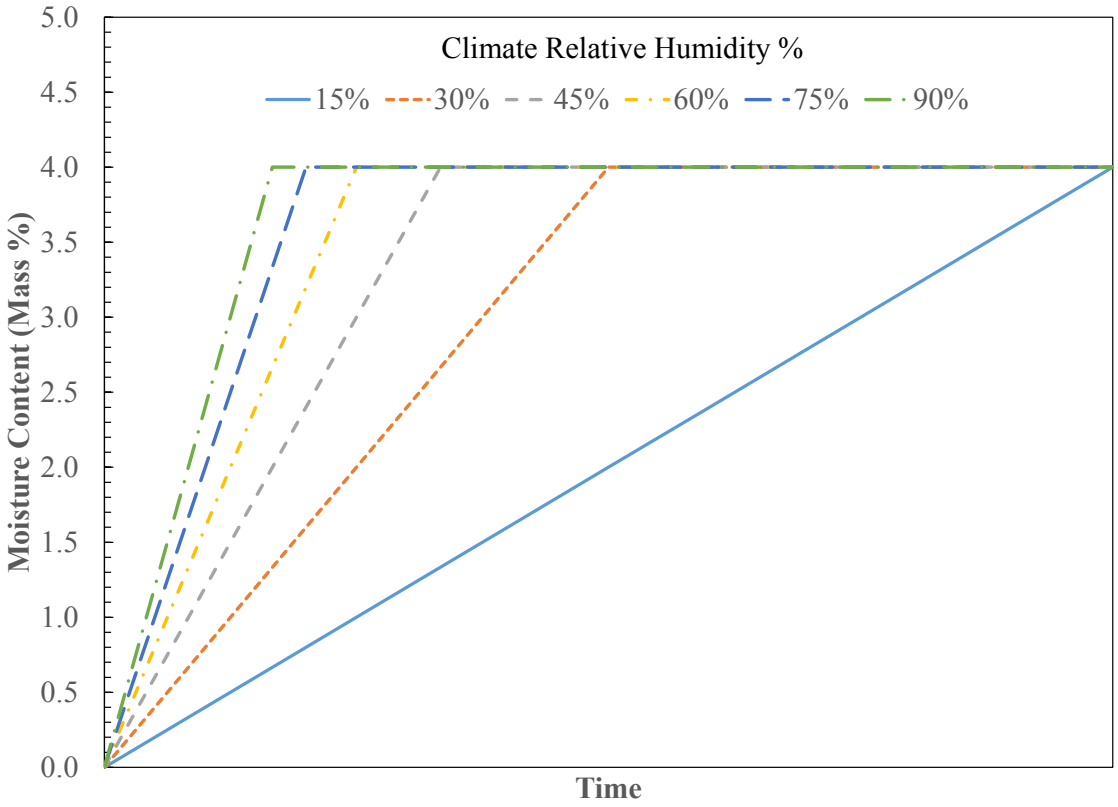

Figure 3-4: Moisture gain at different humidity levels for panels held at higher temperature

3.1.4 Fourth Step – Predicting Panel Degradation

The fourth step of the procedure involves using in-situ or transient data to study the moisture profiles for VIP walls. For this thesis, the in-situ data was collected from an outdoor building envelope test facility located at NRCan's Bells Corners complex in Ottawa. In the long term, it is anticipated that moisture profiles for different climate zones will be available using models. By studying the temperature profiles and surface moisture content next to VIPs within a wall, the amount of time that specific climate conditions are present in the wall can be recorded. By applying the information gained in the third step and using the in-situ date, an estimate can be made regarding the amount of moisture that could accumulate within the panels. For example, in a wall located in southern Ontario, one might expect to see high temperatures and high humidity conditions within wall

assemblies during the summer after wetting periods. By examining the duration of specific temperature and humidity conditions, an estimate can be made on how much moisture has been gained by the panels using step 3. At this point a theoretical thermal performance value for the panels could be determined by relating the expected moisture content back to step 2 which would allow a service life estimate to be made for VIPs integrated into walls located in different climate zones.

3.1.5 Fifth Step – Validation of Results

The fifth and final step of the procedure involves comparing predicted moisture content and thermal resistance to actual moisture gains and thermal resistance results obtained from in-situ testing. The final step would allow for validation and/or calibration of the prediction model.

The scope of this thesis involves step 1 of 5 only. The thesis also provides some discussion on the construction and commissioning of the equipment used to test the thermal resistance of panels through the accelerated ageing procedure.

3.2 Initial VIP Inspection

The vacuum insulation panels used for this work were obtained from two different manufacturers (referred to as PM1 and PM2). The panels from PM1 were obtained in 2011, and although stored safely in a laboratory, they may have experience an unknown level of degradation over time. As such, their change in performance will be quantified from their baseline testing in this thesis. The panels from PM2 were obtained in 2016 and their evaluated thermal resistance should be closer to their manufactured value.

Before any testing on the panels begins, a visual inspection of the panels should be conducted to determine if any of the panels have lost their vacuum. A visual inspection of

the panels cannot quantify the level of vacuum within a panel, however one can tell most of the time if there has been a complete failure of the vacuum or if the vacuum appears intact. A new panel appears stiff and rigid and when fingers are tapped on the surface, the panel sounds crisp compared to panels that have lost their vacuum. Panels which are punctured appear limp, floppy and sounds muffled when tapped. The visual inspection of panels is not an exact process and cannot prevent partially degraded panels from being tested. In a test performed by Kumaran, et al, [26], a panel selected for testing showed no signs of degradation however when the thermal resistance of the panel was calculated it became apparent that the panel had experienced some degradation to its internal vacuum that was not noticeable through visual inspection. A similar occurrence was observed by Conley [37], when evaluating the thermal resistance of a wall section containing VIPs being tested in a guarded hot box (GHB). It was only after thermal images of the wall were taken that it was discovered that one of the panels was not performing at the expected level despite appearing intact during construction of the sample wall section.

Upon selecting panels for testing, the mass of the panel is recorded before proceeding with thermal resistance testing. Obtaining a reference mass for the panels allows for any change of mass to be noted as wetting or drying of the core. Recording the mass of the panels to quantify the amount of moisture accumulating in a panel is a technique that has been successfully used through research [11, 16, 22]. In this thesis, the moisture content of the panels will be used in conjunction with the measured thermal resistance values calculated to quantify ageing and degradation of the panel. A GHP was designed and constructed to accurately measure the thermal resistance of the panels as discussed in Section 3.4.

3.3 Accelerated Ageing Procedure

Given that some panels are constructed differently, and that there are several factors that affect the rate at which moisture transports across a panel's foil, a procedure was developed for this thesis that can be used to test the ageing characteristics of multiple panels. The work conducted will contribute to the on-going efforts in accelerated ageing testing of VIPs.

In order to carry out the first step of the procedure, two pieces of equipment were designed and constructed. The first piece of equipment constructed was the GHP which allows the thermal resistance of insulating materials to be calculated. The second piece of equipment constructed was two climate chambers whereby the VIPs can be stored in an environment with variable temperature and humidity. As discussed earlier, an environment of high temperature and high humidity will increase the moisture content in the VIPs. The aim of the climate chambers is to represent typical environmental conditions found in building envelopes. The specifications of the GHP will be discussed in more detail in the Experimental Setup Section 4 of this thesis. The construction of the climate chambers was completed by a lab colleague, who is continuing the research proposed under this testing procedure to accelerate the ageing of VIP panels.

To complete the first step, two panels from PM1 and PM2 were selected and upon completion of initial panel inspection, the dry thermal resistance of the panels was determined using the GHP testing procedure. The mass of the dry panels was also recorded before the panels from PM1 and PM2 were transferred into the climate chambers. The panels were removed from the chambers at approximate intervals of 30 days to record their mass and evaluate their thermal resistance. During this testing, the temperature and

humidity levels in the climate chambers were set to the same environmental conditions as seen by the VIPs walls constructed at the outdoor building envelope test facility located at Natural Resources Canada (NRCan). Section 3.5 will provide more details about the facility and the in-situ test conditions. Exposing samples to conditions as seen in real applications was a recommendation by Jelle [20] that helps link accelerated ageing to the real life degradation of a product. At the beginning of the experiment, the climate chamber were set to 33℃ with a RH of 90%. These environmental conditions were chosen as they represent the conditions found in an eastern facing wall containing VIPs in the outdoor building envelope facility at NRCan. The in-situ tests revealed that the conditions of 33℃ and RH of 90% results in the highest moisture content therefore these conditions were selected for the climate chamber in order to increase the driving moisture into the panels.. The purpose of this part of the test is not to record the time taken for moisture to transport into the panels but to confirm that moisture would permeate the foils of panels from PM1 and PM2 and subsequently monitor how the panels' thermal resistance performed as moisture content increased. After 30 days in the climate chamber the panels were removed and the mass of the panels was recorded. The aged panels from PM1 and PM2 were then tested for thermal resistance in the GHP to determine how the panels' thermal performance had been affected from the ageing period. The process (i.e., weigh the panels, age the panels, measure the thermal resistance of the panels) was repeated until the panels reached a saturation point where the mass of the panels stops increasing or a point where the panels vacuum fails whichever came first. Results from this test and other accelerated ageing tests were later compared to the results from the in-situ tests at NRCan.

3.4 Thermal Resistance Testing of VIPs Using Guarded Hot Plate

A guarded hot plate allows the thermal resistance of an insulating sample to be tested such that the surface temperatures of the sample can be maintained under conditions seen in real wall sections [32]. ASTM defines the method as absolute as the GHP is a method used for generation of reference standards for calibration of other sensors such as heat flux plates [32]. As outlined in the ASTM standards a GHP apparatus can be configured to operate in a single or double sample setup with the panels either in a horizontal or vertical configuration. For this thesis, the GHP was configured to operate in a double sample configuration with samples held in the vertical orientation. The thermal resistance was calculated as the average thermal resistance of the two samples being tested. Figure 3-5 shows the individual plates of the GHP before the plates were anodized and a secondary guard was placed around the plates. The design and construction of the GHP will be explained in more detail in the Experimental Setup Section 4 of the thesis.

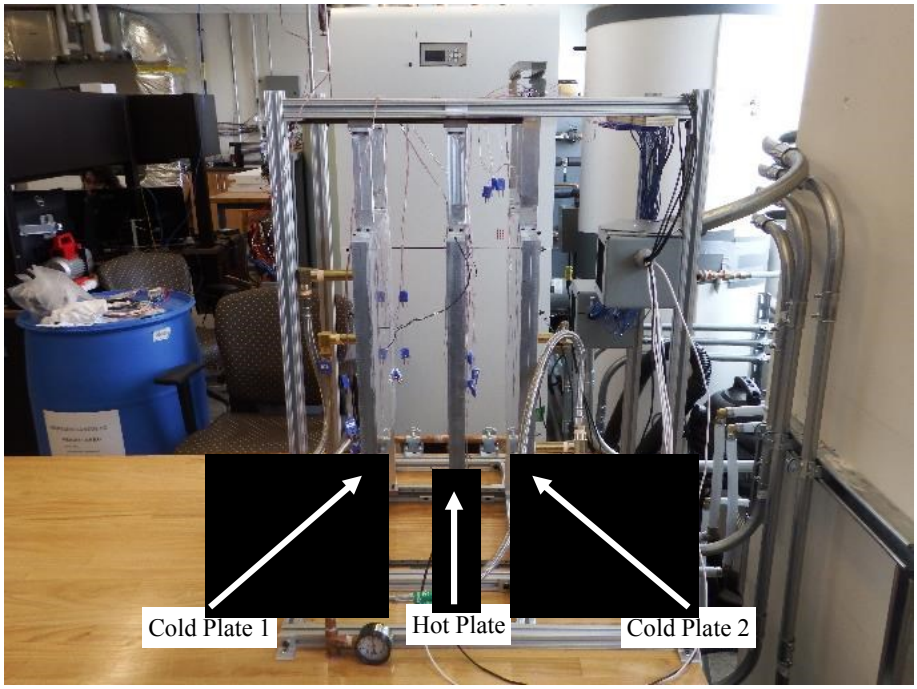

Figure 3-5: GHP before anodizing and secondary guard installation

Two panels were installed in the spaces between the hot and cold plates of the GHP. Samples tested in the GHP can be of different thickness and size. When testing smaller samples, an EPS frame as shown in Figure 3-6 was installed around the sample to ensure coverage of the otherwise exposed heating and cooling surfaces.

Figure 3-6: VIP mounted in EPS frame for GHP testing

The GHP was designed and constructed to allow the plates to slide on linear bearings so that the gap between the hot and cold plates could be adjusted for different sample thicknesses. The insulating samples being tested were held vertically during testing. To ensure that the samples stayed between the plates during testing a lateral force was applied to the plates by clamps. The clamps applied an even pressure across the samples ensuring good contact was made between the surfaces of the samples and the plates of the GHP. To ensure that the amount of clamping pressure was repeatable between tests, marks were scribed into the clamps for each of the samples being tested.

The GHP apparatus was enclosed within a box that could maintain the ambient climate around the GHP. Figure 3-7 shows the secondary guard around the GHP apparatus. The secondary guard held the climate at low humidity levels at the mean temperature of the sample being tested. The secondary guard has a heating element and cooling coils which were used to adjust and maintain the temperature and humidity levels around the GHP. Maintaining a low humidity level around the GHP was used to reduce the amount

of moisture that would otherwise condense on the surface of the cold plate. If moisture did condense in the space between the cold plate and the cold surface of the sample, the contact resistance between the sample and the plate would decrease making the sample appear to have less insulating potential by increasing the rate of energy transfer through the sample.

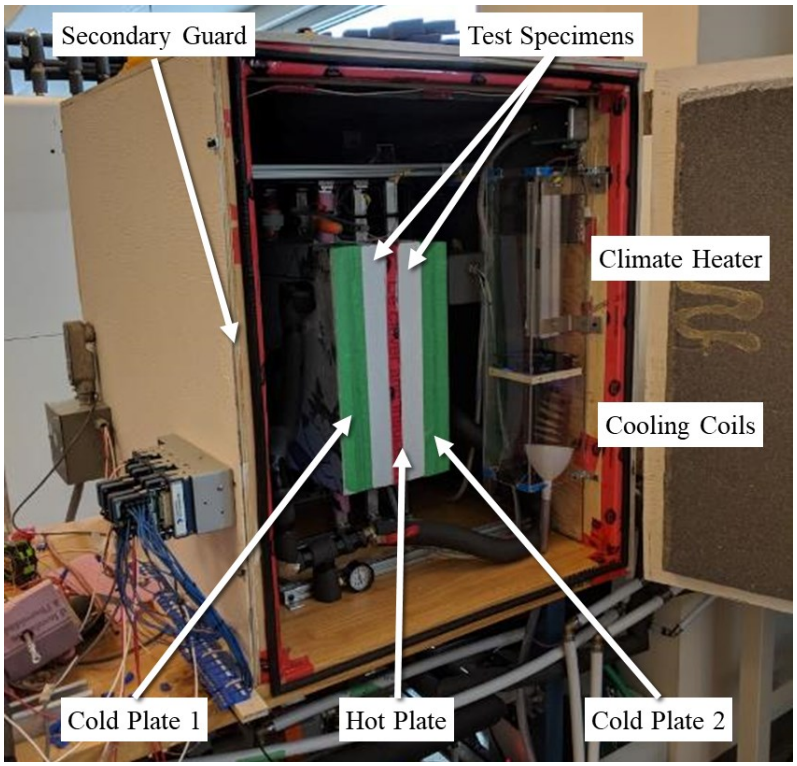

Figure 3-7: GHP with secondary guard for climate control

The operator of the GHP has the ability to control the temperatures of the meter plate, guard ring, cold plates and secondary guard independently. The set point temperatures for the GHP were chosen based on the material being tested and the style of testing being performed. When operating the GHP to calculate the thermal resistance of the VIPs in the accelerated ageing testing, set point temperatures for the hot and cold plates were needed. ASTM standards recommended that when using the GHP approach to evaluate the thermal resistance of samples, the testing conditions should reflect conditions seen in real applications [35]. Based on temperatures expected in walls containing VIPs

the temperature set points in Table 3-1 were considered. The numbers in table Table 3-1 come directly from ASTM standards.

Table 3-1: Initial GHP temperature set points for thermal resistance testing of VIP

Mean Temperature (°C)	Temperature Difference (°C)	
	Small	Large
4	25 ± 5	40 ± 10
10	25 ± 5	40 ± 10
24	25 ± 5	40 ± 10
38	25 ± 5	40 ± 15

A small or large temperature difference across a VIP can affect the uncertainty of the evaluated thermal resistance. Lorenzati, et al, [36] showed that a large temperature difference across a sample would decrease the uncertainty in the calculated results. Bases on these findings a large temperature difference was selected for use in this thesis. Using the conclusions made in their study along with the capabilities of the GHP apparatus, the temperature set point for the GHP thermal resistance testing were refined to the values as seen in Table 3-2.

Table 3-2: GHP temperatures for GHP thermal resistance testing of VIP

Mean Temperature (°C)	Plate Temperatures (°C)		Temperature Difference (°C)
	Hot Plate	Cold Plate	
15	35 ± 0.1	-5 ± 0.1	40 ± 0.2
20	40 ± 0.1	0 ± 0.1	40 ± 0.2
25	45 ± 0.1	5 ± 0.1	40 ± 0.2
30	50 ± 0.1	10 ± 0.1	40 ± 0.2
35	55 ± 0.1	15 ± 0.1	40 ± 0.2

Temperature and power readings were usually taken every minute and averaged over a four-hour period for one averaging period. For each temperature set point, the GHP usually ran five of the four-hour averaging periods. The first four-hour averaging period was taken to allow the sample and the GHP to reach steady state conditions. More details will be presented on this in the Results and Discussion Section 5.1.3. A typical test for

VIPs usually lasts a duration of 100 hours. During this test, five mean temperature set points as indicated in Table 3-2 were tested. In the summer when there is a lot of humidity in the lab the conditioning period before the start of the test may add up to two hours to the beginning of the testing procedure.

Figure 3-8 through Figure 3-11 show a flow chart of the GHP operating procedure. The operator of the GHP starts by inputting initial set point temperatures for the meter plate, guard ring, cold plate, and secondary guard into the LabVIEW program as outlined in Figure 3-8. The operator also specifies the length of duration of averaging period and the number of averaging periods the test will run for Figure 3-10, before starting the test. In Figure 3-8, when the test is started a signal is sent to start a conditioning period for the secondary guard. Once the ambient conditions in the secondary guard are dehumidified the GHP can begin its testing using the first set point. In Figure 3-11 the set point temperatures are then sent to the controls of the plates. As the testing starts a timer starts, and a counter records the number of test completed as shown in Figure 3-10. The first set point for the GHP is tested according to the number of averaging periods for that set point, with each averaging period lasting for a specified time. Figure 3-10 shows how the GHP cycles to the next set point after the number of averaging periods for that set point have been conducted and the GHP continues this pattern until all set points have been tested. Figure 3-9 shows that during testing, continuous monitoring of the secondary guard takes place to maintain a dry environment at the temperature of the sample being tested.

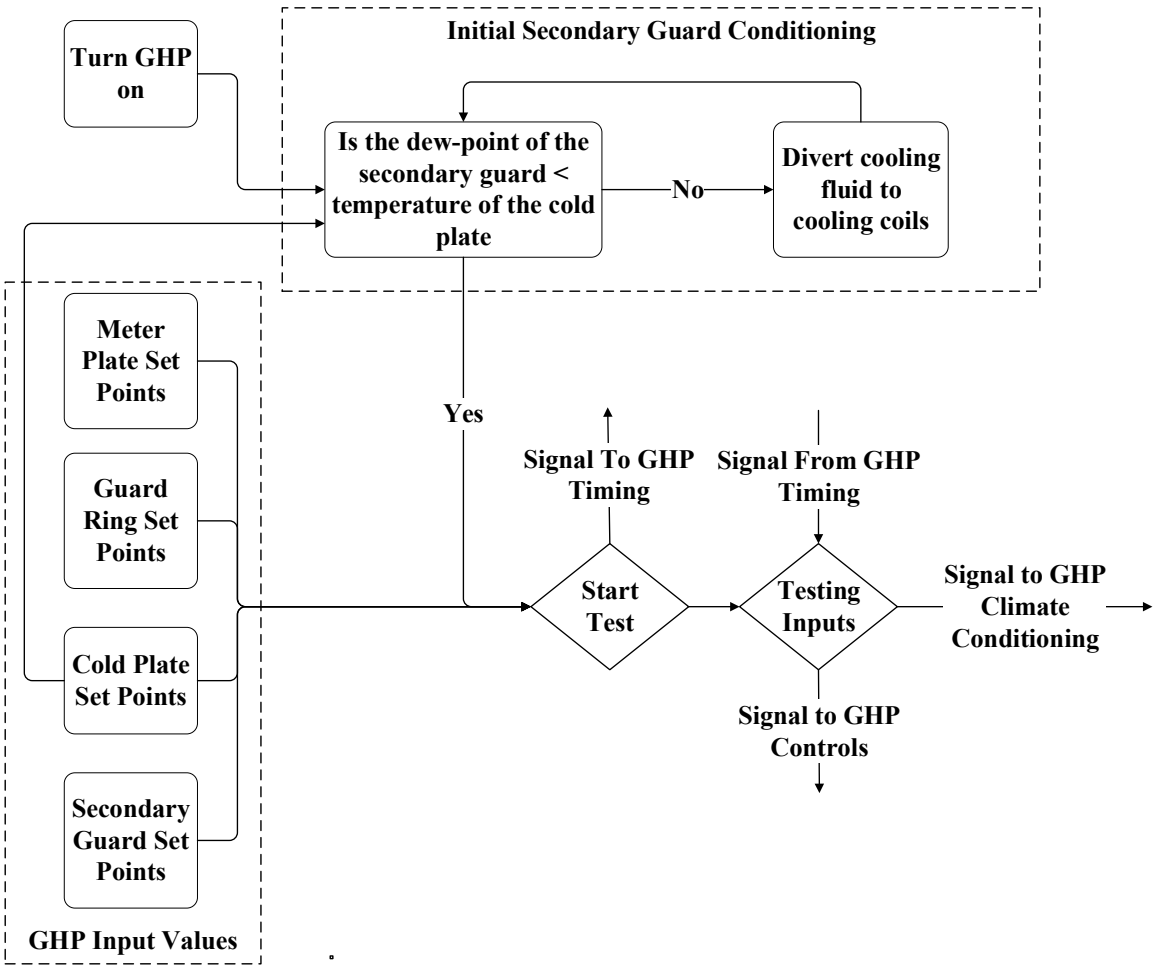

Figure 3-8: GHP start up procedure with input values and initial conditioning of secondary guard

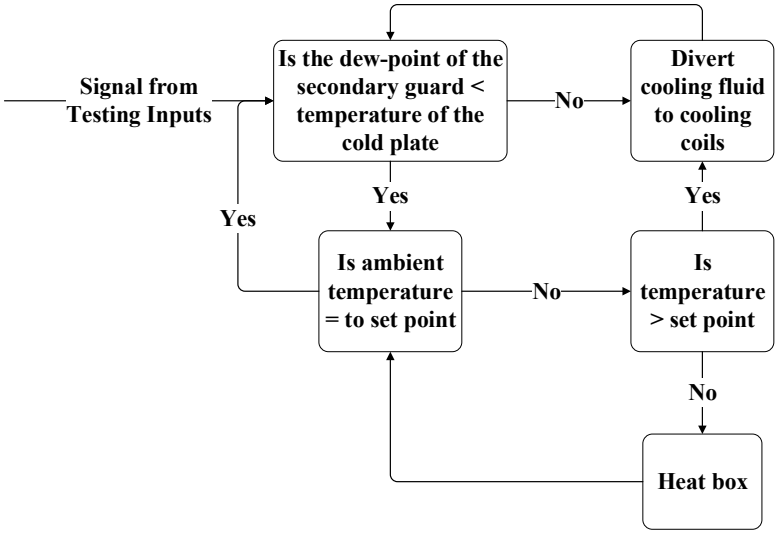

Figure 3-9: GHP continuous conditioning of secondary guard

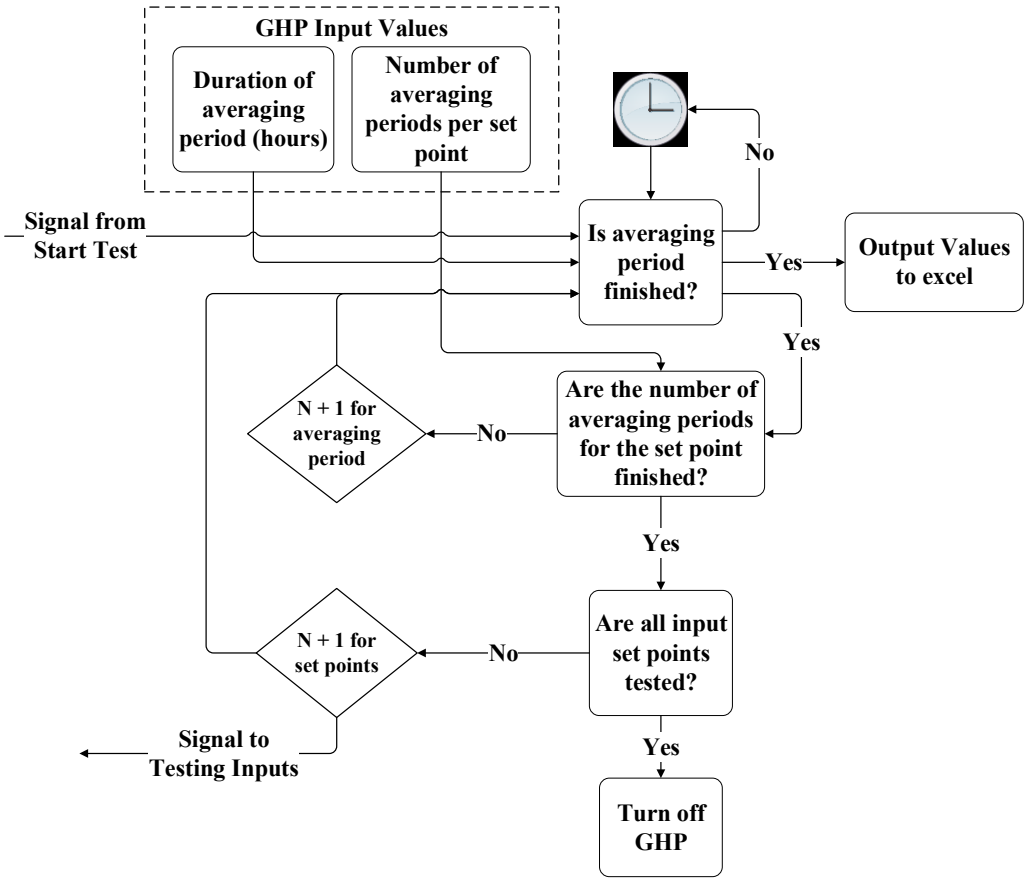

Figure 3-10: GHP timing and set point controls

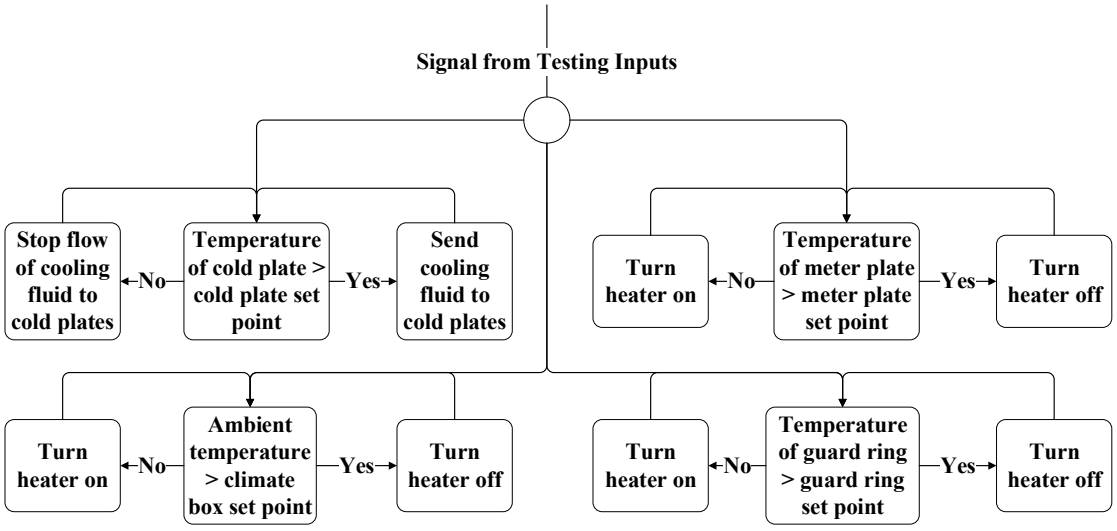

Figure 3-11: GHP controls to maintain plate temperatures and ambient climate

3.5 In-Situ Testing of VIPs

The In-situ component of the new accelerated ageing procedure required a longer time commitment. Work was started on in-situ testing of VIPs in order to validate the newly developed VIP ageing model. In-situ testing will provide a comparison to real life degradation of panels has to be performed. As manufacturers of VIPs and builders are aiming for service lives of approximately 30 years or greater, the rate at which VIPs may degrade in the real applications may be very slow. As this could be the case, one of the first tasks completed was to install panels into a wall section at an outdoor building envelope testing facility, increasing the length of time these panels will be exposed to everyday conditions. Figure 3-12 shows the building envelope testing facility known as the CanmetENERGY Building Envelope Test Hut (CE-BETH) which is located at NRCan's CanmetENERGY-Ottawa's testing facility. NRCan's test hut is capable of testing full wall sections and therefore was used to study the sample walls under in-situ conditions.

Figure 3-12: CanmetENERGY Building Envelope Test Hut (CE-BETH) facility at Canmet NRCan

The interior of CE-BETH is maintained at temperature and humidity levels found in residential homes while the outer surface is exposed to the elements [38]. The internal pressure of the facility is allowed to fluctuate with ambient conditions as the facility is not completely air tight. CE-BETH is a facility designed and built specifically for in-situ testing of building envelopes. The facility is constructed from a shipping container, where three 2.44 m by 2.44 m holes have been cut out of one face to accommodate sample wall sections to be tested. Two of the 2.44 m by 2.44 m openings were allotted for the testing in this thesis. The first 2.44 m by 2.44 m bay was constructed to resemble a wall built to 1960's codes with 2 by 4 studs which has been retrofitted to meet current building standards by adding additional insulation to the exterior of the wall. The 1960's wall was built in two 2.44 m by 1.22 m sections with one section insulated with additional EPS while the other 2.44 m by 1.22 m section was insulated with a composite EPS and VIP layer. Testing a wall built to 1960's standards with and without VIPs provided an opportunity to test how VIPs would perform under a retrofit scenario. The 1960's building standards were selected as there are a large number of older homes within Canada that need to be updated to meet higher insulating standards. The second 2.44 m by 2.44 m wall was constructed to current building standards with 2 by 6 studs. The second wall was also divided into two 2.44 m by 1.22 m sections. The first 2.44 m by 1.22 m section of the new wall was built without VIPs to compare to the second 2.44 m by 1.22 m section that was insulated to a level above current standards using VIPs. The aim of the in-situ testing was to collect hygrothermal data in order to determine how much moisture will be in contact with the panels in a wall section and subsequently how much moisture has accumulated in the VIPs after a specified time frame under normal operation. In order to study the conditions around the VIPs,

instrumentation to measure the temperature, humidity and thermal conductivity on both the hot and cold surfaces of the VIPs were installed throughout the walls. The information gained has shown and will continue to show how moisture accumulates into the wall and under what conditions. The information will be used to develop accelerated ageing conditions and set points for testing VIPs. Developing test conditions that are experienced in real life is important for accelerated testing so that the testing performed can be related back to real time degradation [20]. The four construction styles offer a unique opportunity to monitor the temperature and humidity conditions within different wall types and is the focus in the work done by Conley, et al, [38]. Before the VIPs were installed into the walls, they were numbered and their dry or initial mass was recorded as a baseline weight of the testing. Future work will involve making predictions on the amount of moisture that may have transferred into the panels based on the observed moisture and humidity conditions seen next to the panels.

The wall sections containing VIPs are scheduled to be left in place for a minimum of two years upon which the panels will be removed from the assemblies, and only then will the final results of this testing be known as explained in

Future Work Section 6.2. After removing the VIP from the wall, the mass of the panels will be compared to the dry mass to see if any moisture accumulated within the panels over the time spent in the wall. The thermal resistance of the aged panels will then be tested to compare to the mass and thermal resistance to predictions made. The comparison of the two processes is an important step as it will either validate the predictive approach or be used to calibrate the predictive model. A two year period should allow the panels to degrade and a trend to be identified. The tests were permitted to run for a two

year period at NRCan however, if a longer period could have been secured more pronounced results would have been expected. A similar approach was taken by Schwab et al. [16], where a model was set up to determine the level of degradation a VIP might achieve under normal operations based off of testing conducted in the lab. They were able to validate and calibrate their predictive model based on panel degradation found in VIPs installed in German buildings.

3.6 Thermal Resistance Testing of VIPs Using the Guarded Hot Box

The Guarded Hot Plate apparatus was used for this work as the primary means of testing panel performance. However, to obtain a baseline performance value for dry VIPs in this study, the thermal resistance testing over a large range of temperatures was desired. Due to temperature restrictions of the chiller supplying cooling fluid to the cold plates of the GHP, the mean sample temperatures tested were limited to the range of 15 – 35°C. In order to study how the dry panels performed at lower mean temperatures, the samples were tested in the GHB. Using the GHB allowed for testing of mean sample temperatures as low as -10°C. The GHB is normally used to test full wall assemblies for thermal performance, and works in a similar manner to the GHP. The GHB is constructed with one warm and one cold side that maintain ambient set points on either side of a wall sample. Just like the GHP, the GHB warm side combines a meter section and a guard section to ensure no energy escapes the meter section. Figure 3-13 shows an XPS frame structure constructed to hold the VIP in place while being tested in the GHB, as the GHB normally tests full wall sections and not loose VIPs. The XPS frame was also used to hold the instrumentation needed to calculate the thermal resistance of the VIP. To determine the thermal resistance of the panels, Fourier's law is used. The heat flux sensors are used to

calculate the amount of power flowing through a known area with the thermocouples allowing the temperature difference across the sample to be known.

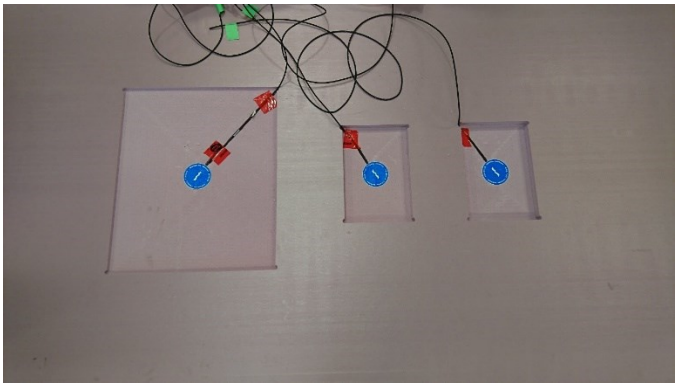

Figure 3-13: Machined pockets to mount VIPs with heat flux sensors installed

In this chapter the details of the accelerated ageing procedure were discussed as well as a description of the equipment used to age and evaluate the degradation of the panels. The next chapter will discuss the design and construction of the equipment used in this thesis and how the accelerated ageing procedure influenced the design of the equipment.

4 Chapter: Experimental Setup

In this section of the thesis a detailed description of the equipment used to evaluate the thermal resistance of the insulation tested in this study will be presented. Chapter 4 provides a system overview of the components that make up the GHP, followed by a detailed description of the hot plate, cold plates, the secondary guard and finally the instrumentation used on the GHP.

4.1 GHP System Overview

As stated earlier, the objective of this study was to develop a technique to accelerate the ageing of VIPs, and in doing so use thermal resistance as the metric to quantify performance degradation. To determine how the insulating performance of VIPs change over time, one must be able to quantify the thermal performance of the panels. The method chosen in this study was to evaluate the thermal resistance of the VIP panels by way of the GHP method as defined in ASTM standard C177 [32]. As outlined in the ASTM standard, there are several configurations for how the GHP could have been constructed, whether it is to be used in a single or double sample configuration and if the GHP is to be operated in the horizontal or vertical orientaiton. The double sample configuration was selected as VIPs are highly insulating material and if only one sample was being tested, it could not be guaranteed that there would be enough insulation on the other side of the hot surface to prevent energy from flowing through it as opposed to the VIP that was being tested. Any energy being lost to the surroundings would lead to an artificially low thermal resistance calculation of the sample being tested and as such the two sided configuration was selected for testing the high thermal resistance of the VIPs. The vertical orientation for the GHP was selected as the VIPs being tested would be compared to VIPs istalled in the same

orientaion in building envelopes. As discussed earlier, the GHP is comprised of a heating plate assembly and two cold plates that support the two insulating samples being tested. Figure 3-7 shows how the two insulating samples were supported between the heater plate and the two cold plates.

During operation a thermal gradient was developed between the hot and cold plates through the insulating sample. By recording the amount of energy needed to maintain the temperature of the hot plate, and the thickness of the sample, Fourier's law can be used to calculate the thermal resistance of the material. Fourier's Law links the rate at which thermal energy q_{x}, transfers through a material to the cross sectional area A, thickness L, thermal conductivity k and the temperature gradient across the sample as seen in Equation (4.1). In Equation (4.1), T_1 and T_2 are the temperatures of the hot and cold plates measured in Kelvin respectively.

$$q_{\mathrm{x}} = \frac{kA}{L}(T_1 - T_2) \tag{4.1}$$

A more detailed layout of the GHP and supporting equipment is shown in Figure 4-1. The hot plate assembly was comprised of two components being the meter plate and the guard ring, which were separated by an insulating air gap. Figure 4-1 shows the hot plate assembly and the embedded heating elements within both the meter plate and guard ring. The cooling plates were supplied with cooling fluid from a closed supply loop which gained its cooling potential from a heat exchanger and a lab supply line. The heat exchanger allowed the cold plates to operate at a range of temperatures independently from constant temperature of the lab supply line. As shown in both Figure 3-7and Figure 4-1 the hot plate and cold plates were held within an enclosure known as the secondary guard. The secondary guard was used to maintain the ambient conditions around the plates, to

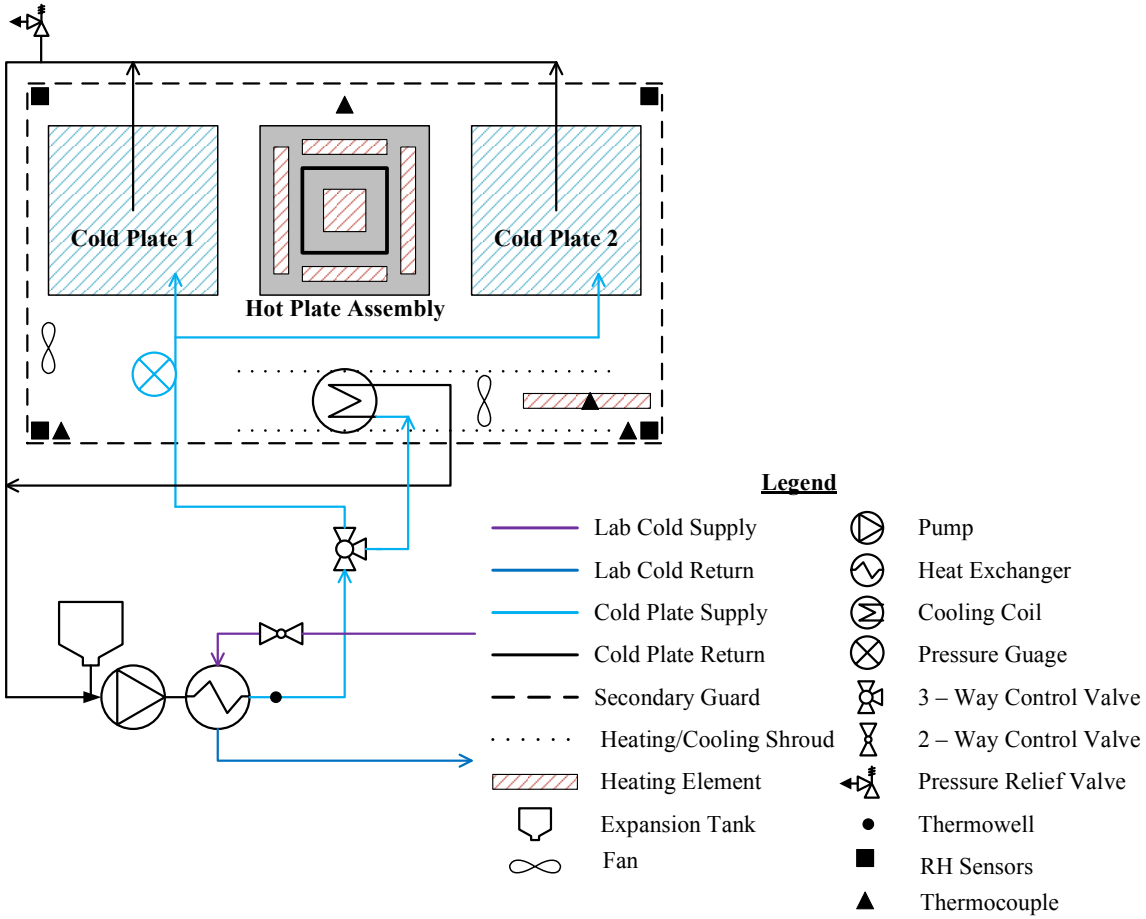

Figure 4-1: System overview for GHP assembly

prevent condensation on the cold plates and to reduce energy loss from the sample during testing. In order to maintain the ambient conditions, the secondary guard was outfitted with a heating element and cooling coil.

4.2 Hot Plate Assembly

Figure 4-2 shows a rendering of the hot plate assembly of the GHP, which consisted of a meter plate, air gap, guard ring and embedded electrical resistance heaters.

In evaluating the thermal resistance of any insulating material, an accurate account of the energy used to maintain the surface temperature of the meter plate during steady state testing was needed. As such the design of the GHP revolved around the meter plate and the steps taken to reduce its energy loss. The meter plate was surrounded by the guard

ring with an insulating air gap between the two plates. The air gap was used as a physical divide between the surfaces of the meter plate and guard ring to prevent conductive energy transfer from the meter plate. When the temperature of the guard ring matches the temperature of the meter plate, there is no energy loss from the meter plate to the guard ring. With this understanding all the energy must travel into the insulating samples being tested along the thermal gradient between hot and cold surface. As there is no standard blueprint for constructing a GHP, a custom GHP was designed and built using ASTM guidelines, to be used for the thermal resistance testing in this thesis.

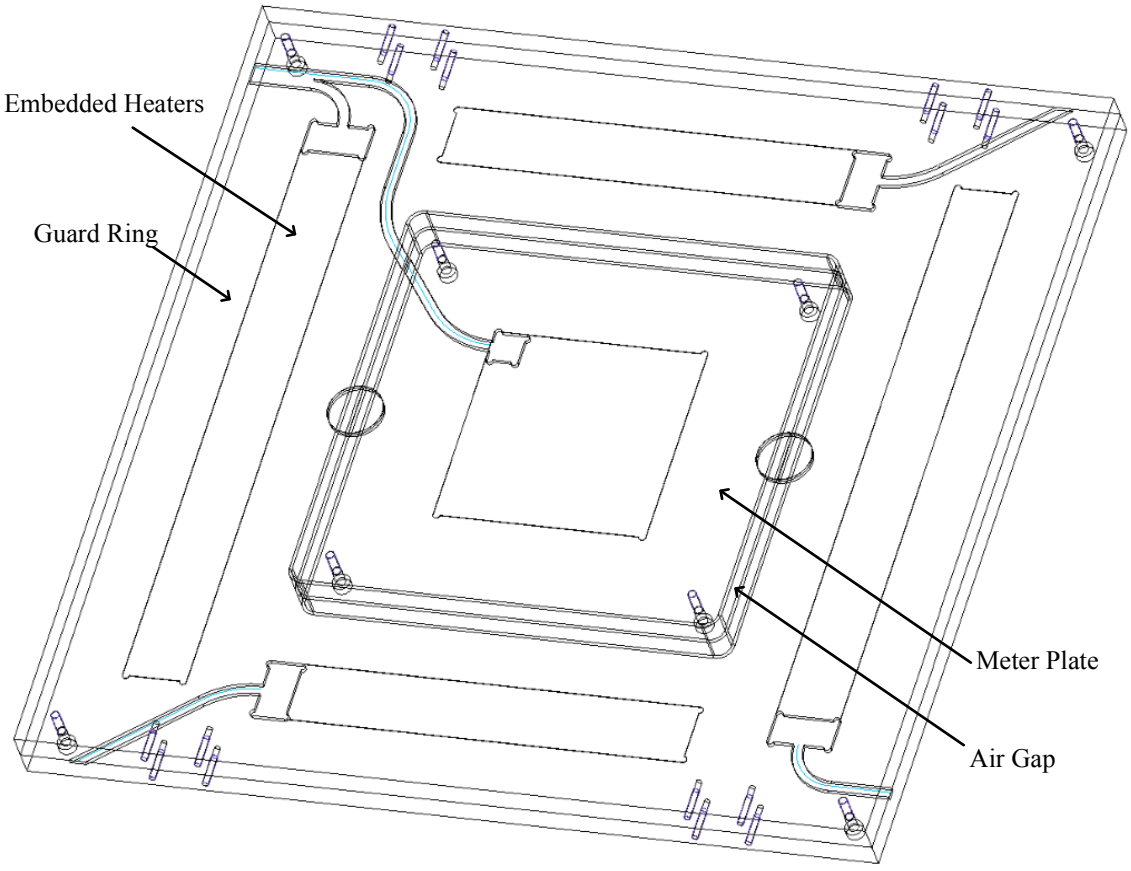

Figure 4-2: Wireframe view of hot plate assembly

Design of the GHP began with the meter plate which was designed to be as large as it possible for the samples being tested. Having a meter plate as close to the sample size as possible allows the evaluated thermal resistance to be representative of true material

characteristics. As materials such as EPS and XPS can be cut to size and VIPs cannot, the design of the GHP focused on the VIPs being tested. As the VIPs being tested in this thesis were of two different sizes the meter plate was limited to the size of the smallest panel which is just under 203 mm in width. Although the panels being tested are rectangular and the size of the meter plate could have been bigger if it were rectangular, the meter plate was designed as a 200 mm square to allow for testing of panels in both the horizontal or vertical orientation. Testing in both orientations would determine if orientation of a VIP in a wall has any effect on panel performance. The meter plate and the matching guard ring have rounded corners as opposed to square, to accommodate machining capabilities which prevented square corners being cut out of the guard ring. To ensure that the surfaces of the hot plates have a uniform emittance the plates were anodized black allowing the plates to emit energy closer to that of a blackbody which is important to ensure that all the energy that enters into the meter plate exits into the sample being tested. Detailed working drawings of the guarded hot plate assembly can be found in Appendix A

Working outward from the meter plate the air gap was designed to meet ASTM C-177 6.4 requirements. Having an air gap too wide could allow for convective currents to form inside the space, transferring energy from the meter plate. ASTM recommends that the area of the gap in the same plane as the surface of the meter plate is to be no more than 5% of the area of the meter plate. In addition to the size of the gap, additional efforts to reduce the chances of convective loops forming, ASTM recommends lightly packing the gap with fibrous insulation. For this set-up, rockwool insulation was used. As mentioned, the plates of the GHP were anodized black to increase their emittance, however as the anodizing process cannot be limited to specific surfaces, the sides of the

meter plate were also anodized. Having the sides of the meter plate and guard ring that face the air gap anodized black was undesirable in preventing energy transfer from the meter plate and as such reflective aluminum tape was added to the sides of the meter plate and guard ring to reduce their emittance and increase their reflectance. Figure 4-3 shows the inner face of the air gap with the aluminum tape adhered to it. With all the measures taken to reduce the energy loss across the air gap and to maintain the plate temperatures of the meter plate and guard ring the same, an average temperature difference of less than 0.1°C was maintained across the gap, which was within the limit specified within the ASTM standards (i.e., not more than 0.2°C).

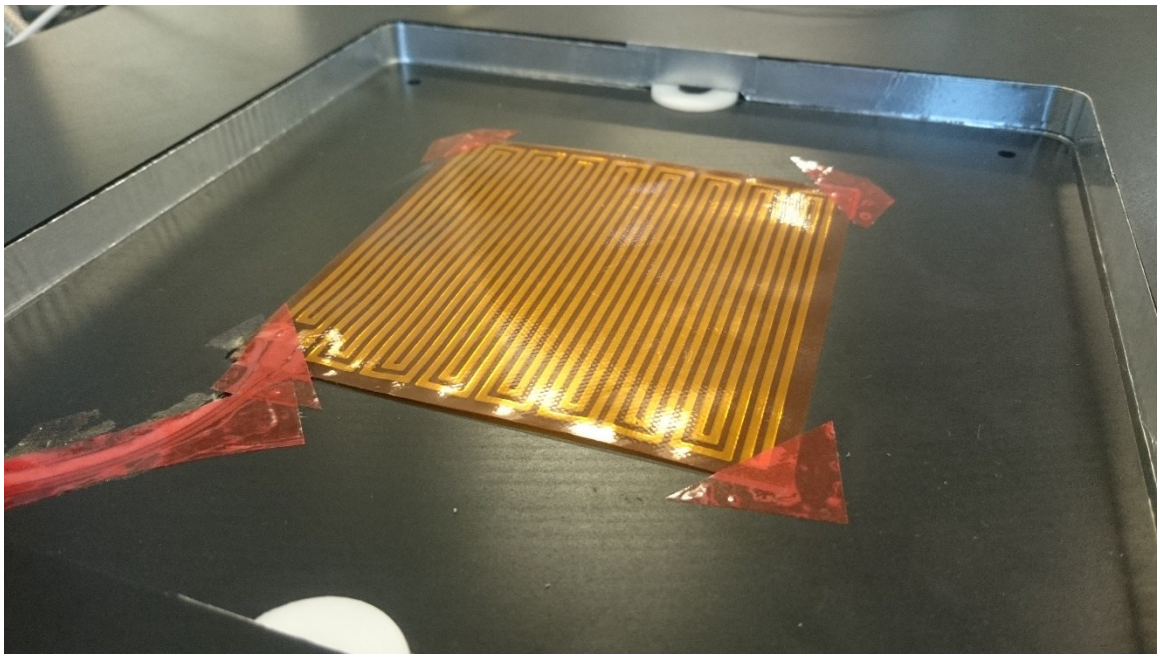

Figure 4-3: Meter plate and guard ring after anodizing with reflective aluminum tape and embedded meter plate heater

The guard ring surrounded the meter plate and was designed to prevent energy loss from the meter plate to the environment. By maintaining the guard ring at the same temperature as the meter plate, no thermal gradient between the plates existed and as such no energy transferred from one to another. The specifications for the size of the guard ring

is outlined in ASTM standards to be half the linear dimension of the meter plate in order to reduce the edge heat loss to acceptable levels. Four electric resistance heaters embedded within the guard ring worked independently of one another to maintain a constant surface temperature around the guard ring. It was important to maintain a constant surface temperature of the guard ring in order to reduce the energy loss from the meter plate. Figure 3-7 shows how EPS insulation was used to frame the guard ring, insulating the guard ring from the ambient environment.

4.3 Cold Plate Assembly

Figure 3-7 and Figure 4-1 both show how the GHP assembly makes use of two cooling surfaces installed on either side of the heating plate. The cooling plates in the GHP setup act as thermal sinks of a uniform surface temperature, maintained by cooling fluid being circulated through internal channels within the plates. Using cooling fluid to cool the plates was chosen as the set-up had access to a circulated glycol line maintained at -10°C. The cold plate assemblies were comprised of two aluminum tooling plates bolted together. Figure 4-4 shows one of the aluminum plates with the cooling channels machined into its face. The plate with the channels was then paired with a non-machined plate, forming internal tubing. An O-Ring was used to ensure fluid remained contained within the closed loop.

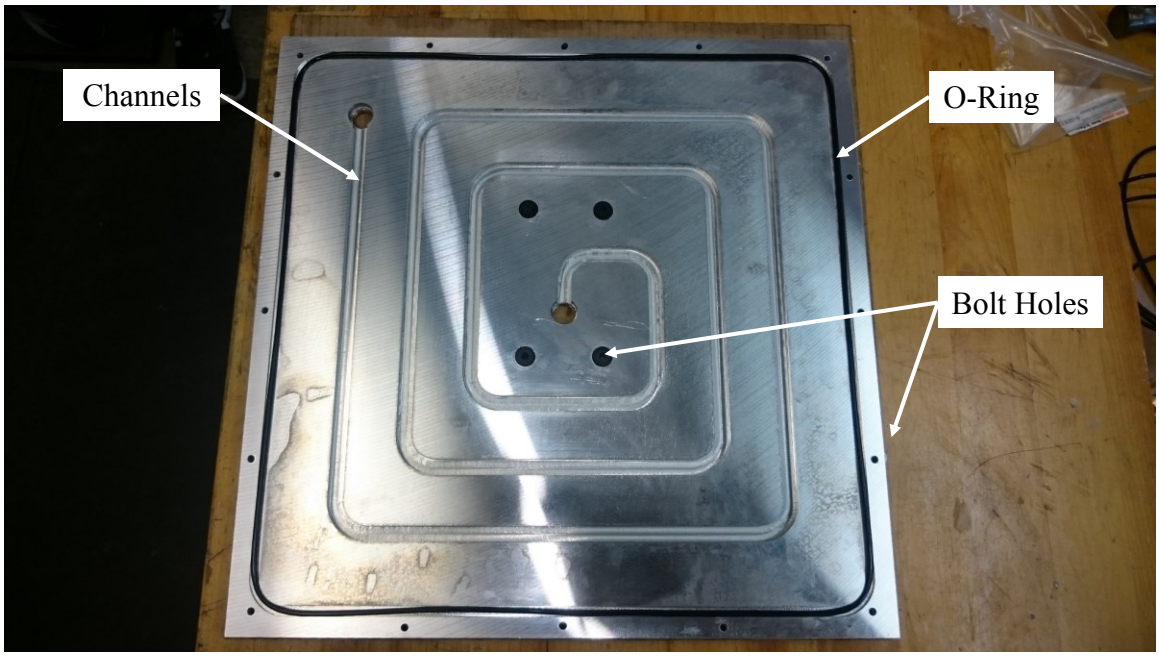

Figure 4-4: Plate with channels cut into it to form internal channels when combined with flat plate

The fluid that circulates through the internal channels removed heat from the plate's surface, cooling the plate to the desired set point temperature. The internal tubing was cut as a serpentine shape spiraling in from the outer edge of the plate to the center. The fluid entered the plates from the outside edge and travelled to the center of the plate. The pattern for the channels was based on layouts used in radiant floor heating, where the perimeter of a room that has all exterior walls is heated before the center of the floor. In this configuration for the radiant floors, some heat is lost to the exterior environment, however the floor remains at a more uniform temperature [39] with the same being true for cold plates where some heat is gained from the exterior edges.

In the design of the cold plates the force that the cooling fluid would exert on the plates needed to be taken into consideration to ensure that the aluminum plates of the cold plate assembly would separate during testing. Determining that the plates would experience a deflection of 0.5 mm, 4 bolts were designed at the center of the plates to give

the system a total safety factor of 63. The calculations for the deflection of the plates can be found in Appendix B .

The cooling fluid used in the cooling loop of the GHP is a 30/70 glycol/water by volume solution, which has a higher viscosity then water and becomes more viscous as the temperature of the liquid decreases [40]. The cooling plates underwent the same black anodizing process as the hot plates with the objective of increasing the surface emissivity. However the decision to anodize the cold plates was also made to protect the aluminum plates from oxidizing and pitting during operation. Figure 4-1 shows how the two cold plate assemblies were connected in parallel to one another, which ensures that the same temperature fluid flowed through both plates. The temperature difference between the two plates did not exceeded 0.2℃ of each other suggesting that the plates are evenly balanced. Once a desired set point temperature was selected for the GHP cooling loop a combination of a thermowell, heat exchanger and proportional control valve as shown in Figure 4-1, were used to monitor, cool and maintain the desired set point fluid temperature. The thermowell was used to monitor the cooling fluid temperature circulating through the GHP loop. A proportional integral control loop reads in the signals sent from the thermowell and controlled a proportional control valve, which varied the supply of cooling fluid into the GHP heat exchanger in order to maintain the desired set point temperature.

As there was almost a meter of pipe after the thermowell and before the cold plates, the cooling fluid gained some energy from the surrounding ambient air in the laboratory despite best efforts to insulate the pipes. To mitigate the effects of the observed rise in temperature of the fluid before reaching the cold plates, a test to develop a correction factor was conducted. A test was set-up where desired cold plate set point temperatures as

indicated in Table 4-1, were input into control program for the GHP and the observed plate temperatures recorded.

Table 4-1: Set points to determine cold plate temperature corrections

Set Point Number	Desired Cold Plate Temperatures (℃)	Actual Cold Plate Temperatures (℃)
1	15.00	15.75
2	10.00	11.29
3	5.00	6.75
4	0.00	2.29

A linear equation was created for both the desired Equation (4.2) and actual Equation (4.3) cold plate temperatures where y_1 and y_2 were the desired and actual plate temperatures.

$$y_1 = -5z_1 + 20 \tag{4.2}$$

$$y_2 = -4.4887z_2 + 20.245 \tag{4.3}$$

Rearranging Equation (4.2) to solve for z_1, and subbing $z_1$into Equation (4.3) in place of z_2 the actual plate temperature value y_2 is given in terms of the desired set point temperature as indicated in Equation (4.4).

$$y_2 = 0.8977y_1 + 2.0452 \tag{4.4}$$

where the difference ΔT in temperatures can then be written as indicated as seen in Equation (4.5).

$$\Delta T = y_2 - y_1 \tag{4.5}$$

Upon completion of the test, a correction factor was developed from the difference in desired temperatures to observed plate temperature and implemented into LabVIEW. The correction factor calls for colder water at the thermowell to make up for the temperature rise along the pipes, allowing the desired set point plate temperature fluid to

actually reach the cold plates. Using the calculated temperature difference cooling fluid is required T_{Req} at the desired temperature minus the difference as given in Equation (4.6).

$$T_{\mathrm{Req}} = y_1 - \Delta T \tag{4.6}$$

Figure 3-7 shows how the cold plate assemblies were each insulated with an EPS backing, to help maintain a uniform plate temperature during testing and reduce condensation forming on the plates and to maintain a constant plate temperature through testing. Even with the EPS backing on the cold plates, ASTM standard C177 Section 6.1 suggests that a climate controlled secondary guard be built around the GHP apparatus to prevent condensation from occurring on the plates.

4.4 Secondary Guard

The purpose of having a secondary guard is to prevent condensation on the cold plates and to reduce the amount of heat loss from the samples being tested by maintaining a dry environment at the mean sample temperature. In this section the construction and equipment used in the secondary guard will be described.

The secondary guard was an insulated box built around the GHP assembly which had two access doors to load samples into the GHP. The secondary guard was insulated with 0.038 m of EPS and outfitted with a heating and cooling capacity to maintain ambient temperature. A vapour barrier sealed the envelope of the secondary guard while weather stripping sealed the openings, preventing moisture from infiltrating the dehumidified space. Two fans were used to circulate air within the secondary guard, ensuring the air was at a uniform temperature throughout the space. One of the fans in the GHP drew air across the cooling coils and forces air across the heater to condition the ambient air while the second was used to mix the air, preventing stratification from forming. As outlined in

the Experimental Procedure Section 3.4 of the thesis the ambient conditions within the secondary guard were determined before and during testing to monitor the temperature and humidity within the space. Four hygrometers and three thermocouples were distributed around the secondary guard to measure the humidity and temperature to calculate the dew-point within the space and determine if the space requires dehumidification.

The dew-point temperature is the saturation temperature corresponding to partial pressure of water vapour. When moist air is cooled to this temperature, the air can no longer retain any additional water, and the air is at an equilibrium point where water enters the air at the same rate that it condenses out of it [41]. If the air is cooled to a lower temperatures then moisture only condenses out of the air and dehumidifies the air. When determining if the secondary guard required dehumidification, a comparison was made between the dew-point of the ambient air and the current cold plate temperature. If the current cold plate temperature was lower or equal to the dew-point of the air in the secondary guard, condensation would form on the surface of the cold plates.

The flow chart in Figure 3-8 outlines the process used to eliminate conditions where condensation could form on the cold plates, where a conditioning period of the secondary guard was conducted before the GHP turned on. In the conditioning period, four hygrometers and three thermocouples measured the humidity and temperature to calculate the dew-point within the space. A comparison was made to the dew-point temperature that would result from the coldest plate temperature and if the current dew-point in the box was greater than that of the plate surface temperature, cooling fluid was diverted through coiling coils in the secondary guard. Cooling fluid, at a temperature that was lower than the surface temperature of the cold plates was diverted through the cooling coils, causing condensation

to form on the cooling coils, which reduces the dew-point within the secondary guard. Cooling fluid was allowed to flow until the dew-point within the guard dropped below the set-point of the cold plate. Removing the moisture reduced the possibility that moisture would accumulate on the cold plates and skew the test results. A flow chart of the starting procedure for the GHP is shown in Figure 3-8 where the set point inputs can be seen on the left with the initial conditioning procedure outlined at the start of the sequence. Monitoring the level of humidity within the climate box continued throughout the testing period and whenever humidity levels were too great cooling fluid was diverted by the 3-way valve to the exposed copper cooling coils installed in the secondary guard. Figure 3-7 outlines the logic used in the dehumidification process. The coils within in the secondary guard provided a surface for the moisture to condense on. The coils were coated with a water repellant coating so that the condensing water dripped off the coils into a funnel that drained from the secondary guard. Moisture was extracted from the air within the secondary guard until the dew-point of the air reached a point that was lower than that of the plate temperature, and at which point the 3-way valve diverted flow back to the cooling plates. The ambient temperature was also monitored during the conditioning loop and if heating or cooling was needed the secondary guard reacted accordingly.

The process used for determining the dew-point temperature was adapted from the ASHRAE handbook fundamentals [41]. The first step in calculating the dew-point temperature of the air in the secondary guard is to calculate the saturation pressure p_{ws} of the water vapour of the air measured in Pa, at the temperature T measured in Kelvin in the secondary guard using Equation (4.7).

$$\ln(p_{\mathrm{ws}}) = C_8/T + C_9 + C_{10}T + C_{11}T^2 + C_{12}T^3 + C_{13}\ln T \qquad \textbf{(4.7)}$$

where p_{ws} is the saturation pressure of water vapour measured in Pascals.

The average temperature of the secondary guard was determined from the four thermocouples in the secondary guard. The variables for Equation (4.7) are listed in Table 4-2.

Table 4-2: Variables for Equation (4.7)

Variable	Value
C_8	-5.8002206 x 10^3
C_9	1.3914993
C_{10}	-4.8640239 x 10^{-2}
C_{11}	4.176478 x 10^{-5}
C_{12}	-1.4452093 x 10^{-8}
C_{13}	6.5459673

After the saturation pressure was calculated the water vapour partial pressure p_w could be calculated by rearranging Equation (4.8) where ϕ is the relative humidity of the air within the secondary guard in decimal format.

$$\phi = \frac{p_w}{p_{ws}}\Big]_{t,p} \tag{4.8}$$

After calculating the partial pressure of water vapour, the dew-point temperature could be calculated using both Equations (4.9) and (4.10). As Equations (4.9) and (4.10) use the water vapour partial pressure in kPa the value obtained for the water vapour partial pressure from Equation (4.8) was converted. If the calculated dew-point values from both Equation (4.9) and (4.10) were greater than or equal to 0°C the dew-point value generated from Equation (4.9) was used, else the calculated dew-point temperature from Equation (4.10) was used.

Between dew-points of 0 and 93°C

$$t_d = C_{14} + C_{15}\alpha + C_{16}\alpha^2 + C_{17}\alpha^3 + C_{18}(p_w)^{0.1984} \tag{4.9}$$

For dew-points below 0°C

$$t_{\mathrm{d}} = 6.09 + 12.608\alpha + 0.4959\alpha^2 \quad \textbf{(4.10)}$$

where t_{d} is the dew-point temperature measured in degrees Celsius, $\alpha = \ln(p_{\mathrm{w}})$ and p_{w} is the water vapour partial pressure measured in kPa. The variables for Equation (4.9) are listed in Table 4-3.

Table 4-3: Variables for Equation (4.10)

Variable	Value
C_{14}	6.54
C_{15}	14.526
C_{16}	0.7389
C_{17}	0.09486
C_{18}	0.4569

In addition to maintaining a dry environment for testing, the secondary guard was also used to maintain the ambient temperature around the GHP apparatus at the mean temperature of the sample being tested as outlined in Section 6.6.1 of ASTM C177 [32]. To determine if heating or cooling was needed in the box, the ambient air temperature of the secondary guard was compared to the set point ambient temperature with a deadband of 0.5℃. Figure 3-7 and Figure 4-1 show how in the secondary guard was heated using an electrical resistance heater embedded in a set of Aluminum fins. To ensure that the heater in the heating fin did not exceed the manufacturer's maximum operating temperature of 120℃ a thermocouple was used to monitor the heaters temperature. When the temperature reached 85℃ the heater was temporarily turned off. Cooling of the secondary guard was supplied by the same cooling coils that dehumidify the space.

4.5 Instrumentation

In this section, a detailed description of the location, function and specification of the instrumentation used to monitor and control different aspects of the GHP will be

presented. The explanation of the instrumentation used for the GHP assembly will start with the meter plate followed by the air gap, guard ring and then the cold plate.

As the temperature and energy used in the thermal resistance calculations were based off the temperature and energy consumed by the meter plate, it would follow that being able to monitor the temperature of the meter plate with accuracy would be preferable. ASTM suggests that the number of sensors on the meter plate is to be no less than ten times the square root of the area $(10 \cdot \sqrt{A})$ or 2 whichever is greater, where A is area of the meter plate in m^2. With the area of one side of the meter plate equaling 0.04 m^2 this comes out to a minimum of 2.01 temperature sensors per face. Figure 4-4 (b,c) shows the layout of the thermocouples on the meter plate. Understanding that 2.01 thermocouples per face was the minimum, each side of the meter plate was fitted with five thermocouples with one central thermocouple and one in each of the four corners as seem in Figure 4-4 (b,c) to ensure that a true representation of the meter plate temperature was being observed. Thermal imaging of the meter plate showed that during testing the meter plate reached and maintained an even set point temperature after 15 minutes of heating from room temperature. Appendix C shows still images of the hot plate assembly heating up in 15 second intervals over a fifteen minute period. In the images it can be seen that the plate heats from the center outward but eventually reaches the uniform set point temperature of 45°C.

The power used to maintain the surface temperature of the meter plate was recorded using a WattNode model WNB-3Y-208-P by Continental Control Systems. The error on the power meter selected was 0.5% of the total power recorded during the test, plus the equivalent of one pulse of energy. More detail on how the uncertainty of the power meter

and thermocouples contribute to the overall uncertainty in the thermal resistance calculations can be seen in Section 4.6 of this thesis. A National Instruments cRIO-9024 compact controller with chassis was used in scan mode to record the voltage signals from a NI-9214 C-Series temperature input module that the thermocouples on the GHP apparatus were hooked up to.

The guard ring surrounded the meter plate and was used to prevent energy loss from the meter plate. Figure 4-4 b and c outline the position of the thermocouples used to monitor the temperature difference between the meter plate and the guard ring, with four gap imbalance measurements taken along the four sides of the meter plate. ASTM C177 suggests that the temperature readings for the gap imbalance be taken from a quarter of length of the sides of the meter plate [32]. The guard ring had four embedded electrical resistance heaters that were controlled independently of one another, which allowed the top, bottom and sides of the guard ring to adjust the surface temperature accordingly. Figure 4-4 b and c shows the four thermocouples used to monitor the temperature of the guard ring close to the air gap. All the thermocouples in the GHP setup were made of Type T 30 gauge wire.

The two cold plates were outfitted with three thermocouples each as shown in Figure 4-4 a and d. The decision to have three thermocouples on the cold plates came after viewing thermal images of the cold plates during initial testing which showed the plates remaining at a uniform temperature within the specified deadband. To ensure that the average temperature of each of plates was recorded, three thermocouples were spread across the plate measuring the temperature close to the inlet, exit and halfway point of the internal channel. Thermal imaging of one of the cold plates cooling down shows the plate

going from room temperature to the set point of -1℃ over a 7.5 minute period in Appendix D . Each of the thermal images was taken at a 15 second interval as the plate cooled.

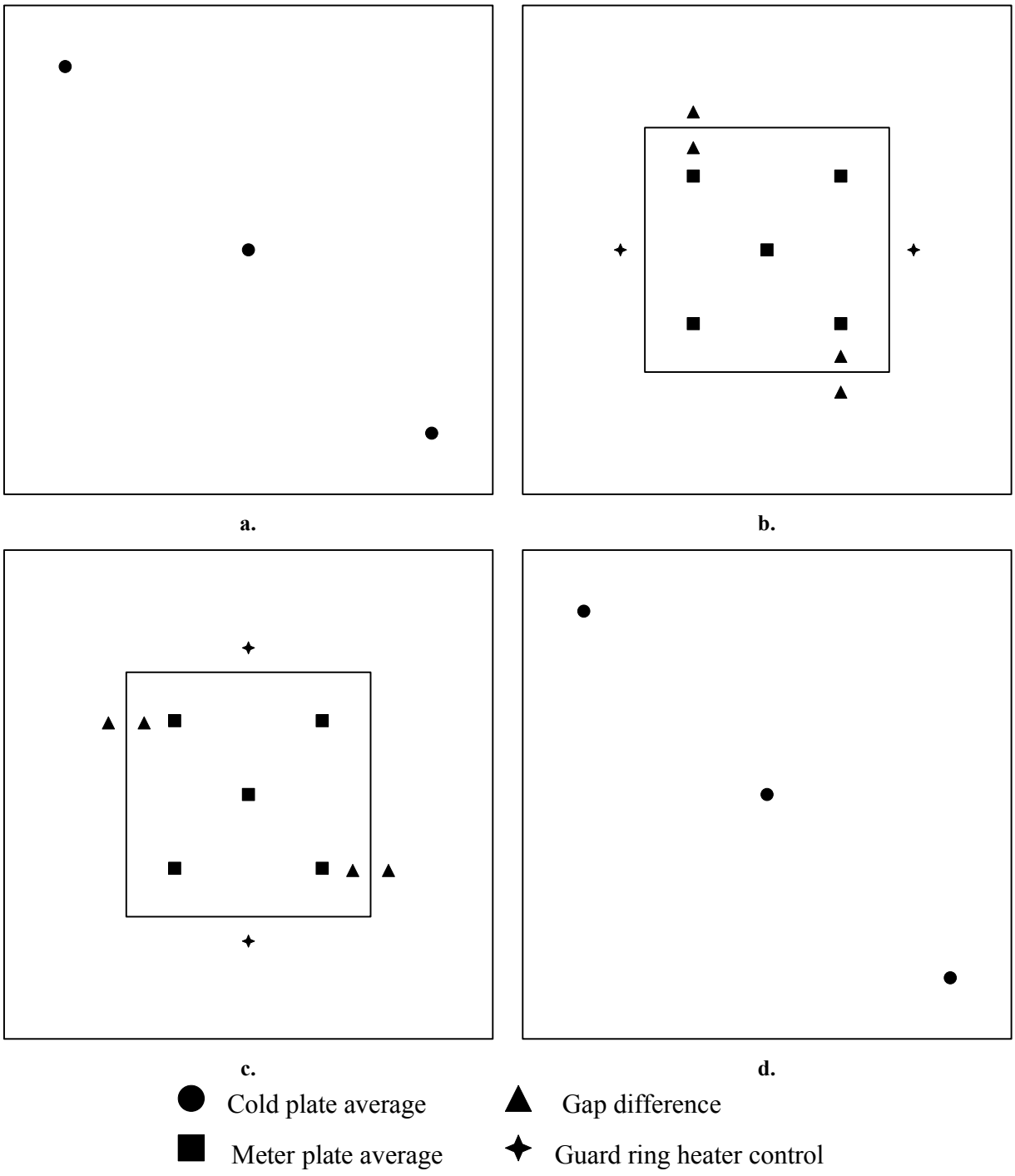

Figure 4-4: Thermocouple layout for hot plates (b.,c.) and cold plates (a.,d.)

4.6 Uncertainty Analysis

In the analysis of the VIPs within this study, the thermal resistance as well as the mass of the panels will be discussed and as such an uncertainty analysis on the measured and calculated results was conducted and can be seen in detail in Appendix E. The uncertainty on the calculated thermal resistance is a function of the temperature difference across the sample and the power used in maintaining the test conditions. As such the uncertainty is specific to each test performed, however it can be expressed in Equation (4.11)

$$u_{R_{SI}} = \pm\sqrt{\left(\frac{A}{q}\cdot\sqrt{(u_s{}^2 + u_r{}^2)_{Cold} + (u_s{}^2 + u_r{}^2)_{Hot}}\right)^2 + \left(-\frac{\Delta T\cdot A}{q^2}\cdot((0.005\cdot q) + (0.04167/t))\right)^2} \quad (4.11)$$

The uncertainty on the measured mass of the panels is a function of the number of readings taken and the scale being used. As the uncertainty of the mass of the panels is dependent on the standard deviation of the readings taken the uncertainty is unique to each time a VIP is weighed. The uncertainty in the mass can be can be represented by Equation (4.12).

$$u_M = \pm\sqrt{(u_r)^2 + (u_s)^2} \quad (4.12)$$

In this chapter, the construction of the GHP and supporting equipment was presented. The next chapter will be discussing the results and observations from the tests conducted on the validation of the GHP and evaluated thermal resistance of the VIPs tested.

5 Chapter: Results and Discussion

In the current chapter the significance of the results from the commissioning of the GHP are discussed along with the results from the initial testing of the VIPs and the significance of the findings to the proposed accelerated ageing procedure. Chapter 5 begins with a discussion on the testing of the capabilities of the secondary guard around the GHP, testing the performance of the GHP against known materials and ensuring the tests performed were conducted at steady state conditions. Chapter 5 then discusses the tests conducted to develop the temperature set points used in the testing of VIPs, the results from the initial VIP testing before discussing the results from climate ageing the panels and thermal performance of the panels after ageing. As the GHP apparatus was specifically built to evaluate the thermal resistance of materials, it was imperative the accuracy was determined to allow for successful analysis of panel ageing.

5.1 Commissioning of the GHP

After the GHP was constructed, a commissioning period was undertaken to ensure that the GHP produced results comparable to industry. Ensuring the GHP functions as intended was important to allow the testing of VIP to be conducted with confidence.

5.1.1 Effect of ambient air temperature on GHP results

As previously mentioned, a secondary guard around the GHP apparatus was used to prevent moisture from condensing on the cold plates and reduced the amount of energy loss from the sample by maintaining the ambient temperature around the sample at the mean temperature of the sample being tested. In the commissioning phase of the GHP, a test was conducted to determine how much of an effect the ambient temperature had on the energy loss of the system and subsequently the thermal resistance of the sample

being tested. To test the effects that the ambient temperature had on the evaluated thermal resistance of a sample, a test was devised where the ambient temperature of the secondary guard was decreased around the GHP while VIPs were tested under constant plate conditions. In these tests, the panels from PM2 were tested with set point temperatures of 5°C, 25°C and 45°C for the cold plate, secondary guard and meter plate respectively. The objective for this test was to determine the maximum allowable deviation from the mean sample temperature that the ambient conditions can stray for a test to be still be considered successful. The results from the test presented in Figure 5-1, show that as the ambient temperature decreases compared to the mean sample temperature, the measured value for the thermal resistance decreases. In the test, the ambient conditions were allowed to drop to a maximum of 5°C below mean sample temperature, to the surrounding laboratory temperature of 20°C. When the secondary guard was allowed to drop by 5°C, the thermal resistance of the VIP being tested dropped by 7.6% compared to the thermal resistance calculated when the ambient space was maintained at the mean sample temperature of 25°C. The conclusion taken from this test is that a drop up to 0.5°C of the ambient temperature in the secondary guard is the maximum allowable deviation the ambient temperature can be from the mean sample temperature for a test to still be considered successful. At a temperature difference of 0.5°C, the difference in calculated thermal resistance compared to the thermal resistance calculated with no difference in ambient temperature, was within the 2.3% uncertainty on the measured values, meaning that within 0.5°C any difference in evaluated thermal resistance could be due to instrumentation error vs an actual difference in performance, and if the difference is greater than 0.5°C the thermal resistance would be artificially low due to an increased loss of energy through the sample.

The results obtained from this test were then used to assess the validity of future testing where the temperature difference between the secondary guard and the mean plate temperature were compared to determine if the difference was within 0.5℃ of each other. If the difference was greater than 0.5℃ the results were scraped and the test was rerun.

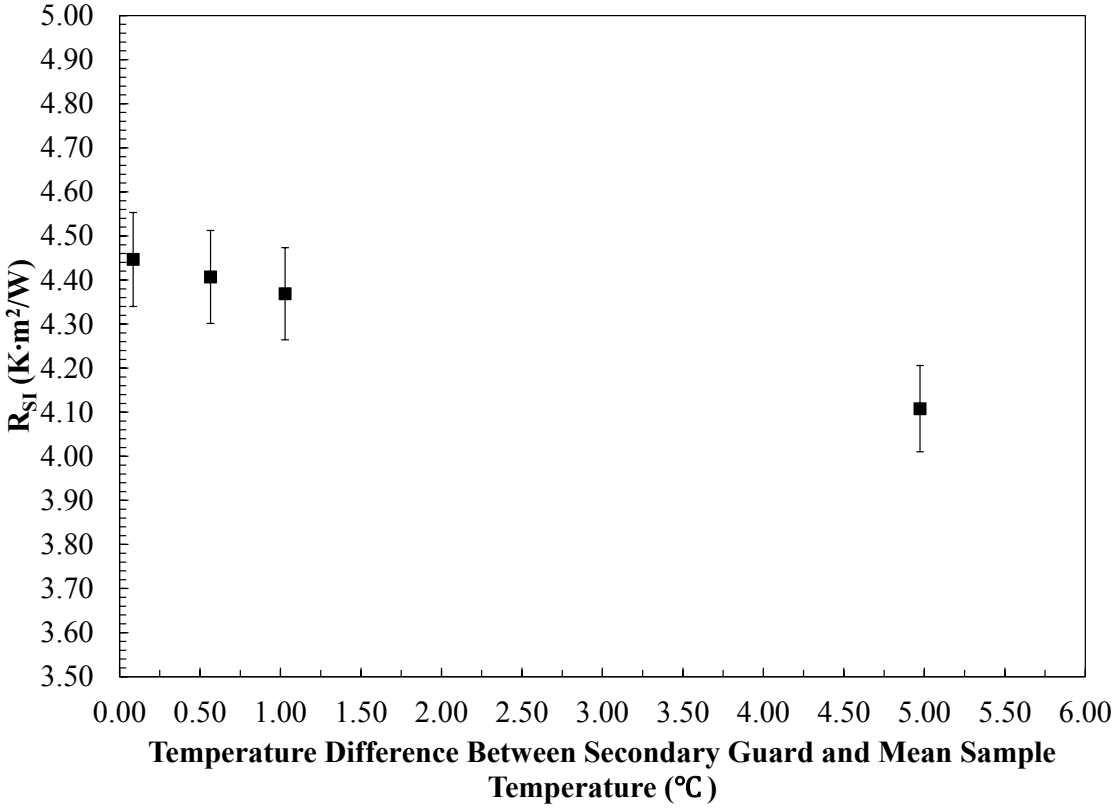

Figure 5-1: Temperature Difference Between Secondary Guard & Mean Sample Temperature

5.1.2 Validation of GHP to Industry Specified Materials

Before evaluating the thermal resistance of a VIP of unknown and/or changing thermal resistance, a verification process was conducted on the GHP to determine if the GHPs evaluated thermal resistance was accurate when testing against materials of specified standards. The two materials that were used to validate the performance of the GHP were expanded polystyrene (EPS) and extruded polystyrene (XPS) as these materials are held to industry specified standards and are readily available for testing in varying thicknesses.

Both EPS and XPS are manufactured from polystyrene however, EPS is made from many expanded polystyrene beads where XPS is extruded from a mold from a mass of polystyrene. For this testing ASTM standards were consulted to determine the industry specified testing temperatures for EPS and XPS. The recommended testing temperature was a mean sample temperature of 24℃ with a temperature difference of 22℃ across the sample. The ASTM recommended temperature was used to validate the performance of the GHP against EPS and XPS of industry specified standards.

The EPS used in the validation process was of Type 2 EPS with a thickness of 0.050 m, and an expected thermal resistance of R_{SI} 1.41 $K \cdot m^2/W$. The thermal resistance of the EPS was evaluated over a 16 hour period at the ASTM set point temperatures. The resulting thermal resistance was evaluated to be R_{SI} 1.39 ± 0.05 $K \cdot m^2/W$. The difference of 1.4% between the expected and calculated results are within the 3.7% uncertainty on the calculated thermal resistance, suggesting that the GHP is an accurate means of evaluating thermal resistance. Validation of the GHP using EPS was conducted two additional times between VIP testing to ensure that the performance of the GHP was not changing through usage with the second test performed in the middle of VIP testing and the third at the end of VIP testing. Results of the EPS testing are shown in Table 5-1. The findings from the testing done on EPS during the testing period show that the GHP procedure is repeatable and accurate.

Table 5-1: Summary of validation testing using EPS throughout VIP testing

Test Number	1	2	3
R_{SI} ($K \cdot m^2/W$) Calculated	1.40 ± 0.05	1.39 ± 0.05	1.39 ± 0.05

Validation testing of the GHP was also conducted using XPS of a thickness of 0.038 m, with an expected R_{SI} 1.32 K·m^2/W. Like the EPS, testing of the XPS was conducted over a 16 hour period resulting in a calculated R_{SI} 1.34 ± 0.03 K·m^2/W. Again the difference of 1.5% between the expected and calculated result is within the 2.6% uncertainty of the calculated value showing that the GHP is capable of testing insulating materials to a high degree of accuracy.

Additional testing of XPS was conducted to determine if the GHP would be capable of testing insulating samples of different thicknesses and of higher insulating capacity. In this testing the thermal conductivity as well as the thermal resistance were evaluated. Thermal conductivity for the XPS was evaluated as thermal conductivity is a material property. Thermal conductivity is not dependent on the thickness of the sample and it should remain constant over the different thicknesses tested. However the manufacturer specifications for the thermal conductivity differed for each thickness of the XPS evaluated and as such a constant thermal conductivity was not observed. The three thicknesses of XPS used in the testing were 0.015 m, 0.025 m and 0.038 m. The results from the testing of different thickness of XPS are summarized in Table 5-2, and are compared to the expected thermal resistance and thermal conductivity value as specified by the manufacturer. As seen from the results in Table 5-2, both the evaluated thermal conductivity and thermal resistance of the XPS remained within the uncertainty limits of the expected manufactures values across all thicknesses tested. The test also showed that the GHP can successfully test materials of different thicknesses with accuracy.

Table 5-2: Summary of GHP validation testing using XPS of different thickness

Thickness (m)	R_{SI} ($K \cdot m^2/W$)		Thermal Conductivity (mW/m·K)	
	Expected	Measured	Expected	Measured
0.015	0.50	0.53 ± 0.01	30.0	28.5 ± 0.75
0.025	0.88	0.91 ± 0.02	28.4	27.8 ± 0.75
0.038	1.32	1.34 ± 0.03	28.7	28.5 ± 0.75

5.1.3 Ensuring that Steady State Conditions were Achieved

When using the GHP approach for evaluating the thermal resistance of insulating material, care must be taken to ensure that the equipment and sample reach steady state conditions before analyzing any of the data. The GHP reaches steady state conditions when the system has reach an operating level where the surface temperatures of the sample are constant and the energy needed to maintain the meter plate temperature is supplied to the heating element at a constant rate. As explained in the Experimental Procedure Section 3 of the thesis, each set point was divided into five averaging periods at four hours each. Before settling on four hours for the length of time of each averaging period, a test was conducted to determine how long the GHP would take to reach steady state conditions. In this test VIPs from PM2 were installed into the GHP and the averaging periods for the GHP were set to 1 minute intervals. The GHP was allowed to run for 20 hours to capture the time that steady state conditions were achieved and 1 minute intervals were used to ensure there was enough resolution when analyzing the data to determine the moment steady state was reached. For this test the set point temperatures were set as follows: 5°C, 25°C and 45°C for the cold plate, secondary guard and meter plate. Figure 5-2 shows that the meter plate, secondary guard and cold plates reached their set point temperatures within the first 15 minutes of testing. To ensure that the GHP reaches steady state conditions a period must be reached where the heating element is turning on at even intervals and that the amount

of power being used at each interval is constant. Figure 5-3 is a plot of the power consumption of the meter plate used through the testing period. A settling period for the power consumed was observed at the two hour mark. After two hours the heater came on at 19 minute intervals and provided approximately 12.5 Watts of power for approximately 1 minute periods as shown in Figure 5-3. The dip in the data at approximately the three hour mark can be attributed to a heating period being split between two time periods on the power meter. As the power was split between the two time periods the amount of power consumed in each instant was less than the 12.5 Watts per time step during steady state. This test helped determine that a 4 hour averaging period was an acceptable length of time for steady state conditions to be reached for a VIP being evaluated for thermal resistance.

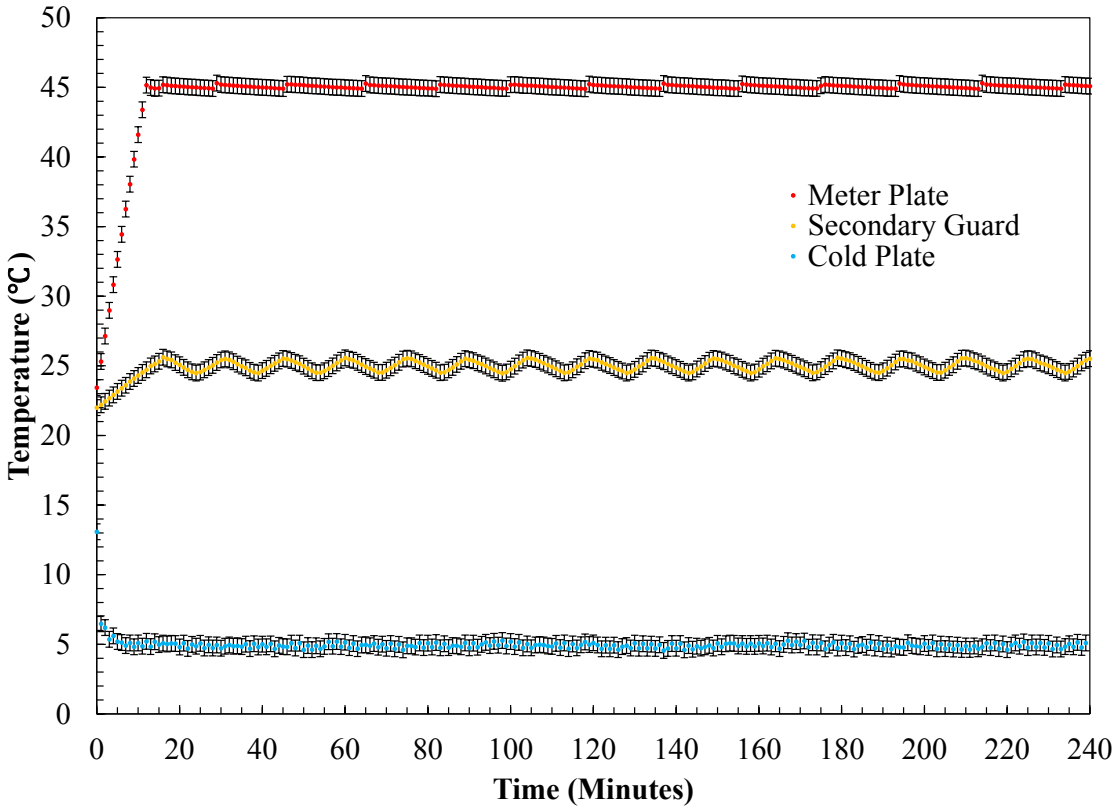

Figure 5-2: Temperature readings during GHP steady state testing

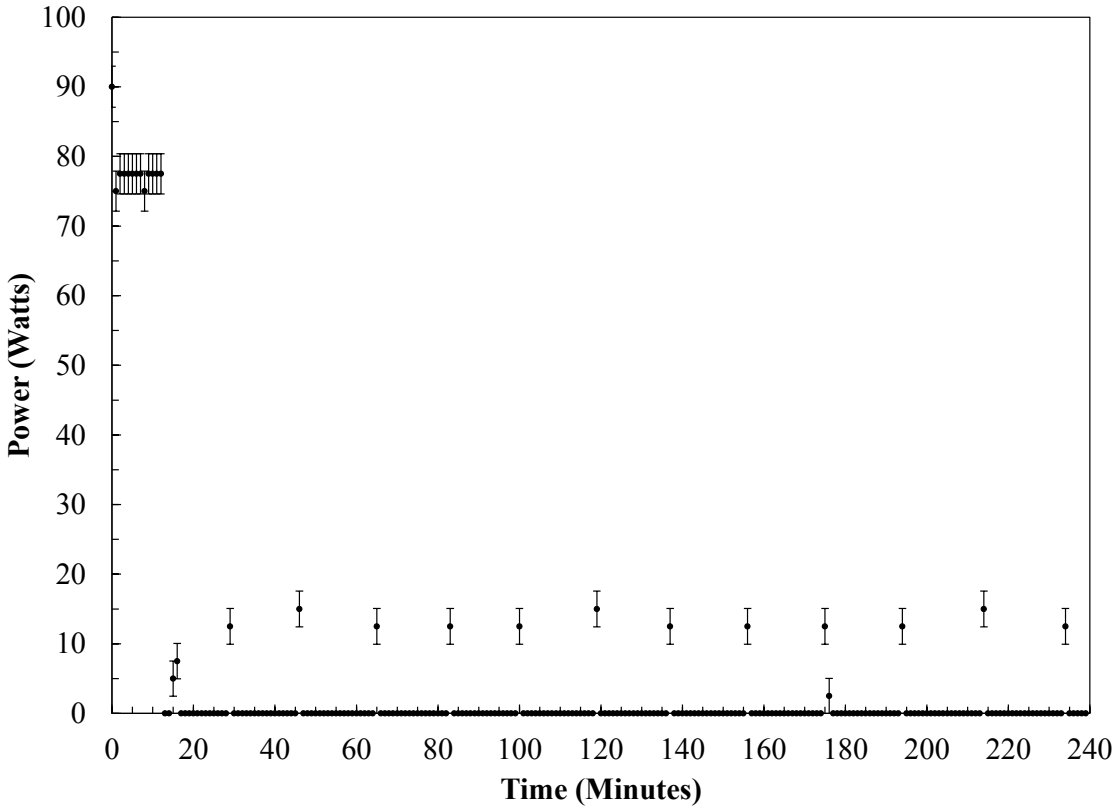

Figure 5-3: Power consumption during GHP steady state testing

5.2 Testing to Develop Temperature Set Points for VIP Testing

As outlined in the Experimental Procedure Section 3, temperature set points for the GHP had to be developed to evaluate the thermal performance of VIPs. To ensure that the selected 40℃ temperature difference would be acceptable in respect to the uncertainty in the calculations of thermal resistance as well as reaching a settling point of thermal resistance, a test was performed on panels from both PM1 and PM2. In this test, panels from both manufacturers were tested in the GHP while the mean panel temperature of 24℃ was held constant and the temperature difference across the sample increased. The objective of this test was to find the temperature difference where the thermal resistance

decreased until a point where the difference between each test became negligible. An outline of the test set point temperatures that were used in the test are shown in Table 5-3.

Table 5-3 Plate temperatures for temperature difference testing

Set Point #	Cold Plate (°C)	Meter Plate (°C)	Temperature Difference (°C)
1	13	35	22
2	9	39	30
3	4	44	40
4	-1	49	50
5	-6	54	60

The results obtained from PM1 can be seen in Figure 5-4 which shows that as the temperature difference across the panels increased, the uncertainty in the measured value decreased from approximately 3.7% at ΔT 22°C to 1.6% at ΔT 60°C. In Figure 5-4 it can also be seen that the evaluated thermal resistance of the VIP also decreases as the temperature difference across the VIP increased which was a trend observed by Lorenzati, et al [36]. In analyzing the results from this test it was determined that the optimal temperature difference across the panels from PM1 was actually 60°C as the uncertainty of in the value was the lowest and the thermal resistance appeared to have reached a settling point. Upon completion of the testing of the panels from PM1, panels from PM2 were tested through the same conditions.

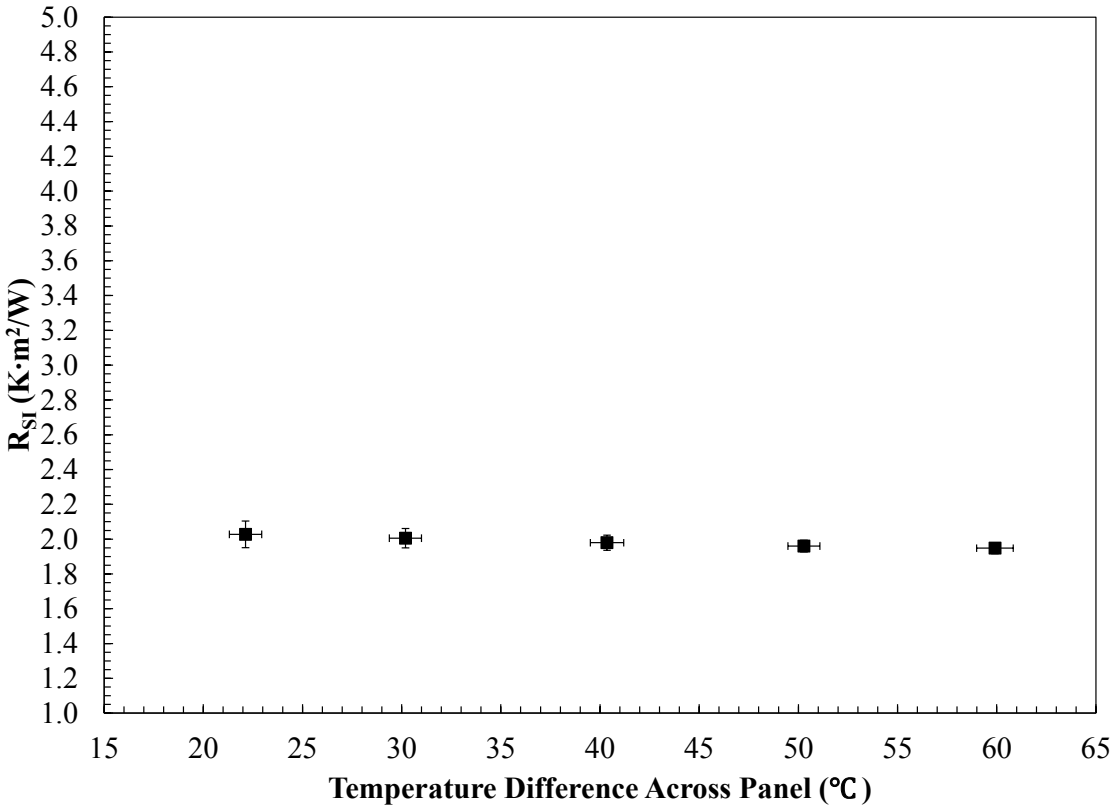

Figure 5-4: Increasing temperature difference across PM1 with mean temperature constant

The results obtained from the testing of the panels from PM2 showed different results compared to PM1. The results from PM2 testing are shown in Figure 5-5 where a high thermal resistance value can be seen at lower temperature differences and a low thermal resistance value can be seen at the high temperature difference. The results from this testing showed that temperature differences across VIPs can have a large effect on the performance of the product with an approximate 11% decrease from a 22℃ ΔT to 60℃ΔT. The results from the panels of PM2 suggest that the VIPs have an optimum range of performance for the product. These results also highlight that importance of evaluating the thermal resistance of panels through a range of temperatures as the thermal resistance is a function of both average temperature and temperature difference. Taking into consideration the results from the testing of PM1 and PM2 as well as the capabilities of the

GHP in regards to its maximum and minimum temperatures, the 40℃ temperature difference across the panels was selected. A 40℃ temperature difference was selected as it helped keep the uncertainty in the evaluated thermal resistance down and it allowed for the most flexibility in testing of difference mean panel temperatures.

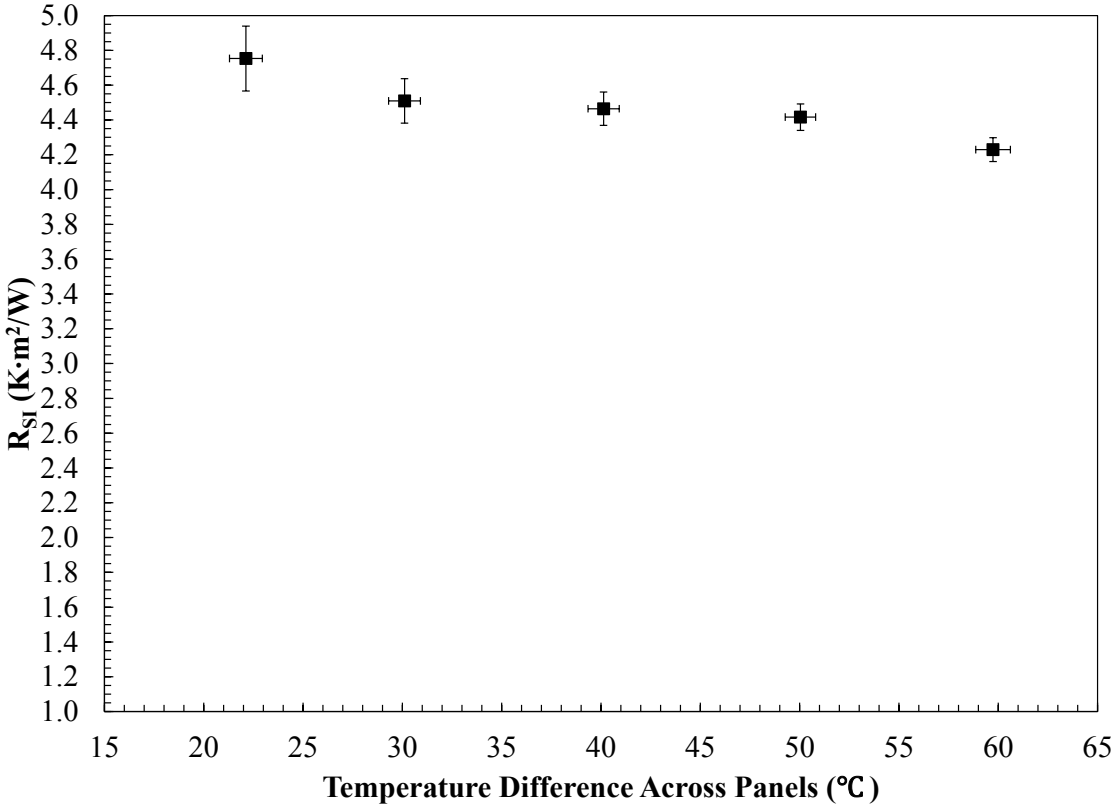

Figure 5-5: Increasing temperature difference across PM2 with mean temperature constant

5.3 Thermal Resistance Testing

In order to quantify the level of degradation a VIP experiences during accelerated ageing, a baseline for its thermal performance must be established. Baseline thermal resistance testing is done using unaged or dry panels to determine their highest performance level. As not all panels are manufactured equally as outlined in a study by Kumara et al. [26], where a spread of 14% in evaluated thermal resistance was seen between the highest and lowest performing panels, all panels used in this thesis are tested

before accelerated ageing to obtain a value for their thermal resistance. The baseline testing was performed for a set of panels from both PM1 and PM2 using the GHP testing procedure as outlined in the Experimental Procedure Section 3 of the thesis. Baseline testing was conducted with a 40°C temperature difference across the panels with mean panel temperatures tested from 15 to 35°C. In order to appreciate the thermal resistance of the VIPs, EPS was also tested through the same procedure with all results presented below. The thicknesses of the samples tested will also be listed so that a comparison can be made between the materials.

5.3.1 EPS Thermal Resistance Testing

Testing of EPS was done in order to give a comparison for the VIPs tested in this study. The testing of the 0.058m thick EPS was conducted through the same set point temperatures that were selected for the VIPs. The results from the testing of the EPS are shown in Figure 5-6 which shows the dependence of thermal conductivity on temperature. Over the 20°C temperature range, the EPS dropped approximately 6% from low to high mean temperature. The uncertainty in the measured value at 15°C was larger than the rest of the calculated uncertainties as the cold plate was fluctuating in temperature through the 16 hour period and as such a larger standard deviation in the recorded temperatures was recorded.

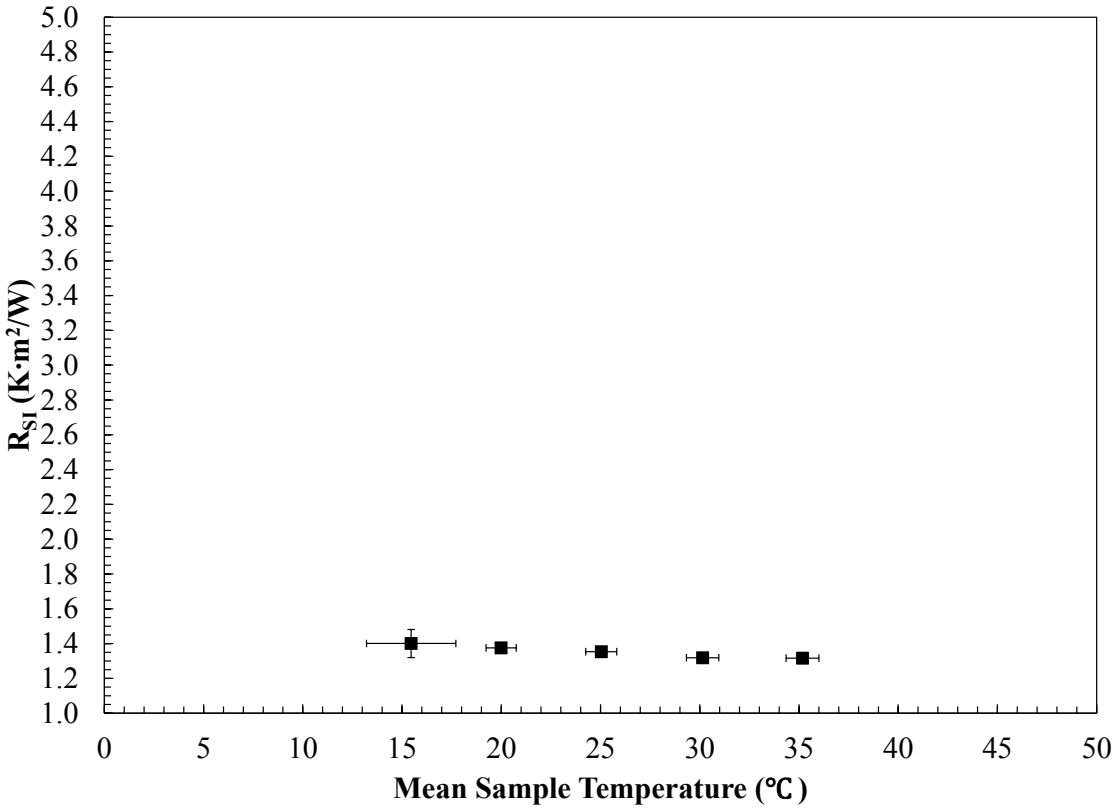

Figure 5-6: Thermal resistance testing of EPS

5.3.2 PM1 Baseline Thermal Resistance

Two VIPs from PM1 were selected and promptly labeled panels 1 and 2 for identification purposes through testing. The mass of the two panels was recorded before testing to determine if individual panels absorbed water at different rates, and can be seen in Table 5-4. The panels from PM1 had a measured thickness of 0.01m and were the thinnest VIPs tested. Before evaluating the thermal conductivity of the panels from PM1, information as to their expected thermal performance was obtained in the form of previous work conducted by Conley and Cruickshank [31]. In the paper the same panels from PM1 were constructed into a wall assembly and tested in a GHB apparatus to quantify the amount of thermal bridging occurring in a wall constructed with VIPs. In Figure 5-7 a point from their testing can be seen next to the results from this thesis, having an average

center of panel thermal resistance of 2.38 K·m^2/W when tested at a mean panel temperature of approximately 12.5°C. These results were used as a guide to compare calculated thermal resistances from PM1 in this thesis. Figure 5-7 presents the thermal resistance of the two panels from PM1 as a function of the mean panel temperature, illustrating how the thermal resistance of the material decreases as the mean sample temperature increases. Interpolating from the results obtained in this thesis for a thermal resistance value at 12.5°C a value of 2.38 K·m^2/W could be possible. Comparing this calculated thermal resistance value to that of Conley and Cruickshank, [31] shows that the evaluated thermal resistance values from the GHP for panels from PM1 are in the range of expected values. In Figure 5-7 the thermal resistance of the VIPs can be seen to drop as the mean sample temperature of the panel increases, and in this test the panels experienced a drop of approximately 3.8% over a 15°C temperature difference. Looking back to the results of the EPS thermal resistance testing, the EPS experienced a 6% drop over the same 15°C range of mean temperatures. Comparing the results from the VIPs suggests that the thermal resistance of VIPs are less dependent on mean temperature compared to EPS. Determining how dry VIPs thermal resistance is affected by the mean sample temperature was considered an important characteristic, in order to make the comparison to panel that have been aged. The comparison would determine if the amount of moisture content of a panel affects the rate at which the thermal resistance changes with temperature.

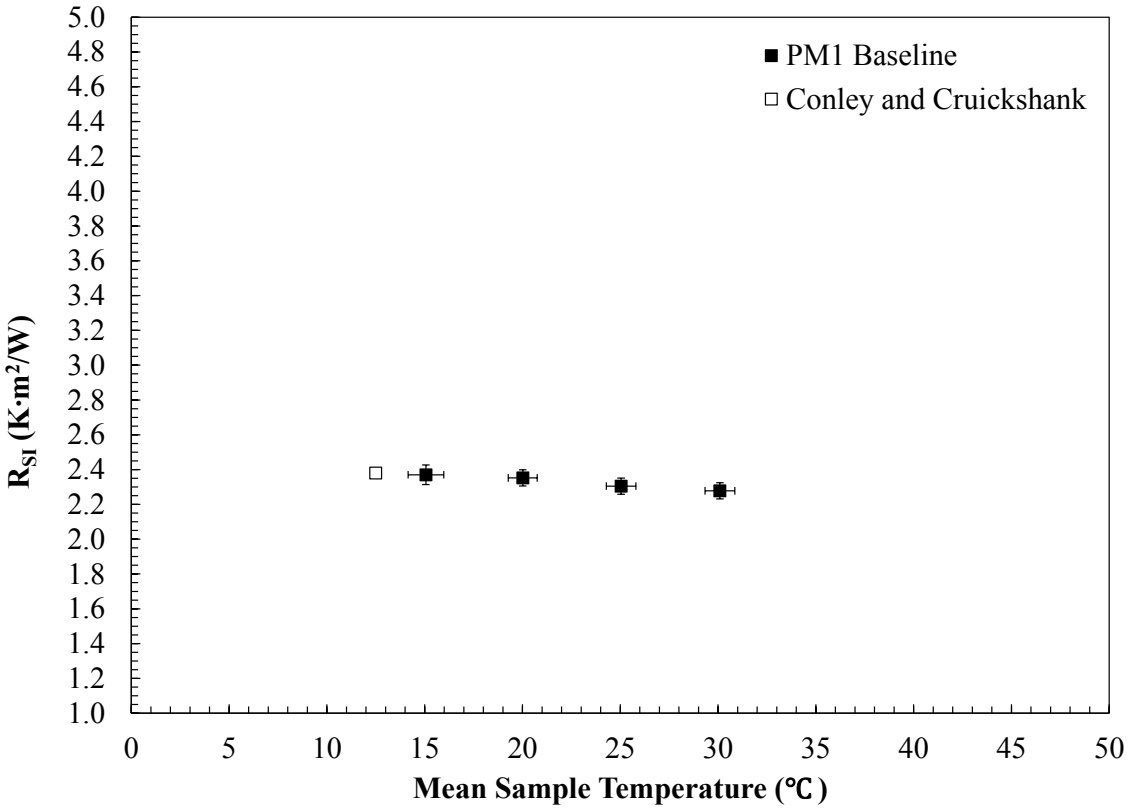

Figure 5-7: Baseline thermal resistance testing for panels from PM1

5.3.3 PM2 Baseline Thermal Resistance

Similarly to the baseline testing of panels from PM1, the mass of two panels from PM2 was recorded before testing in the GHP, and is shown in Table 5-4. The same testing conditions were used as the testing of panels from PM1 to keep test parameters consistent through testing. Compared to the panels from PM1 the VIPs from PM2 were thicker and had a measured thickness of 0.02 m. The evaluated thermal resistance values gives the impression that the panels from PM2 are a superior product to the panels from PM1, however when the thermal conductivities of the two panels are compared the two manufactures are very similar. Figure 5-8 shows how the evaluated thermal resistance of panels from PM2 decreased as the mean sample temperature increased, with a drop of 4% from 15℃ to 35℃ which is lower than the drop for EPS across the same range.

Between 15℃ to 30℃ the panels dropped approximately 3.2% compared to the 3.8% from PM1. These results from the testing of the panels from PM2 suggest that the thermal resistance is the least dependent on mean temperature compared to panels from PM1 and to EPS. Despite the baseline thermal resistance testing of panels from PM1 and PM2 showing less temperature dependence then EPS, the results still show a dependence on mean sample temperature, which suggests that future testing of VIP should continue to test at different mean temperatures in order to understand how mean temperature and moisture content affect the thermal resistance.

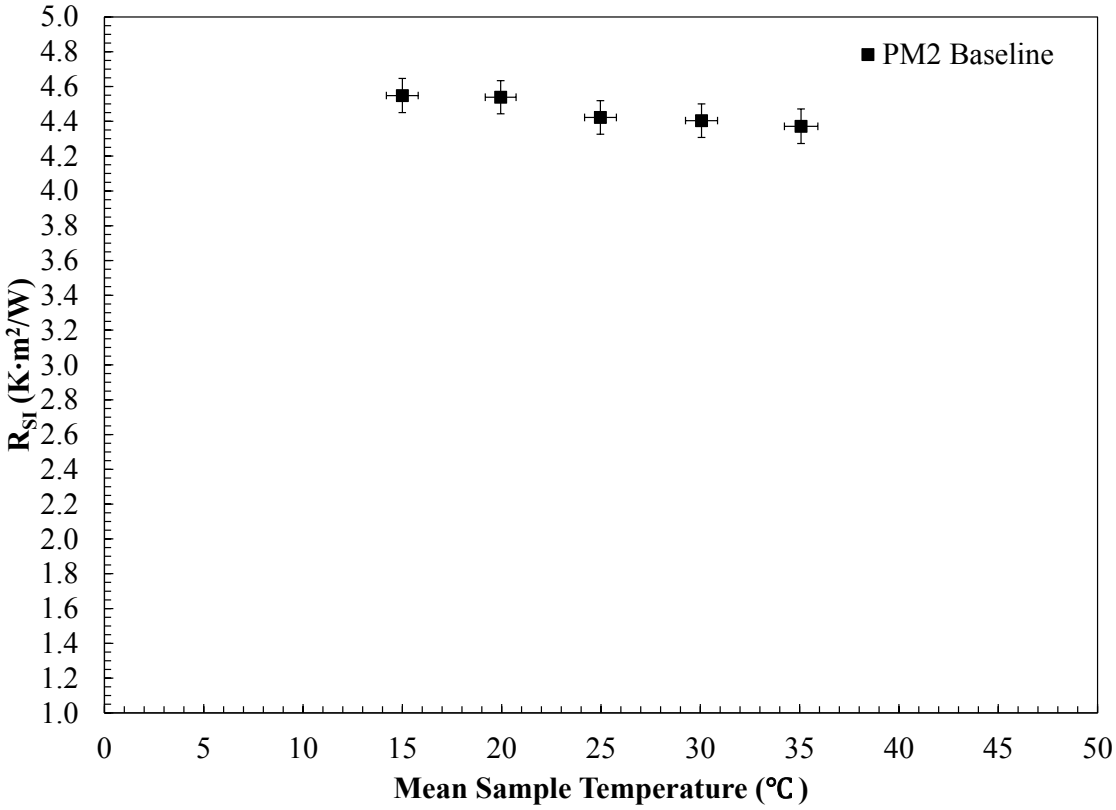

Figure 5-8: Baseline thermal resistance testing for panels from PM2

5.4 Moisture Content of Panels

Research has shown that as moisture accumulates within a VIP the thermal resistance of the panel decreases [22], and that moisture can transfer across the foil of the

panel at a faster rate compared to air [25]. One of the objectives of this thesis was to prove that the moisture content of panels could be altered from exterior climate conditions and if the moisture content of the panels were altered, how does the increased moisture content affect the thermal resistance. As outlined in the Accelerated Ageing Procedure Section 3.3 of Experimental Procedure, panels form both PM1 and PM2 were stored in climate chambers maintained at 33℃ with a RH of 90%. For this part of the larger accelerated ageing testing of VIP the rate at which the moisture defuses into the panels was not being monitored as this will be studied in more depth in future works.

The panels from PM1 and PM2 were loaded into a climate chambers and held there for approximately 30 days. At the end of the 30 day period the panels were removed and the mass of the panels was recorded before the thermal resistance of the panels was evaluated. The mass of the panels before and after ageing is shown in Table 5-4, which shows that all the panels gained moisture during their period in the climate chamber. The panels from PM1 experienced a larger moisture gain compared to panels from PM2 under the same amount of time, suggesting that the foil of the panels from PM1 are more susceptible to moisture transport compared to that of PM2.

The results from this set of testing showed that the moisture content of the panels could indeed be altered by holding the panels in a climate chamber in a warm and humid environment. The significance of this testing is that with the equipment in the lab the moisture content of VIPs can be altered, which will allow for future testing to be conducted to determine if the rate of transport of moisture into a VIP can be affected by different temperature and humidity levels. If the VIPs within this thesis responded in the same manner as the panels in the testing conducted by Schwab et al. [15, 16], where a 4%

increase in mass due to moisture gain caused a 50% increase in thermal conductivity of the panels, the panels from PM1 and PM2 would need to gain approximately 33 g and 9.8 g of moisture respectively to see the same level of degradation.

Table 5-4: Mass of panels from PM1 and PM2 before and after climate ageing

Manufacturer	Panel #	Baseline mass (g)	After First Ageing mass (g)	Difference (g)	% Difference
PM1	1	834.06 ± 0.04	835.85 ± 0.08	1.79	0.21
	2	851.06 ± 0.04	852.78 ± 0.14	1.72	0.20
PM2	1	245.13 ± 0.21	245.31 ± 0.04	0.17	0.07
	2	247.39 ± 0.14	247.47 ± 0.03	0.08	0.03

5.5 Thermal Performance of Panels after Ageing

After holding the panels in the climate chamber the panels were removed and their thermal resistance was evaluated using the GHP. The objective for the testing after the climate ageing was to determine how the thermal resistance of the panels was affected, if any, by the increase in moisture content. In this section of the thesis, the obtained results of the thermal resistance testing after ageing for both panel manufactures are presented, along with a discussion of the significance of the findings.

5.5.1 PM1 Thermal Resistance after Ageing

As seen in the previous section, the panels from PM1 gained approximately 0.2% moisture during their period in the climate chamber. The panels were then tested in the GHP under the same conditions as in the baseline testing, in order to make a direct comparison of the results. As seen in Figure 5-9 the evaluated thermal resistance values after ageing were lower than the unaged thermal resistance values across the whole range of sample temperatures tested. On average the thermal resistance decreased by 5% through the ageing process, which shows that an increase in moisture content has a negative impact

on the thermal resistance of VIPs from PM1. The second observation made of the results from the testing was that the dry panels thermal resistance dropped by approximately 3.8% between the mean temperatures of 15℃ and 30℃ where the drop for the aged panels was greater at 4.4% across the same range. The larger drop of thermal resistance across the range of temperatures suggests that as the mean temperature increases and the moisture content of a VIP increases the rate that thermal resistance decreases increases. The fact that thermal resistance of VIPs are changing with both temperature and moisture content makes a good argument for testing VIPs through a range of temperatures to determine how VIPs respond to moisture content and mean temperature.

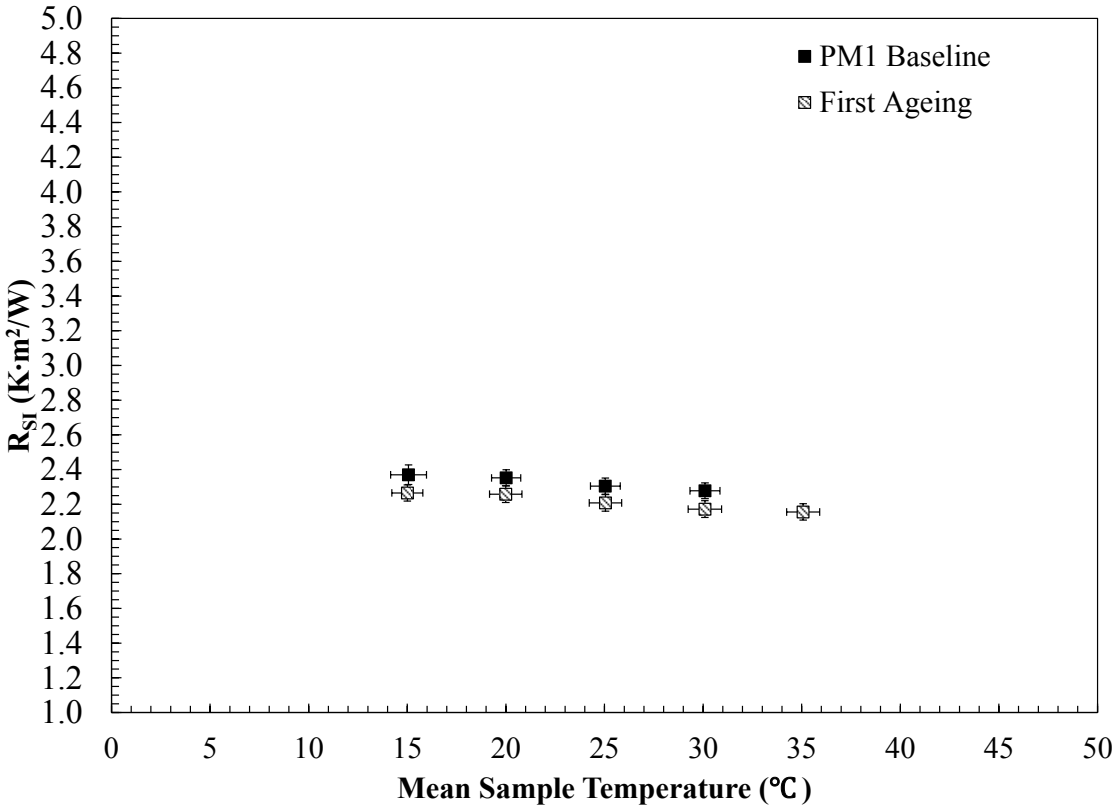

Figure 5-9: Thermal resistance testing for panels from PM1 after ageing

5.5.2 PM2 Thermal Resistance after Ageing

In an identical process, the panel from PM2 were also evaluated for thermal resistance after ageing. The panels from PM2 experience a lower gain of moisture compared to panels from PM1, gaining approximately 0.05% mass over the ageing period. Figure 5-10 shows that just like the panels from PM1 the thermal resistance of the panels was affected by the gain of moisture across all the sample temperatures tested. The thermal resistance values that were calculated showed a decrease of 6.5% compared to values obtained from the dry panels. The drop in performance was not expected based on how little moisture was gained in the panels. It can be seen that despite the amount of moisture that transports across the foil, moisture within a panel negatively affects the thermal resistance of a panel. As the foil composition of the panels is closely guarded by the manufacturers, the foil type and composition of the panels from PM2 is not known. It would appear that the foil of PM2 is less susceptible to moisture transport than that of PM1, which is why the amounts of moisture transported across the panels are different. During testing, it was also noted that panels from PM1 had a desiccant within the panel core while the panels from PM2 did not. Comparing the results from PM1 to PM2, the panels from PM1 experienced a larger moisture gain but a lower decrease in performance compared to the panels from PM2 suggesting that the internal desiccant had some effect in contributing to the difference in performance levels. It would be interesting to see how panels from PM2 would perform if an internal desiccant was added to absorb the minimal moisture gain.

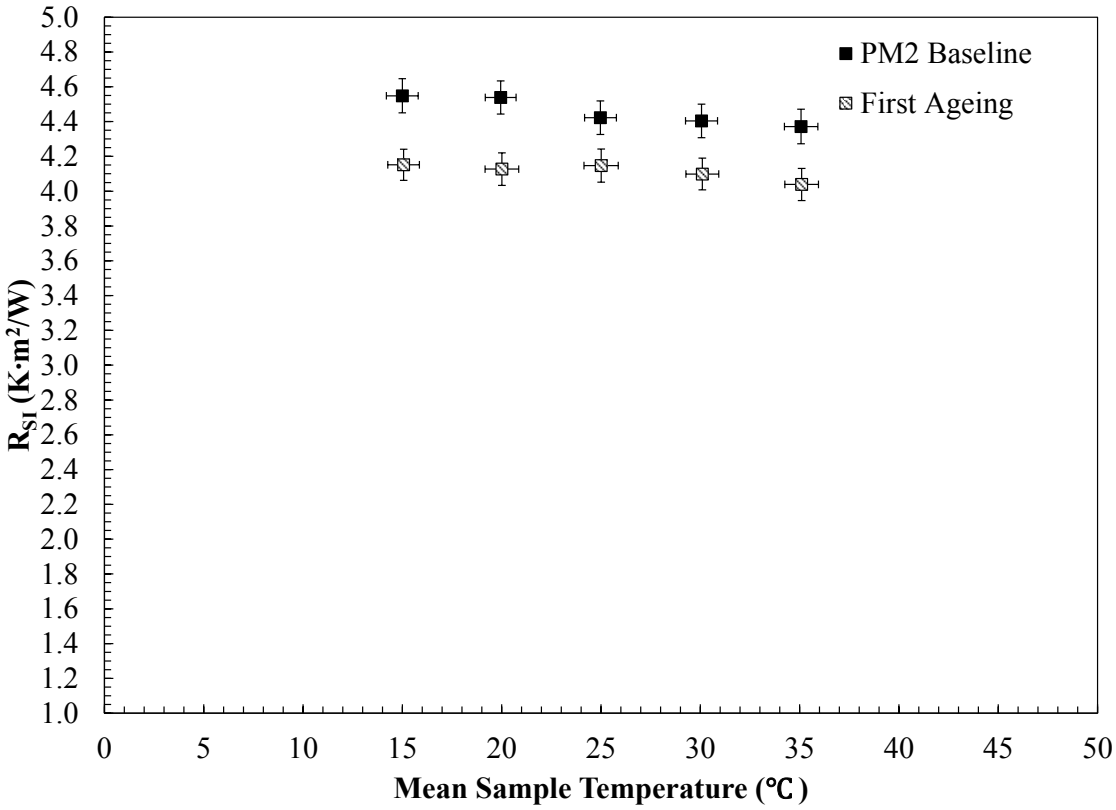

Figure 5-10: Thermal resistance testing for panels from PM2 after ageing

The conclusions taken from the thermal resistance testing after ageing of the panels is that the thermal resistance of the panels is negatively affected by moisture content of the panels, and that different panels experience different levels of degradation based on the amount of moisture accumulated within the core. As this was only the first ageing period, more testing will need to be conducted to determine how panels degrade including, if more of the panels from both PM1 and PM2 can be aged in the same manner, and if they experience the same level of degradation. Additional testing on the panels used in this thesis will also determine how already aged panels will degrade, with regards to further intake of moisture and degradation of thermal resistance over further 30 day ageing periods.

6 Chapter: Conclusions and Future Work

6.1 Conclusions

As building codes in Canada are responding to the need to conserve and reduce the amount of energy being used within both residential and commercial buildings, the amount of insulation needed within buildings envelopes is increasing along with wall thickness. To meet the energy and space saving requirements of today's building market, builders and owners are looking for new materials and practices to insulate their walls and vacuum insulation panels have shown potential to meet or exceed today's high insulating levels while keeping the thickness of the building envelope down. However, the unknown lifespan and ageing characteristics of VIPs may deter some builders from using them within their projects for fear that the panels may fail or cause degradation to the structure prematurely.

The objective of this thesis was to present an accelerated ageing procedure for VIPs that can link results from accelerated ageing to real time degradation. A detailed outline of the new accelerated ageing procedure that quantifies how the thermal resistance of VIPs are both dependent on temperature and percent moisture content within the panels was presented. In this work, climate chambers were used to accelerate the degradation of VIPs and a GHP was used to evaluate the thermal resistance of the panels. Currently in-situ testing of VIPs within a wall section at NRCan is providing the real time degradation of panels as well as the climate conditions around VIPs within wall sections. Future work will use the climate profiles found around the panels from in-situ testing to determine how much time panels spend under specific temperature and humidity conditions within the wall and from this the level of degradation of the panels will be determined using the

degradation values obtained during accelerated testing. Subtasks were created to ensure that the thesis achieved this objective, with the list of subtasks outlined in the Section 1.4. The following section is a summary of the major findings or conclusions from each of the subtasks and how the subtasks were completed.

Through a review of the literature on VIPs it was determined that the moisture content within a panel's core from the transport of moisture across the foil cover, due to warm and humid environmental conditions, caused the greatest loss in insulating capacity. A 4% increase in mass due to moisture gain within a VIP has the potential to increase the thermal conductivity of a panel by 50%. When comparing the degradation resulting from moisture content a 5% gain in internal pressure results in a minimal increase in thermal conductivity. Despite only achieving a 0.2% change in mass of the panels due to moisture a drop in thermal resistance was observed. Had the panels been held in the climate chamber for longer it is hypothesized that they would have continued to gain moisture until reaching a saturation point.

In order to quantify the level of thermal resistance of the VIPs within this thesis a GHP was designed, constructed and its performance evaluated according to ASTM standards. The GHP and supporting equipment were specifically designed to meet the needs of the study and as such working and assembly drawings were made for each part and for the final assembly. After completion of the GHP assembly the construction of the secondary guard around the GHP began. The secondary guard was designed to maintain the ambient climate around the samples being tested to ensure a dry and temperature controlled environment around the sample.

Upon completion of the assembly a validation of the performance of the GHP was conducted using EPS and XPS to ensure that the results obtained from the GHP were accurate to industry specified standards. Type 2 EPS of 0.05 m thickness was tested at three instances throughout testing to ensure the performance of the GHP was staying consistent. The expected thermal resistance for Type 2 EPS of this thickness was R_{SI} 1.41 $K \cdot m^2/W$ and the average of the three EPS tests was R_{SI} 1.39±0.05 $K \cdot m^2/W$ showing that the GHP is both precise and accurate. Validation of the GHP was also conducted using various thicknesses of XPS which showed that the GHP was capable of successfully testing materials of different thicknesses. The validation of the GHP performance allowed further testing of samples of unknown thermal performance to be conducted with confidence.

Baseline testing for the VIPs was conducted using dry panels with the thermal performance of the panels evaluated through a range of mean temperatures. The baseline performance testing for the VIPs from both manufacturers was performed using a range of mean temperatures and a temperature difference of 40°C across the panels. The panels from PM1 experienced a decrease of 3.8% thermal resistance from low to high (15°C - 30°C) mean temperature values tested where panels from PM2 saw a 3.2% drop across the same temperatures. Comparing these values to EPS tested through the same range of mean sample temperatures which saw a drop of 6% thermal resistance, shows that VIPs are more stable in terms of their thermal resistance across the temperature range tested.

An objective of this thesis was to prove that the moisture content of VIPs could be altered by climate conditions surrounding the panels, and as such VIPs were held in a

climate chamber at 33℃ with a RH of 90% for a period of 30 days. Before climate ageing the mass of the panels were recorded for comparison. Upon completion of the ageing period the panels from PM1 experiencing approximately a 0.2% increase in mass from an initial mass of 840 g, where panels from PM2 experienced approximately 0.05% increase in mass from an initial 246 g due to the increase in moisture content. These results proved that the moisture content of VIPs can be altered due to climate conditions around the panels.

To prove that the thermal resistance of VIPs would be negatively affected by the addition of moisture within the panels, the climate aged panels from both PM1 and PM2 were evaluated for thermal resistance using the GHP. The VIPs from PM1 and PM2 experienced an average drop in thermal resistance of 5% and 6.5% respectively. The drop in thermal resistance of the panels from PM2 showed a larger drop than expected for the amount of moisture gained and it was concluded that this was due to the lack of desiccant within the panel to absorb the moisture gained. The results from this testing showed that moisture within a VIP has a negative impact on the thermal resistance of the panels.

The conclusions drawn in this thesis suggests that the proposed accelerated ageing procedure is worth exploring and that the equipment within the lab is capable of measuring the change of mass and quantifying the drop in thermal performance of panels held in climate chambers. The equipment designed, constructed and validated has and will continue to allow for thermal resistance evaluation of VIP and other insulating material within the lab. It is with the work performed in this thesis and the suggested future work that a method can be developed to determine the rate at which the VIP in the study will degrade. Depending on the accuracy and ease of use of this proposed method, it could become a new standard in accelerated ageing of VIP to determine service life.

6.2 Future Work

The work performed in this thesis will contribute to the development of accelerated ageing testing on VIPs, in order to determine an effective service life for the panels within building envelopes. In the Experimental Procedure Section 3 of the thesis the proposed accelerated ageing method was outlined and divided into four steps. In this investigation step two was started with the ageing of the VIPs for 30 days in the climate chambers. Future work of ageing the panels until saturation would be required in order to finish this step and currently there is another project underway that will be working to complete this step.

Moving through to the third step of the proposed ageing procedure, work will need to be conducted to collect data for these rates. As two climate chambers were constructed one chamber can be dedicated to finishing step two of the procedure while the other can start on the first temperature and humidity testing for the third step. Once the first chamber is finished with the second step of testing it can then be used alongside the second chamber to complete the first temperature set point of the moisture accumulation rates in step three.

The first part of step four has been started where panels have been constructed into a wall and are being held in-situ at the CE-BETH facility at Canmet NRCan. The panels were weighed before being installed into the wall along with instrumentation used to monitor the climate around the panels and have been in place for close to a year at the point of writing. Through two year the climate conditions will be monitored and the data will be used to predict the thermal resistance of the panels at the time they are removed from the wall. At the end of two years the panels will be removed from the walls and the new mass of the panels recorded. The difference in mass will give the predicted moisture content

and thermal resistance values a true degradation value to compare with which can then be used to validate or calibrate the predictive model.

During testing, it was not determined if moisture alone was contributing to one panel manufacturers degradation due to the small amount of moisture intake and the uncertainty in the recorded mass. Future testing will be needed in order to determine if other factors are contributing to the degradation of the panels. Future testing could investigate the use of a foil lift off device to measure if dry gases are entering the panel and contributing to panel degradation. To decrease the uncertainty in the measured mass of panels, future work will be needed to investigate if taking more readings to increase the sample size or a more precise scale is needed. By reducing the uncertainty on the measured mass and making use of a test for internal pressure of aged panels, future testing maybe able to isolate the effects of moisture and internal pressure on the VIPs.

References

[1] Natural Resources Canada. Office of Energy Efficiency., "Energy Use Data Handbook Tables," Natural Resources Canada. Office of Energy Efficiency., 02 January 2018. [Online]. Available: http://oee.nrcan.gc.ca/corporate/statistics/neud/dpa/menus/trends/handbook/tables.cfm. [Accessed 28 10 2016].

[2] Alberta Energy Efficiency Alliance, "Resources - ENERGY EFFICIENCY IN THE PROVINCIAL BUILDING CODE," 2009. [Online]. Available: http://www.aeea.ca/resources. [Accessed 23 January 2018].

[3] Natural Resources Canada. Office of Energy Efficiency., "2012 R-2000 Standard," Natural Resources Canada. Office of Energy Efficiency., 2012. [Online]. Available: http://publications.gc.ca/pub?id=9.695654&sl=0. [Accessed 18 January 2018].

[4] Natural Resources Canada. Office of Energy Efficiency., "Energy Star Canada," Natural Resources Canada. Office of Energy Efficiency., 02 January 2018. [Online]. Available: http://www.nrcan.gc.ca/energy/products/energystar/18953. [Accessed 21 February 2018].

[5] Passive House Institute, "Criteria for the Passive House, EnerPHit and PHI Low Energy Building Standard," Passive House Institute , Darmstadt, 2015.

[6] City of Ottawa, "Part 13 - Rural Zones (Sections 211-236) RR - Rural Residential Zone (Sec. 225-226)," 10 March 2017a. [Online]. Available: http://ottawa.ca/en/part-13-rural-zones-sections-211-236#rr-rural-residential-zone-sec-225-226.

[7] IEA/ECBCS Annex 39, "Vacuum Insulation - Panel Properties and Building Applications," 2005.

[8] P. Mukhopadhyaya, K. M. Kumaran, G. Sherrer and D. van Reenen, "An Investigation on Long-Term Thermal Performance of Vacuum Insulation Panels (VIPs)," in *10th International Vacuum Insulation Symposium, Vacuum Insulation Panels: Advances in Applications*, Ottawa, Canada, 2011, pp. 143--148.

[9] IEA/ECBCS Annex 39, "HiPTI - High Performance Thermal Insulation".

[10] P. Mukhopadhyaya, K. Kumaran, N. Normandin, D. van Reenen and J. Lackey, "High-performance vacuum insulation panel: development of alternative core materials," *Journal of Cold Regions Engineering,* pp. 103--123, 2008.

[11] H. Simmler and S. Brunner, "Vacuum insulation panels for building application: Basic properties, aging mechanisms and service life," *Energy and Buildings,* pp. 1122-1131, 2005.

[12] Kevothermal , "Kevothermal Vacuum Insulation Panels," Kevothermal, 2013. [Online]. Available: http://www.kevothermal.com/index.html. [Accessed 12 January 2018].

[13] Va-Q-Tec, "Va-Q-vip F Product Data Sheet," 1 July 2015. [Online]. Available: http://www.va-q-tec.com/en/download-center/download.html?pid=370&aid=367. [Accessed 16 May 2016].

[14] T. L. Bergman, A. S. Lavine, F. P. Incropera and D. P. Dewitt, Fundamentals of Heat and Mass Transfer, Jefferson City: John Wiley & Sons, Inc., 2011.

[15] H. Schwab, U. Heinemann, A. Beck, H.-P. Ebert and J. Fricke, "Permeation of different gases through foils used as envelopes for vacuum insulation panels," *Journal of Thermal Env. & BLDG. SCI.,* vol. 28, no. 4, pp. 293-317, 2005.

[16] H. Schwab, U. Heinemann, A. Beck, H.-P. Ebert and J. Fricke, "Prediction of service life for vacuum insulation panels with fumed silica kernel and foil cover," *Journal of thermal envelope and building science,* vol. 28, no. 4, pp. 357-374, 2005.

[17] H. Schwab, U. Heinemann, J. Wachtel, H.-P. Ebert and J. Fricke, "Predictions for the increase in pressure and water content of vacuum insulation panels (VIPs) integrated into building constructions using model calculations," *Journal of Thermal Env. & BLDG. SCI.,* vol. 28, no. 4, pp. 327-344, 2005.

[18] J.-H. Kim, F. Edmond Boafo, S.-M. Kim and J.-T. Kim, "Aging performance evaluation of vacuum insulation panel (VIP)," *Case Studies in Construction Materials,* vol. 7, no. 2214-5095, pp. 329 - 335, 2017.

[19] R. Kunivc, "Vacuum Insulation Panels (VIP)-An Assessment of the Impact of Accelerated Ageing on Service Life," *Journal of Mechanical Engineering,* vol. 58, pp. 598-606, 2012.

[20] B. P. Jelle, "Accelerated climate ageing of building materials, components and structures in the laboratory," *Journal of materials science,* pp. 6475-6496, 2012.

[21] R. Baetens, B. P. Jelle, J. V. Thue, M. J. Tenpierik, S. Grynning, S. Uvslokk and A. Gustavsen, "Vacuum insulation panels for building applications: A review and beyond," *Energy and Buildings,* vol. 42, pp. 147-172, 2010.

[22] H. Schwab, U. Heinemann, A. Beck, H.-P. Ebert and J. Fricke, "Dependence of Thermal Conductivity on Water Content in Vacuum Insulation Panels with Fumed Silica Kernels," *Journal of Thermal Env. & BLDG. SCI.,* vol. 28, no. 4, pp. 319-326, 2005.

[23] Smithers Rapra, "Tire Testing," Smithers Rapra, 10 January 2018. [Online]. Available: https://www.smithersrapra.com/testing-services/by-sector/automotive/tire-testing. [Accessed 21 January 2018].

[24] Nordic Council of Ministers, "Building Materials and Components in the Vertical Position NT BUILD 495," Nordtest, Finland, 2014.

[25] E. Wegger, B. P. Jelle, E. Sveipe, S. Grynning, A. Gustavsen, R. Baetens and J. V. Thue, "Aging effects on thermal properties and service life of vacuum insulation panels," *Journal of Building Physics,* vol. 35, no. 2, pp. 128-167, 2011.

[26] K. M. Kumaran, P. Mukhopadhyaya, J. Lackey, N. Normandin and D. van Reenen, "Properties of vacuum insulation panels: Results from experimental investigations at NRC Canada," in *Proceedings of the Joint NSC-NRC Workshop on Construction Technologies*, Taipei, Taiwan, 2004.

[27] S. Brunner and H. Simmler, "In situ performance assessment of vacuum insulation panels in a flat roof construction," *Elsevier,* vol. 82, pp. 700-707, 2008.

[28] P. Mukhopadhyaya, D. MacLean, J. Korn, D. van Reenen and S. Molleti, "Building application and thermal performance of vacuum insulation panels (VIPs) in Canadian subarctic climate," *Energy and Buildings,* vol. 85, pp. 672-680, 2014.

[29] ASTM International, "ASTM C518 - 17 Standard Test Method for Steady-State Thermal Transmission Properties by Means of the Heat Flow Meter Apparatus," West Conshohocken, 2017.

[30] ASTM International, "ASTM C1363 - 11 Standard Test Method for Thermal Performance of Building Materials and Envelope Assemblies by Means of a Hot Box Apparatus," West Conshohocken, 2011.

[31] B. Conley and C. A. Cruickshank, "Evaluation of Thermal Bridges in Vacuun Insulation Panel Assemblies Through Steady-State Testing in a Guarded Hot Box," in *International Building Performance Simulation Association*, 2016.

[32] ASTM International, "ASTM C177-13 Standard Test Method for Steady-State Heat Flux Measurements and Thermal Transmission Properties by Means of the Guarded-Hot-Plate Apparatus," West Conshohocken, PA, 2013.

[33] J. P. Holman, "Thermal Conductivity," in *Heat Transfer Tenth Edition* , New York, McGraw-Hill, 2010, pp. 5-9.

[34] ASTM International, "ASTM C578-17 Standard Specification for Rigid, Cellular Polystyrene Thermal Insulation," West Conshohocken, PA,, 2017.

[35] ASTM International, "ASTM C1058/C1058M-10 (Reapproved 2015) Standard Practice for Selecting Temperatures for Evaluating and Reporting Thermal Properties of Thermal Insulation," West Conshohocken, PA, 2015.

[36] A. Lorenzati, S. Fantucci, A. Capozzoli and M. Perino, "VIPs thermal conductivity measurement: test methods, limits and uncertainty," *Energy Procedia,* pp. 418-423, 2015.

[37] B. Conley, Thermal Evaluation of Vacuum Insulation Panels within Residential Building Envelopes, Ottawa ON: Carleton University, 2017.

[38] B. Conley, C. Baldwin, C. A. Cruickshank and M. Carver, "Challenges of High RSI-Value Building Envelop Retrofits," in *15th Canadian Conference on Building Science and Technology*.

[39] M. Miller, "Radiant Loop Layout Patterns," HPAC Heating Plumbing Air Conditioning, 1 December 2013. [Online]. Available: https://www.hpacmag.com/features/radiant-loop-layout-patterns/. [Accessed 22 March 2018].

[40] The DOW Chemical Company, "Engineering and Operating Guide for Dowfrost and Dowfrost HD inhibited propylene glycol-based heat transfer fluids," February 2008. [Online]. Available: https://www.dow.com/webapps/lit/litorder.asp?filepath=heattrans/pdfs/noreg/180-01286.pdf. [Accessed 4 February 2018].

[41] ASHRAE, 2013 ASHRAE Handbook Fundamentals SI Edition, Atlanta, GA: ASHRAE, 2013.

[42] A. P. Boresi, R. J. Schmidt and O. M. Sidebottom, Advanced Mechanics of Materials, John Wiley & Sons, Inc., 1993.

[43] McMaster-Carr, "McMaster-Carr, M5 x 0.8 mm Thread, 30 mm Long," 23 May 2016. [Online]. Available: https://www.mcmaster.com/#91292a192/=1bb79qc. [Accessed 27 January 2018].

[44] S. R. Figliola and E. D. Beasley, Theory and Design for Mechanical Measurements, Fourth Edition, Hoboken: John Wiley & Sons, Inc., 2006.

[45] C. Baldwin, "Design and Construction of an Experimental Apparatus to Assess the Performance of a Solar Absorption Chiller with Integrated Thermal Storage," Carleton University, Ottawa, 2013.

[46] Continental Control Systems, LLC, " Continental Control Systems, LLC WattNode Pulse Installation and Operation Manual," 30 November 2011. [Online]. Available: https://ctlsys.com/wp-content/uploads/2016/10/Manual_WNB_Pulse.pdf. [Accessed 13 March 2018].

[47] Intelligent-LAB, "Intelligent-LAB Centigram Balance," Intelligent-LAB, [Online]. Available: https://www.intelligentwt.com/wp-content/uploads/2016/06/Laboratory-Classic-PBW-Data-Sheet.pdf. [Accessed 16 April 2018].

Appendices

Appendix A Guarded Hot Plate Working and Assembly Drawings

The working drawings presented in this section were created as working guides for the machine shop to reference when machining the individual components of the GHP. The drawings also act as a reference to show how the GHP was constructed. In this appendix the working drawings for all the components of the GHP can be seen along with the assembly drawings for the cold plates and hot plate.

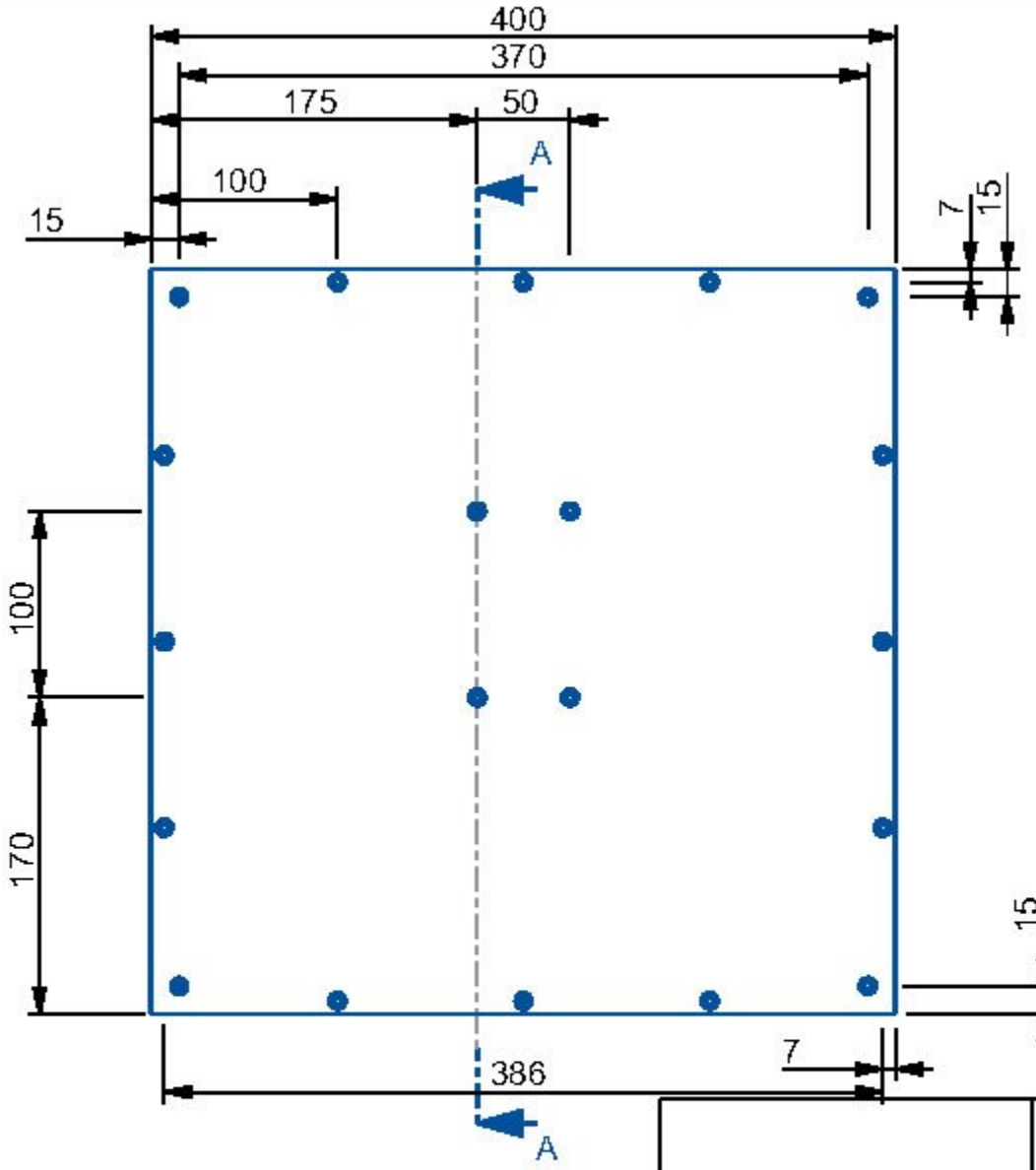

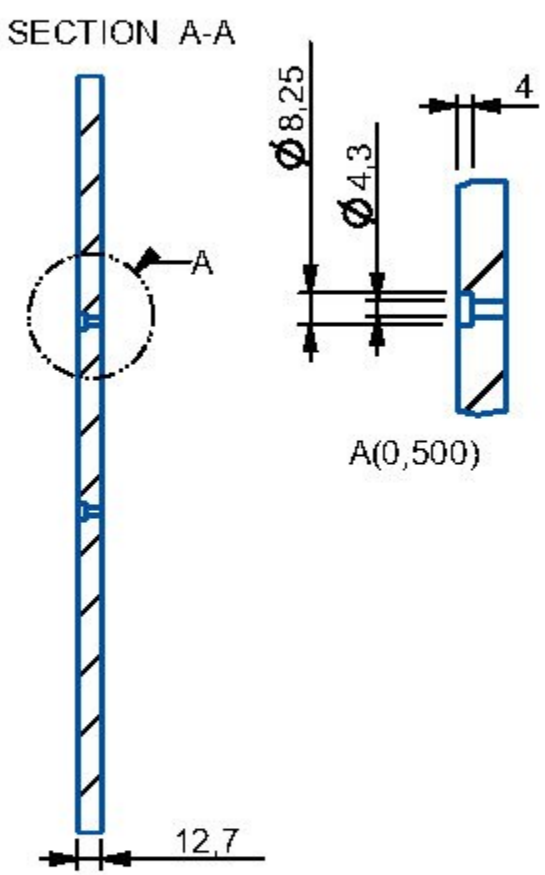

Note: some views lack hidden lines for clarity.
Unless stated tolerance +-0.254mm or 10/1000 inch

	Cold Plate Flat	
	DRW FILE: COLD_PLATE_FLAT	
	MOD FILE: COLD_PLATE_FLAT	
	SCALE: 0.250	MATL: Mic 6
Black Anodized	DRW by: A Hayes	SHEET:1 of 1
Units: mm	DATE: Dec-12-17	TYPE: PART

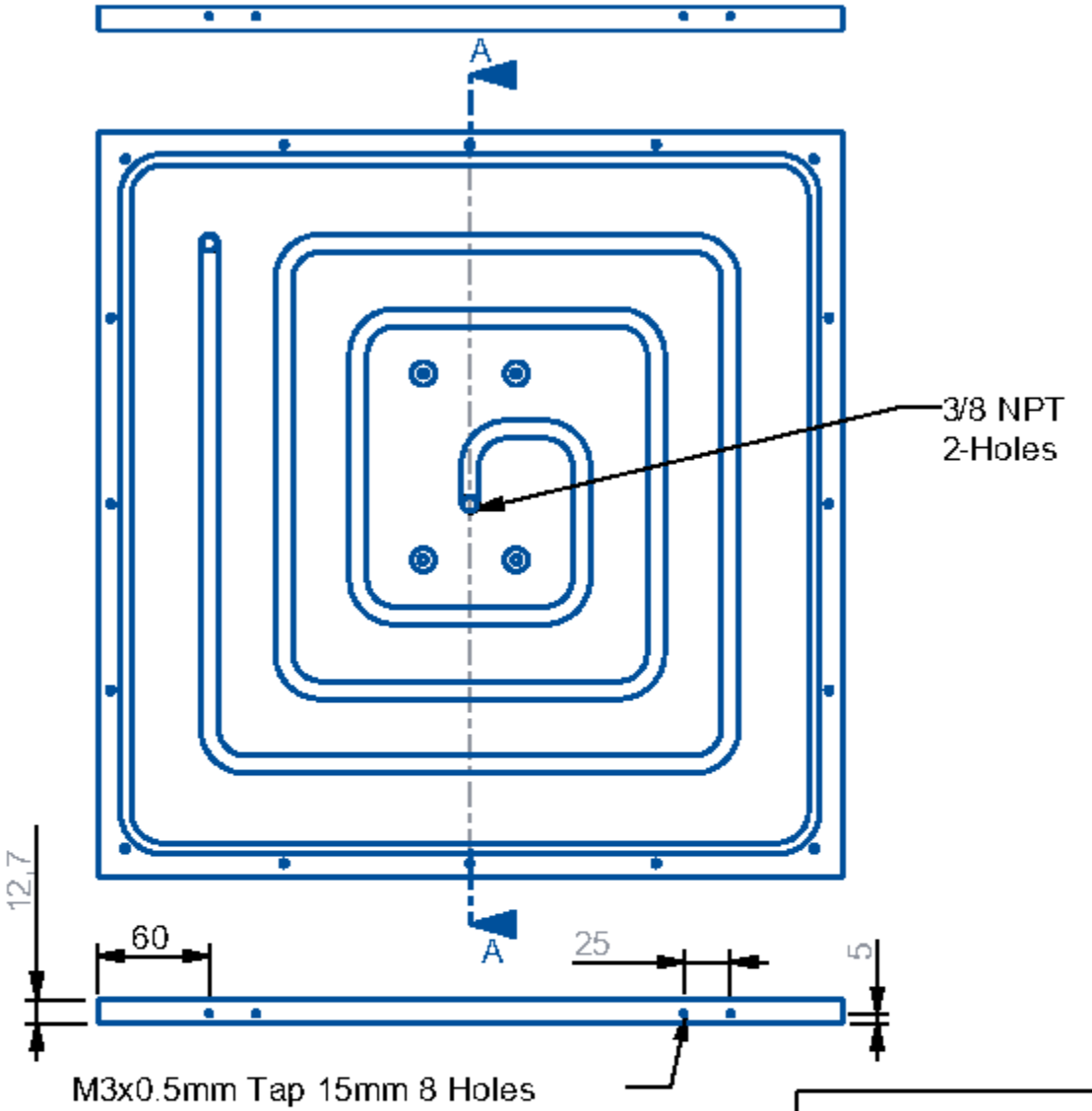

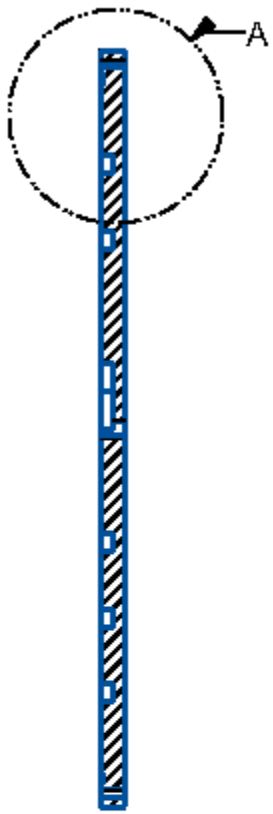

SECTION A-A

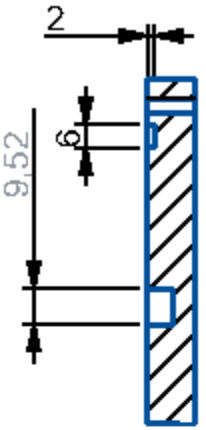

A(0,500)

Note: some views lack hidden lines for clarity. Unless stated tolerance +-0.254mm or 10/1000 inch

	Cold Plate Channel	
	DRW FILE: COLD_PLATE_CHANNEL	
	MOD FILE: COLD_PLATE_CHANNEL	
	SCALE: 0.125	MATL: Mic 6
Black Anodized	DRW by: A Hayes	SHEET: 1 of 2
Units: mm	DATE: Dec-12-17	TYPE: PART

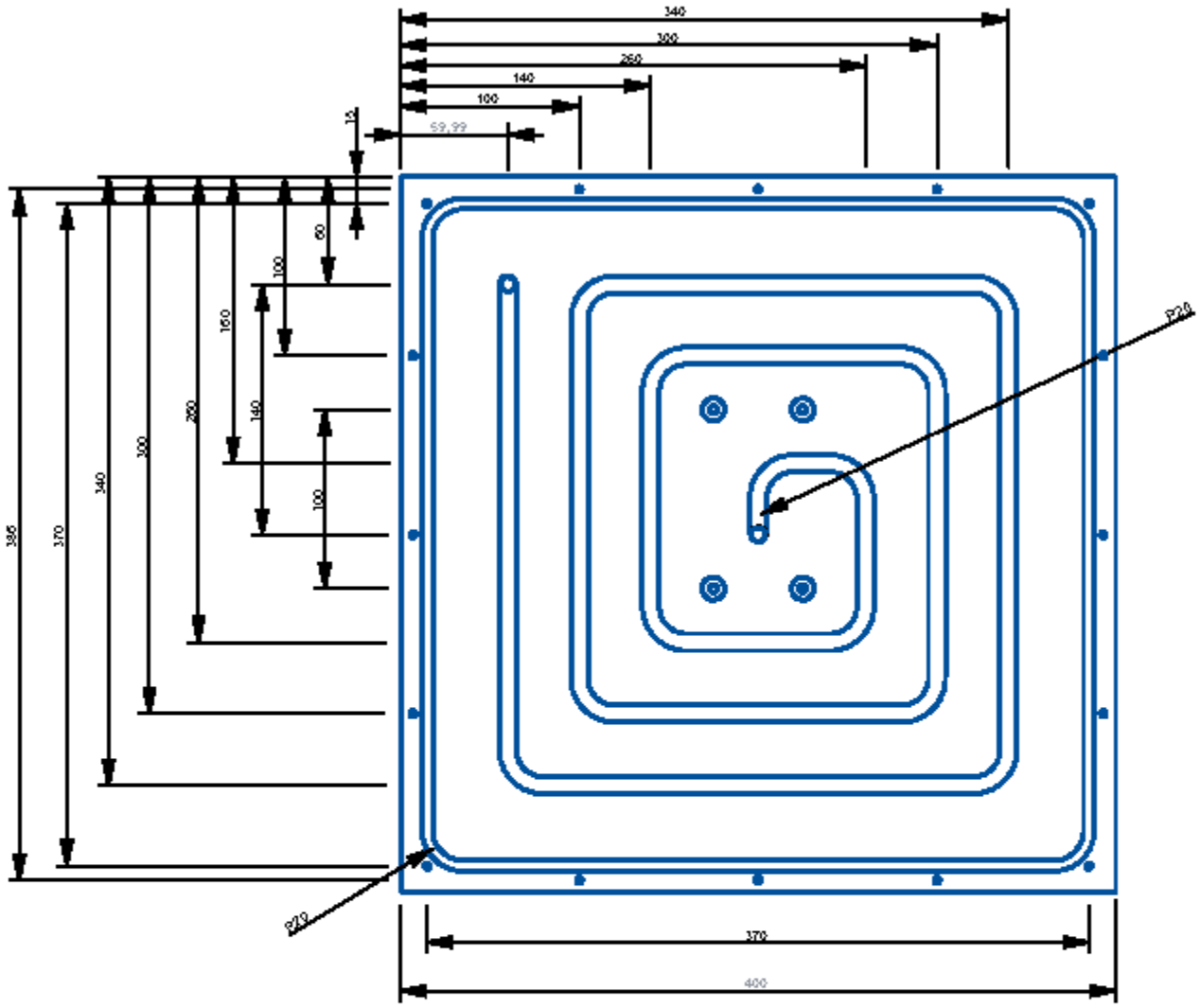

	Cold Plate Channel	
	DRW FILE: COLD_PLATE_CHANNEL_2	
	MOD FILE: COLD_PLATE_CHANNEL	
	SCALE: 0.250	MATL: Mic 6
Black Anodized	DRW by: A Hayes	SHEET:2 of 2
Units: mm	DATE: Dec-12-17	TYPE: PART

Note: some views lack hidden lines for clarity. Unless stated tolerance +-0.254mm or 10/1000 inch

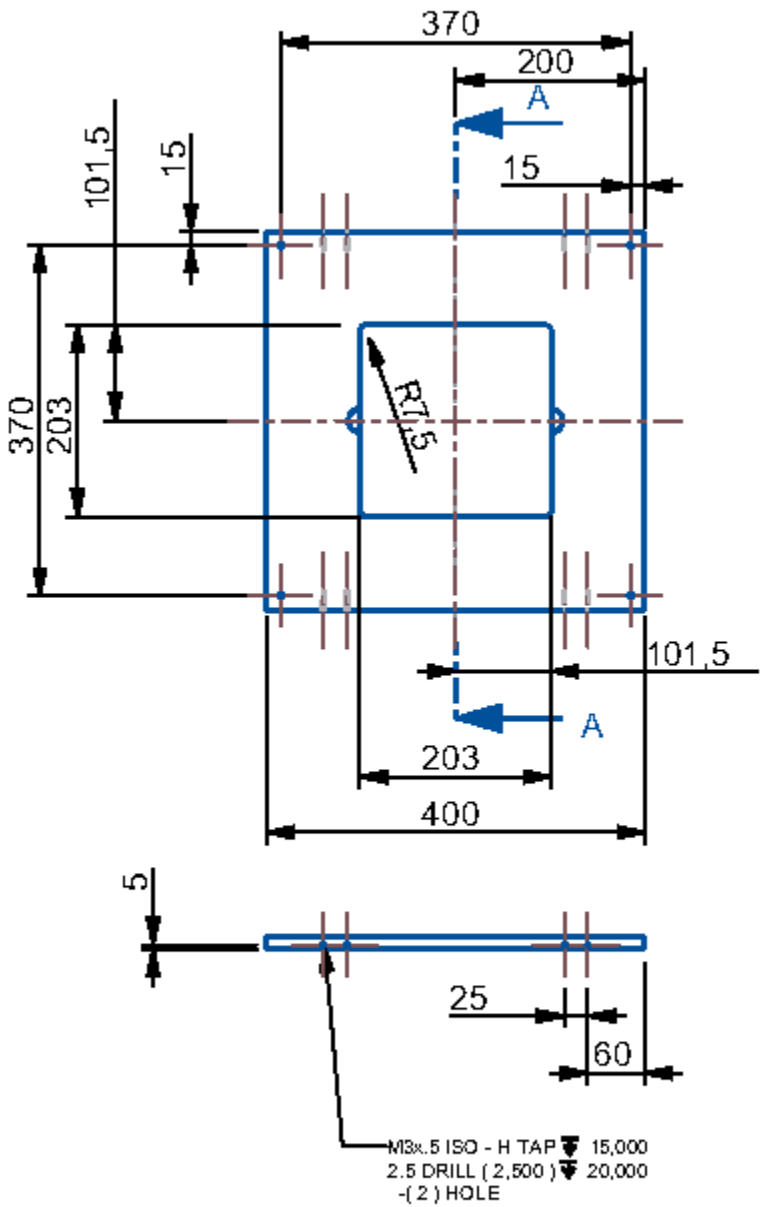

SECTION A-A

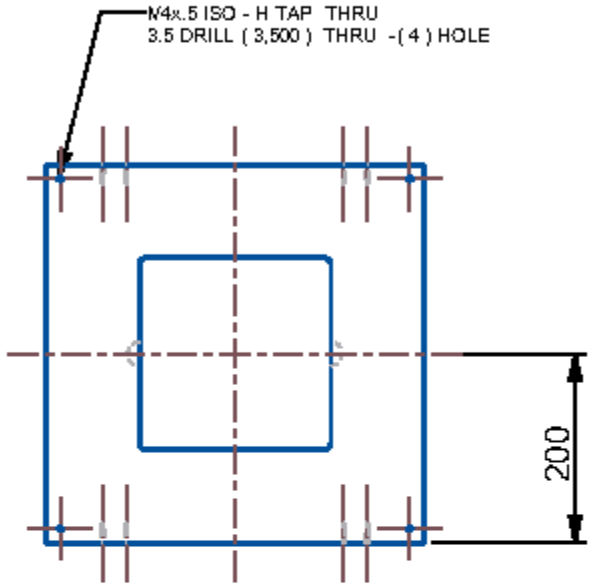

Note: some views lack hidden lines for clarity.
Unless stated tolerance +-0.254mm or 10/1000 inch

	Guard Ring Top	
	DRW FILE: GUARD_RING_TOP	
	MOD FILE: GUARD_RING_TOP	
	SCALE: 0,125	MATL: Mic 6
Anodized Black	DRW by: A Hayes	SHEET:1 of 2
Units: mm	DATE: Nov-08-16	TYPE: PART

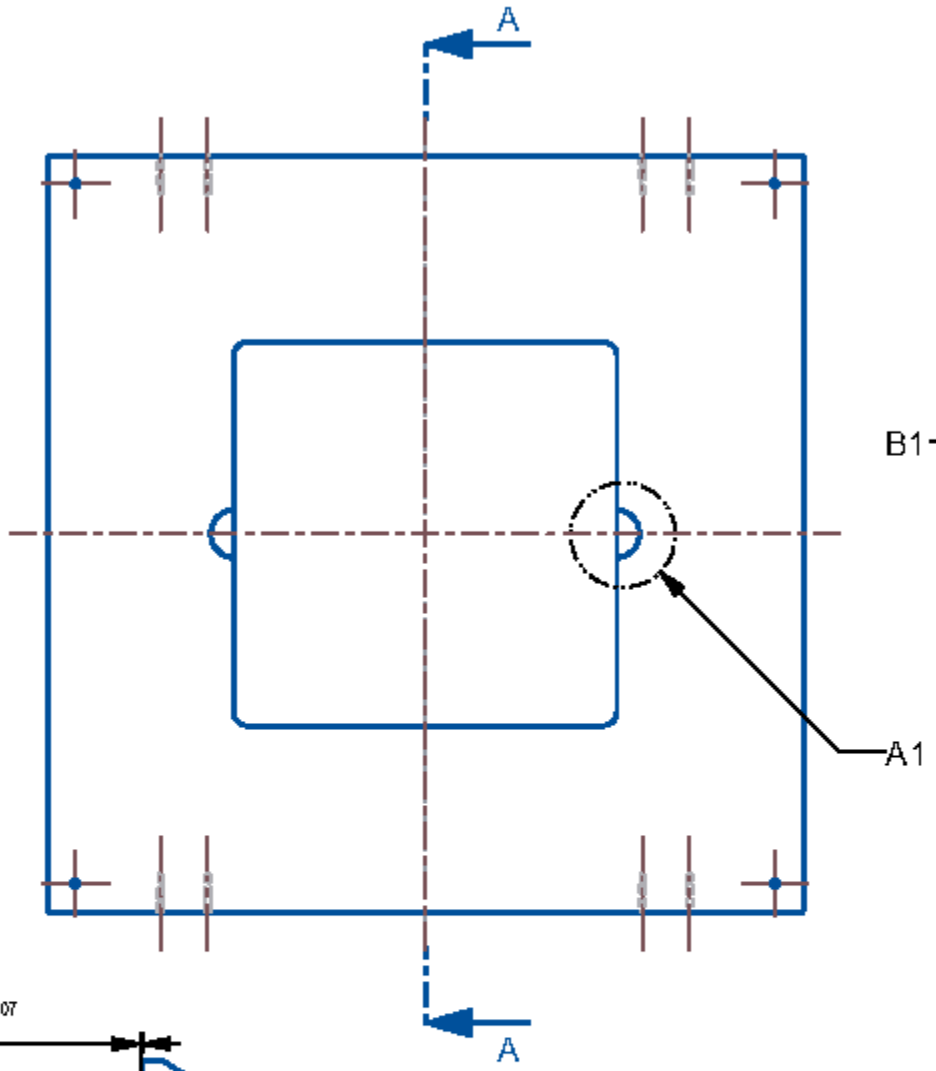

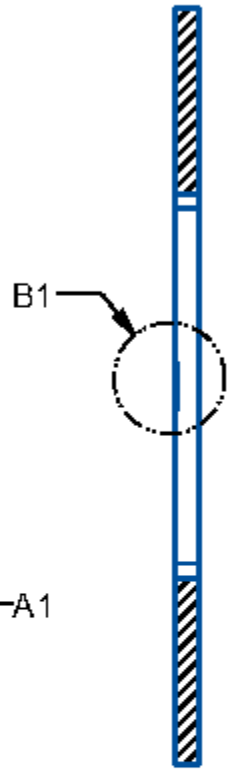

SECTION A-A

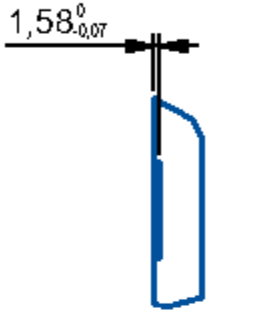

B1(0,500)

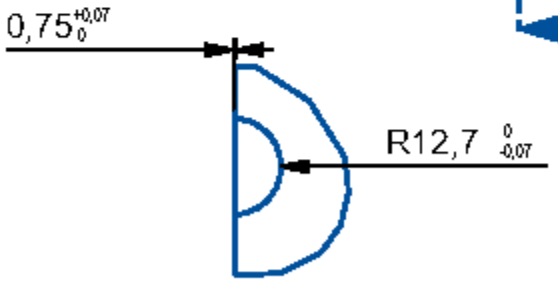

A1(0,500)

Note: some views lack hidden lines for clarity.
Unless stated tolerance +-0.254mm or 10/1000 inch

	Guard Ring Top	
	DRW FILE: GUARD_RING_TOP_2	
	MOD FILE: GUARD_RING_TOP	
	SCALE: 0,125	MATL: Mic 6
Anodized Black	DRW by: A Hayes	SHEET:2 of 2
Units: mm	DATE: Nov-08-16	TYPE: PART

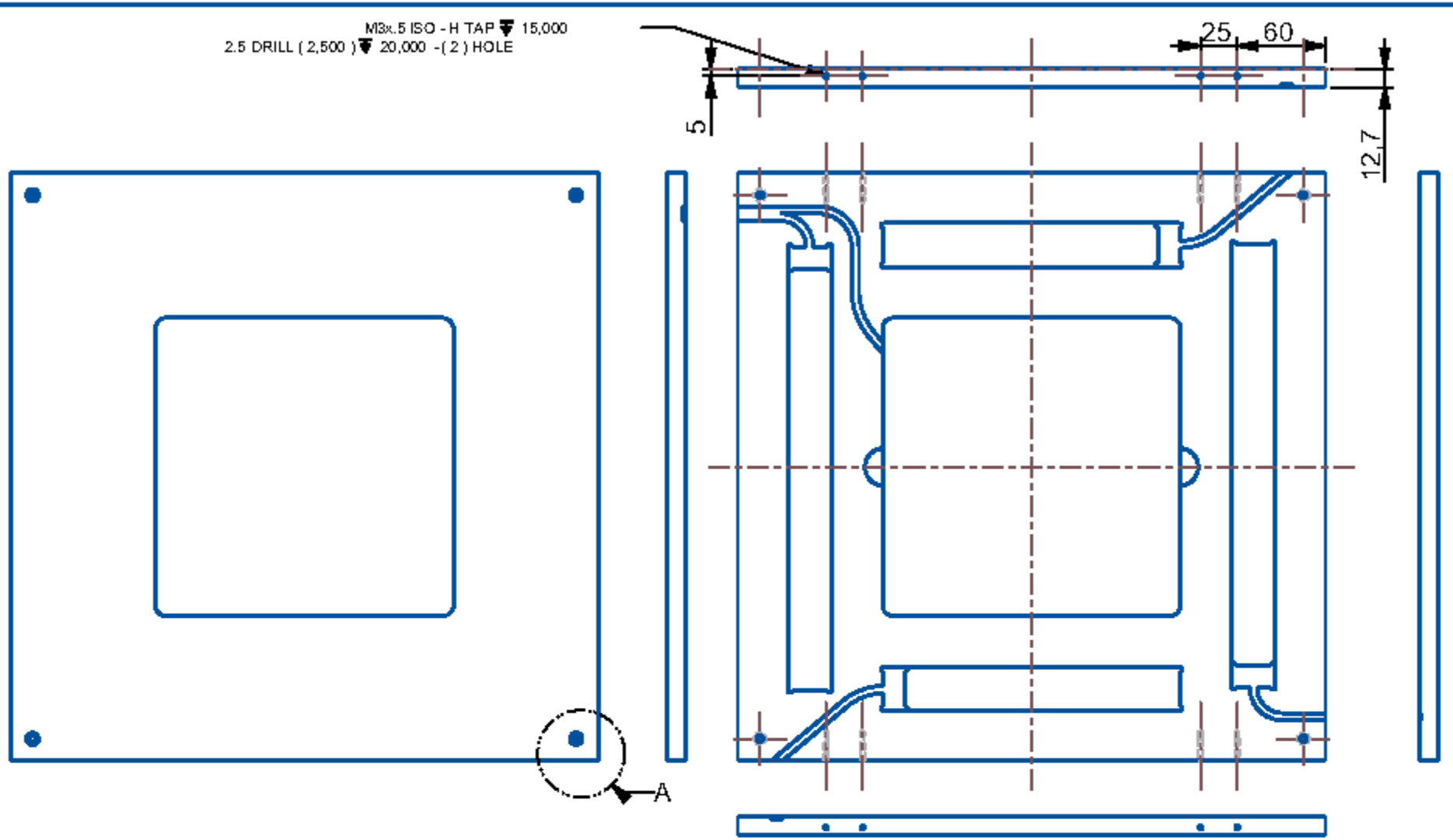

Note: some views lack hidden lines for clarity.
Unless stated tolerance +-0.254mm or 10/1000 inch

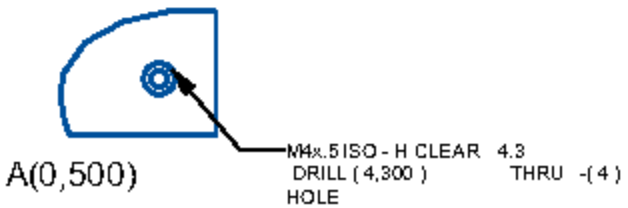

	Guard Ring Bottom	
	DRW FILE: GUARD_RING_BOTTOM	
	MOD FILE: GUARD_RING_BOTTOM	
	SCALE: 0,250	MATL: Mic 6
Anodized Black	DRW by: A Hayes	SHEET:1 of 3
Units: mm	DATE: Nov-08-16	TYPE: PART

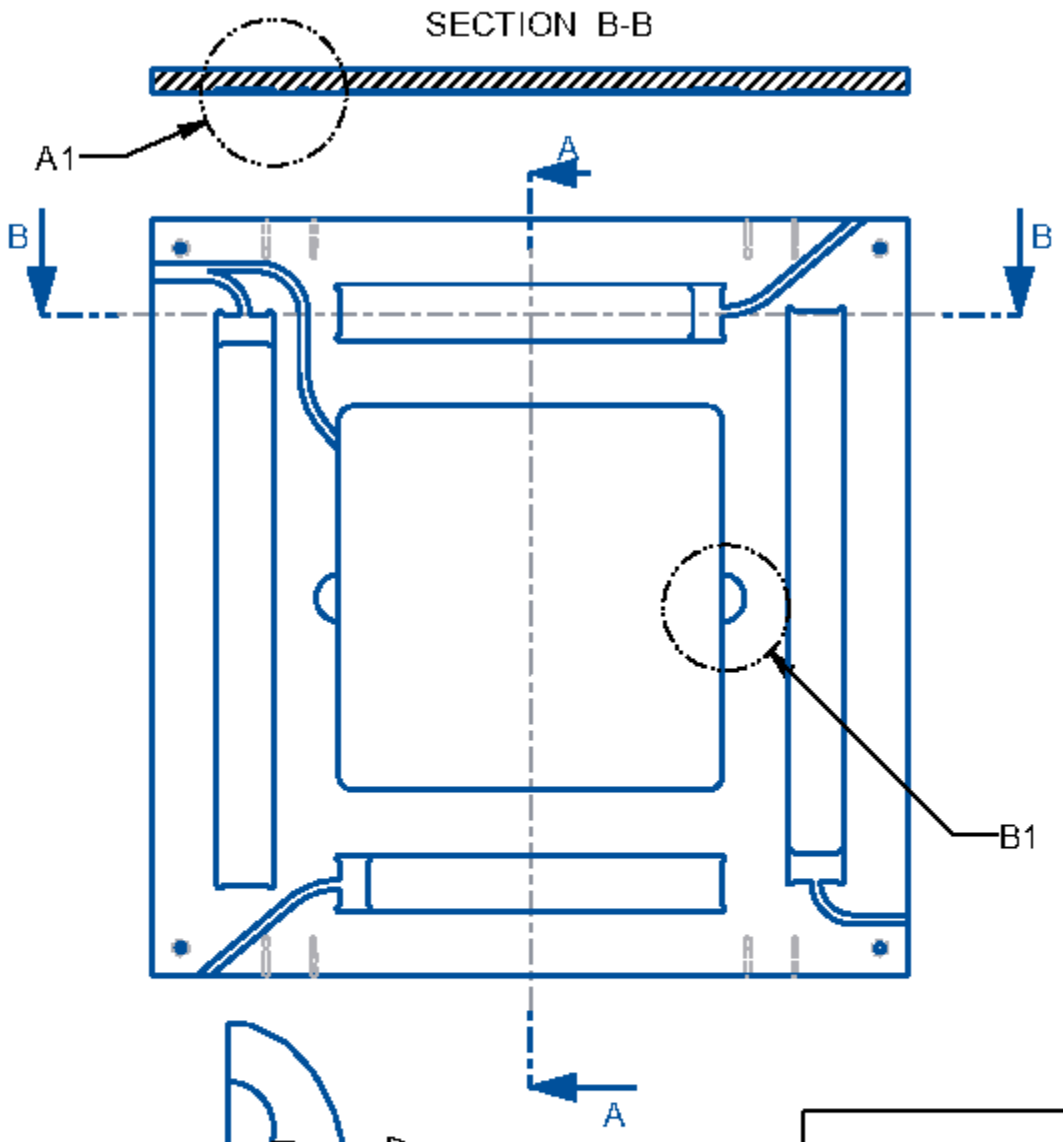

B1(0,500)

SECTION A-A

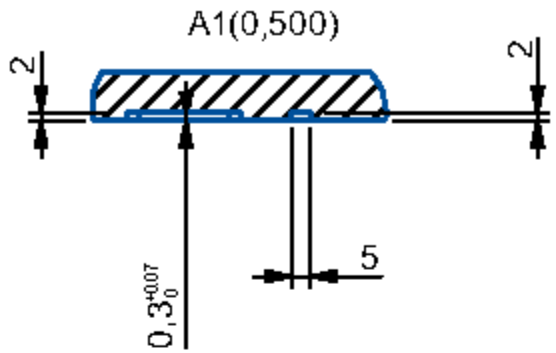

Note: some views lack hidden lines for clarity.
Unless stated tolerance +-0.254mm or 10/1000 inch

	Guard Ring Bottom	
	DRW FILE: GUARD_RING_BOTTOM_2	
	MOD FILE: GUARD_RING_BOTTOM	
	SCALE: 0,250	MATL: Mic 6
Anodized Black	DRW by: A Hayes	SHEET:2 of 3
Units: mm	DATE: Nov-08-16	TYPE: PART

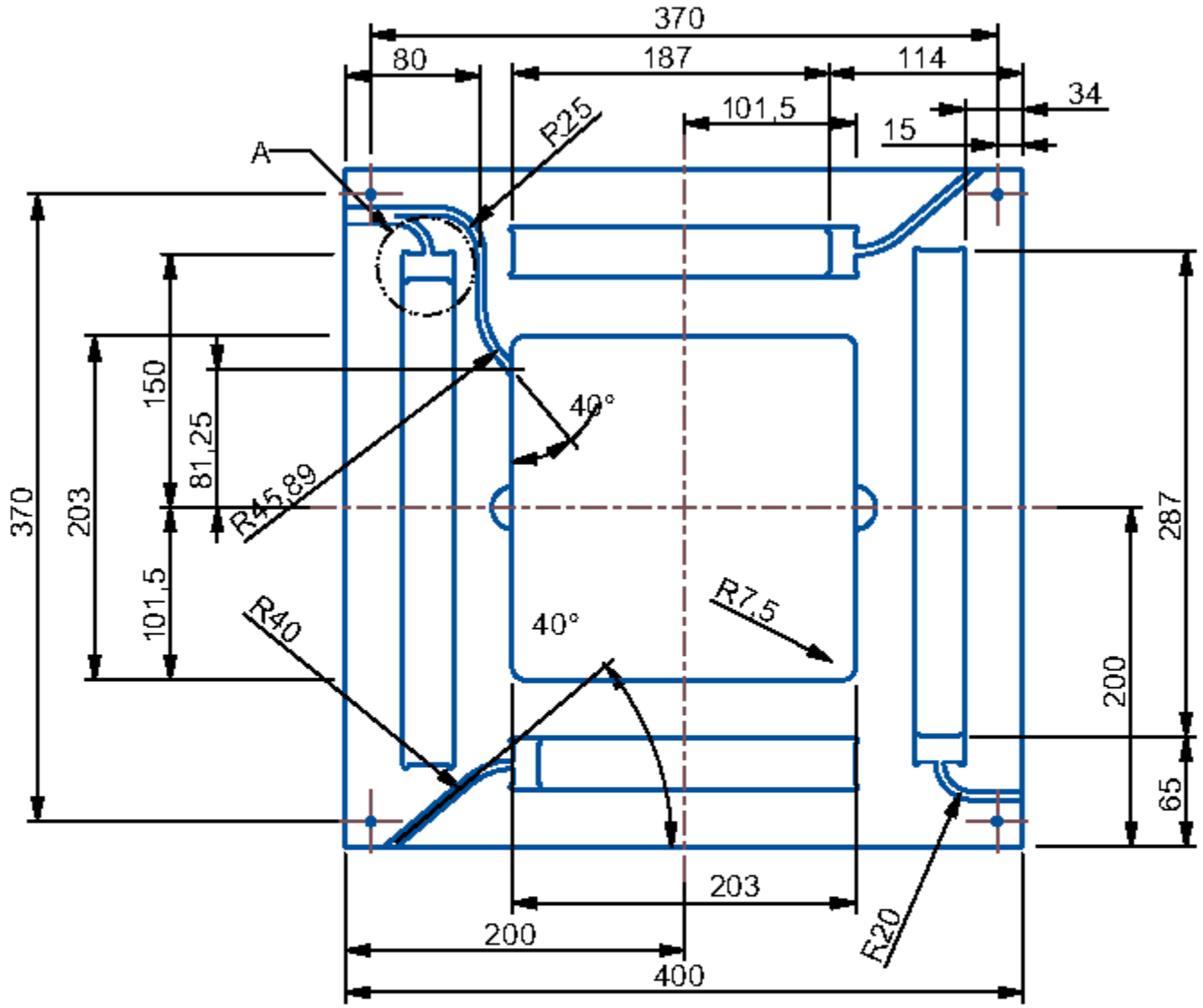

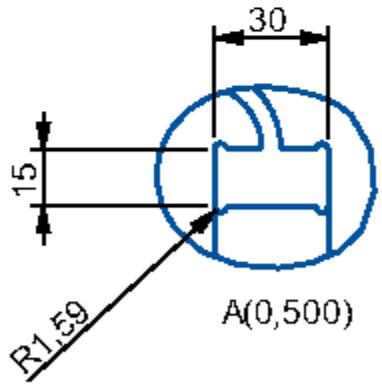

Note: some views lack hidden lines for clarity.
Unless stated tolerance +-0.254mm or 10/1000 inch

	Guard Ring Bottom	
	DRW FILE: GUARD_RING_BOTTOM_3	
	MOD FILE: GUARD_RING_BOTTOM	
	SCALE: 0,250	MATL: Mic 6
Anodized Black	DRW by: A Hayes	SHEET:3 of 3
Units: mm	DATE: Nov-08-16	TYPE: PART

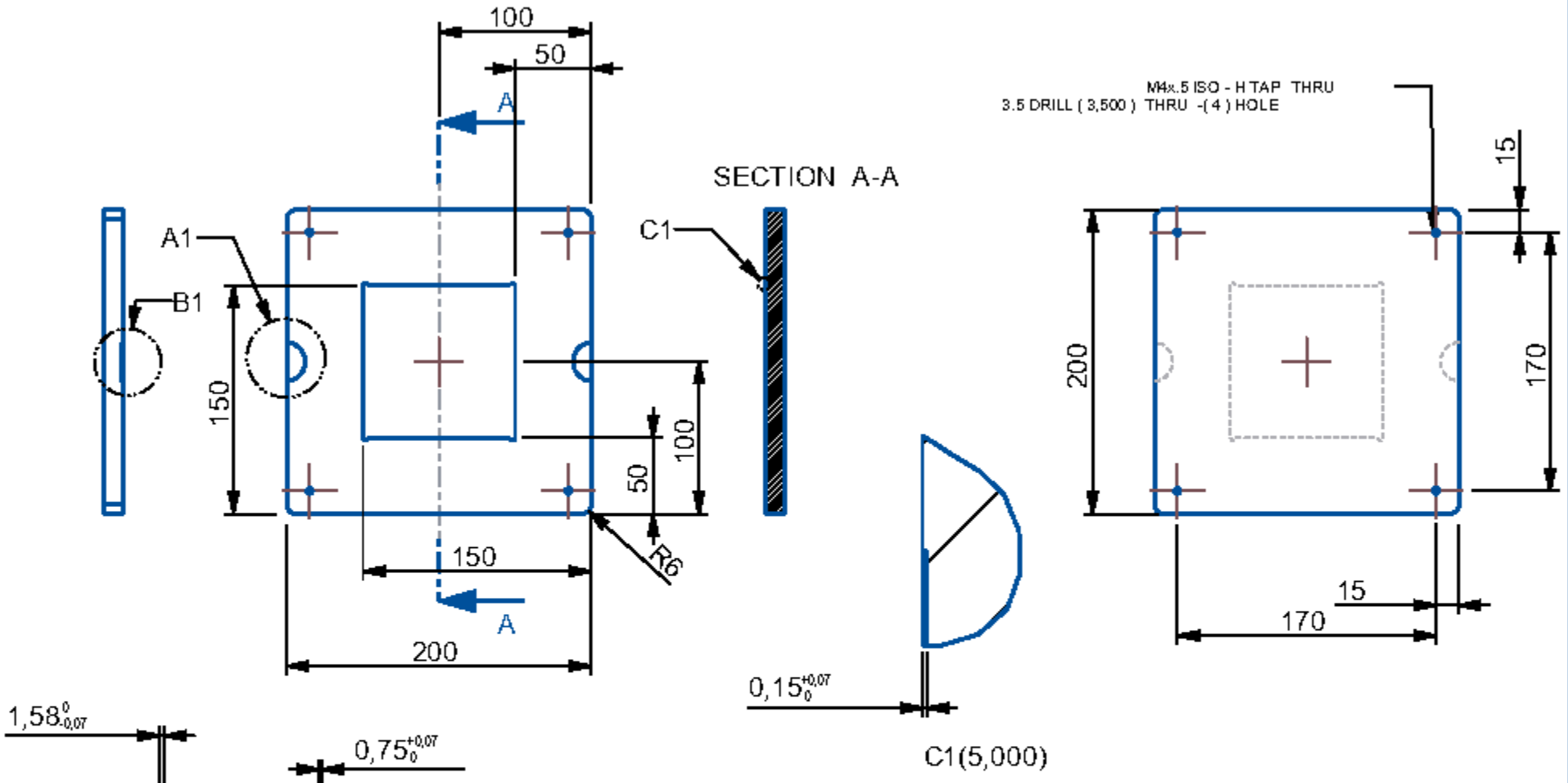

Note: some views lack hidden lines for clarity.
Unless stated tolerance +-0.254mm or 10/1000 inch

	Meter Plate Top	
	DRW FILE: METER_PLATE_TOP	
	MOD FILE: METER_PLATE_TOP	
	SCALE: 0,250	MATL: Mic 6
Anodized Black	DRW by: A Hayes	SHEET:1 of 1
Units: mm	DATE: Nov-08-16	TYPE: PART

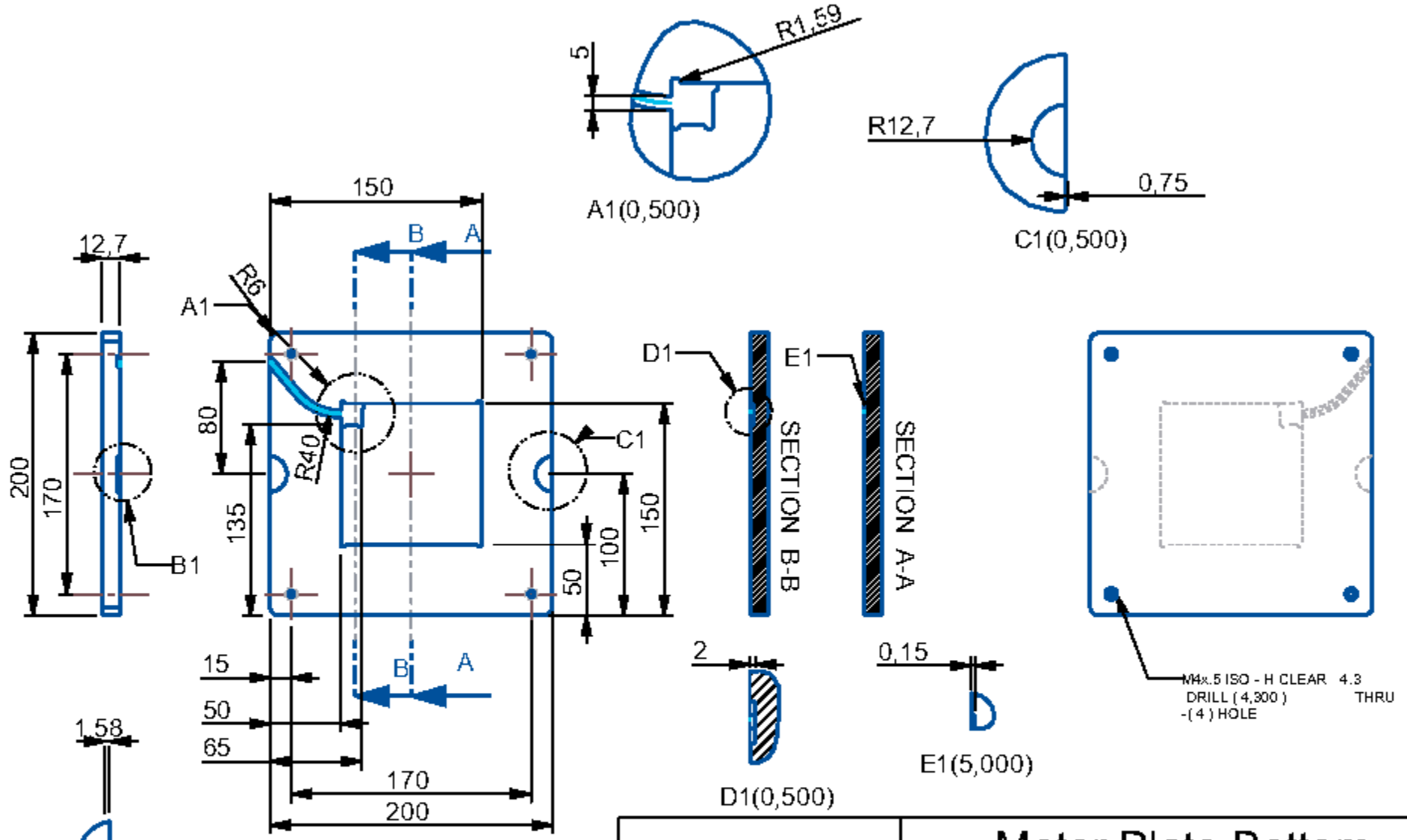

Note: some views lack hidden lines for clarity.
Unless stated tolerance +-0.254mm or 10/1000 inch

	Meter Plate Bottom	
	DRW FILE: METER_PLATE_BOTTOM	
	MOD FILE: METER_PLATE_BOTTOM	
	SCALE: 0,250	MATL: Mic 6
Anodized Black	DRW by: A Hayes	SHEET:1 of 1
Units: mm	DATE: Nov-08-16	TYPE: PART

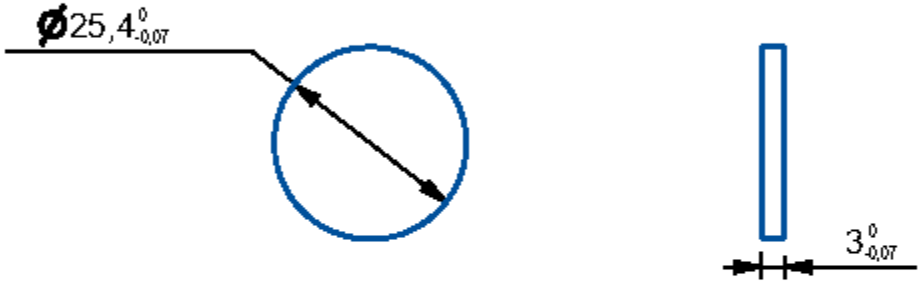

Note: some views lack hidden lines for clarity.
Unless stated tolerance +-0.254mm or 10/1000 inch

	Meter Plate Spacer	
	DRW FILE: METER_PLATE_SPACER	
	MOD FILE: METER_PLATE_SPACER	
	SCALE: 1,000	MATL: Polyoxymethylene
	DRW by: A Hayes	SHEET:1 of 1
Units: mm	DATE: Nov-08-16	TYPE: PART

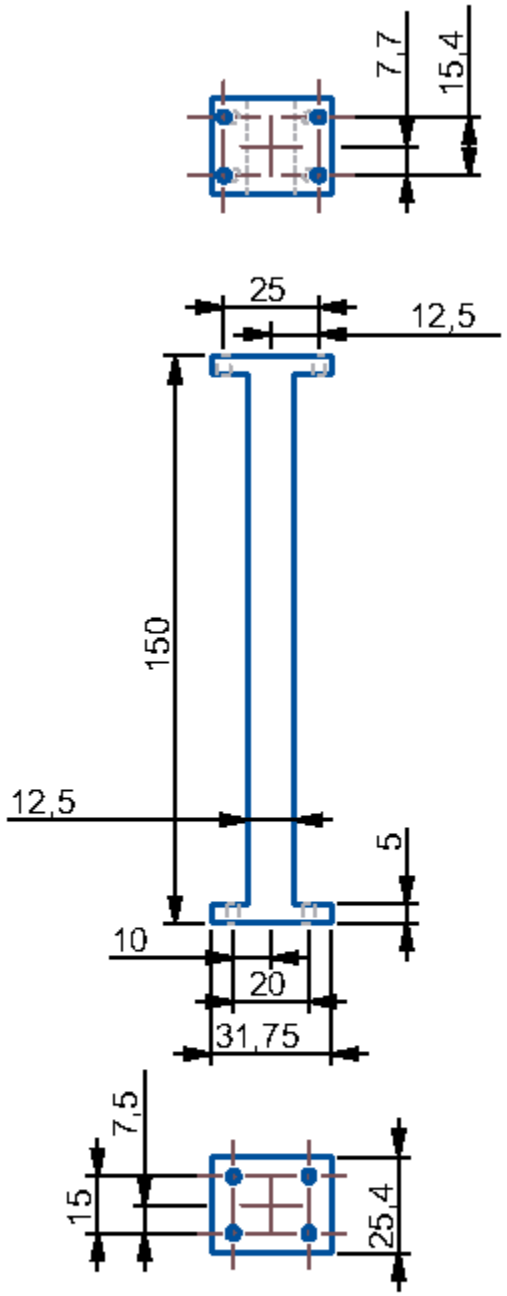

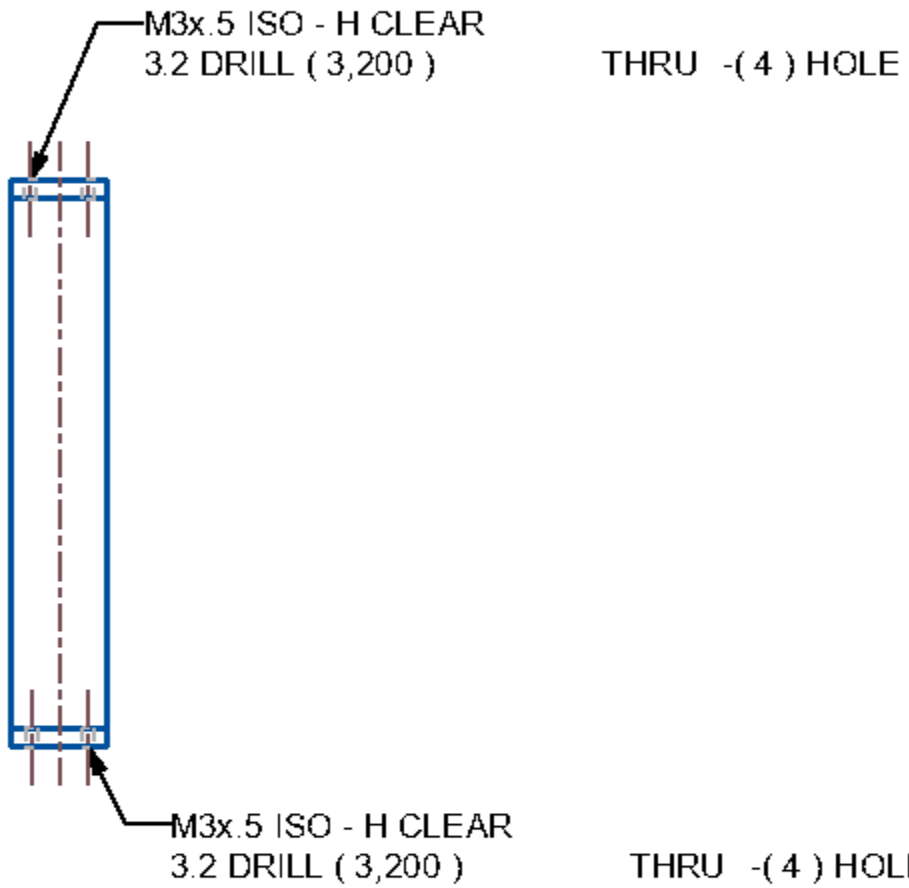

Note: some views lack hidden lines for clarity.
Unless stated tolerance +-0.254mm or 10/1000 inch

	Short Leg	
	DRW FILE: SHORT_LEG	
	MOD FILE: SHORT_LEG	
	SCALE: 0,500	MATL: Aluminum
	DRW by: A Hayes	SHEET:1 of 1
Units: mm	DATE: Dec-12-17	TYPE: PART

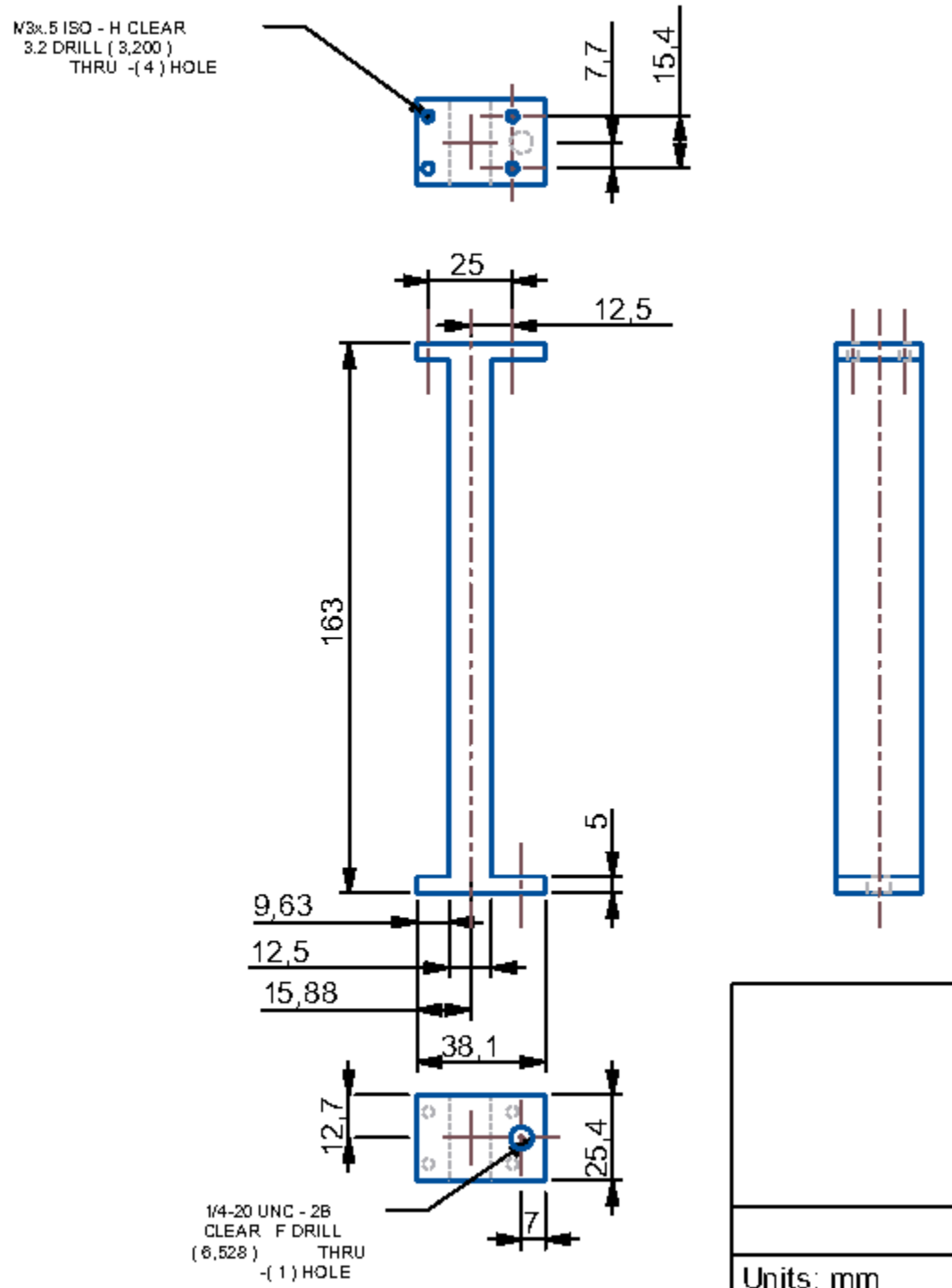

Note: some views lack hidden lines for clarity.
Unless stated tolerance +-0.254mm or 10/1000 inch

	Long Leg	
	DRW FILE: LONG_LEG	
	MOD FILE: LONG_LEG	
	SCALE: 0,500	MATL: Aluminum
	DRW by: A Hayes	SHEET:1 of 1
Units: mm	DATE: Dec-12-17	TYPE: PART

ITEM NO	PART NUMBER	QTY	DESCRIPTION	NOTES
1	COLD_PLATE_CHANNEL	1	cold_plate_channel.prt	
2	COLD_PLATE_FLAT	1	cold_plate_flat.prt	
3	LONG_LEG	4	long_leg.prt	
4	MC_9452K382	1	O-Ring 1/8 by 18" ID	McMaster Carr

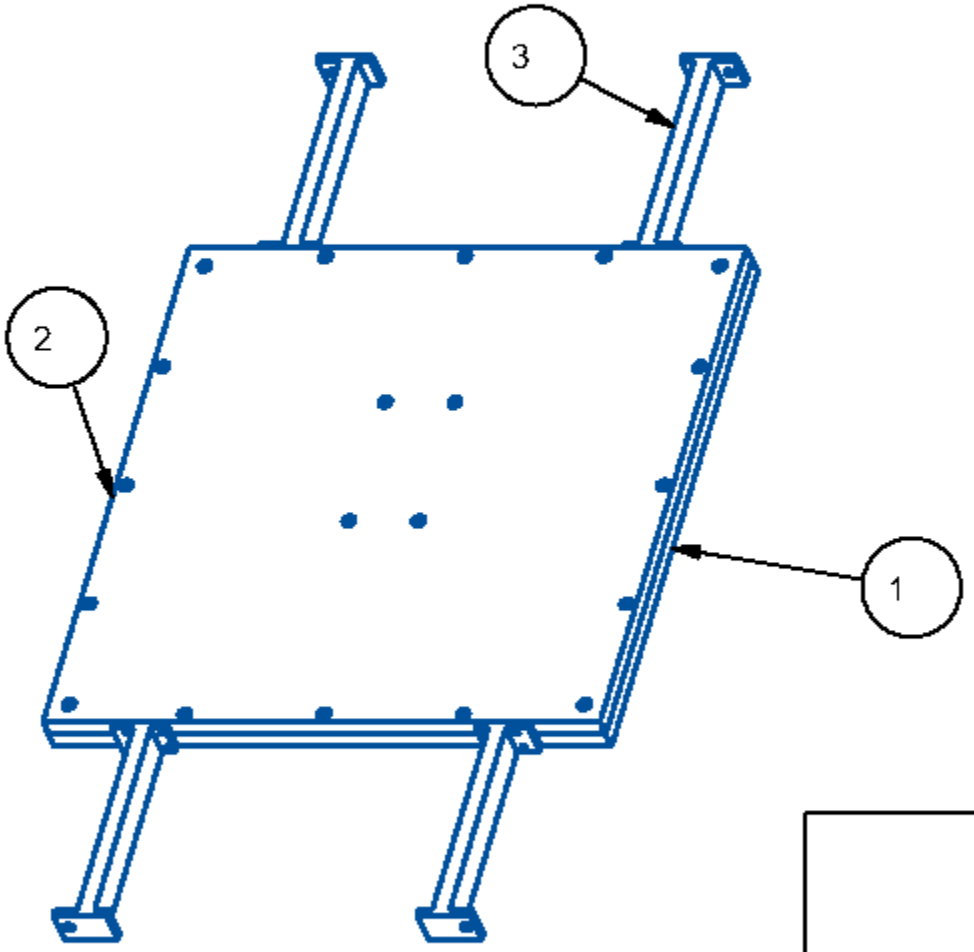

	Cold Plate Fixed Assembly	
	DRW FILE: COLD_PLATE_FIXED	
	MOD FILE: COLD_PLATE_FIXED	
	SCALE: 0.2	
	DRW by: A Hayes	SHEET:1 of 1
	DATE: Dec-12-17	TYPE: ASSEM

ITEM NO	PART NUMBER	QTY	DESCRIPTION	NOTES
1	COLD_PLATE_CHANNEL	1	cold_plate_channel.prt	
2	COLD_PLATE_FLAT	1	cold_plate_flat.prt	
3	MC_9880K2	4		McMaster Carr
4	SHORT_LEG	4	short_leg.prt	
5	MC_9452K382	1	O-Ring 1/8 by 18" ID	McMaster Carr

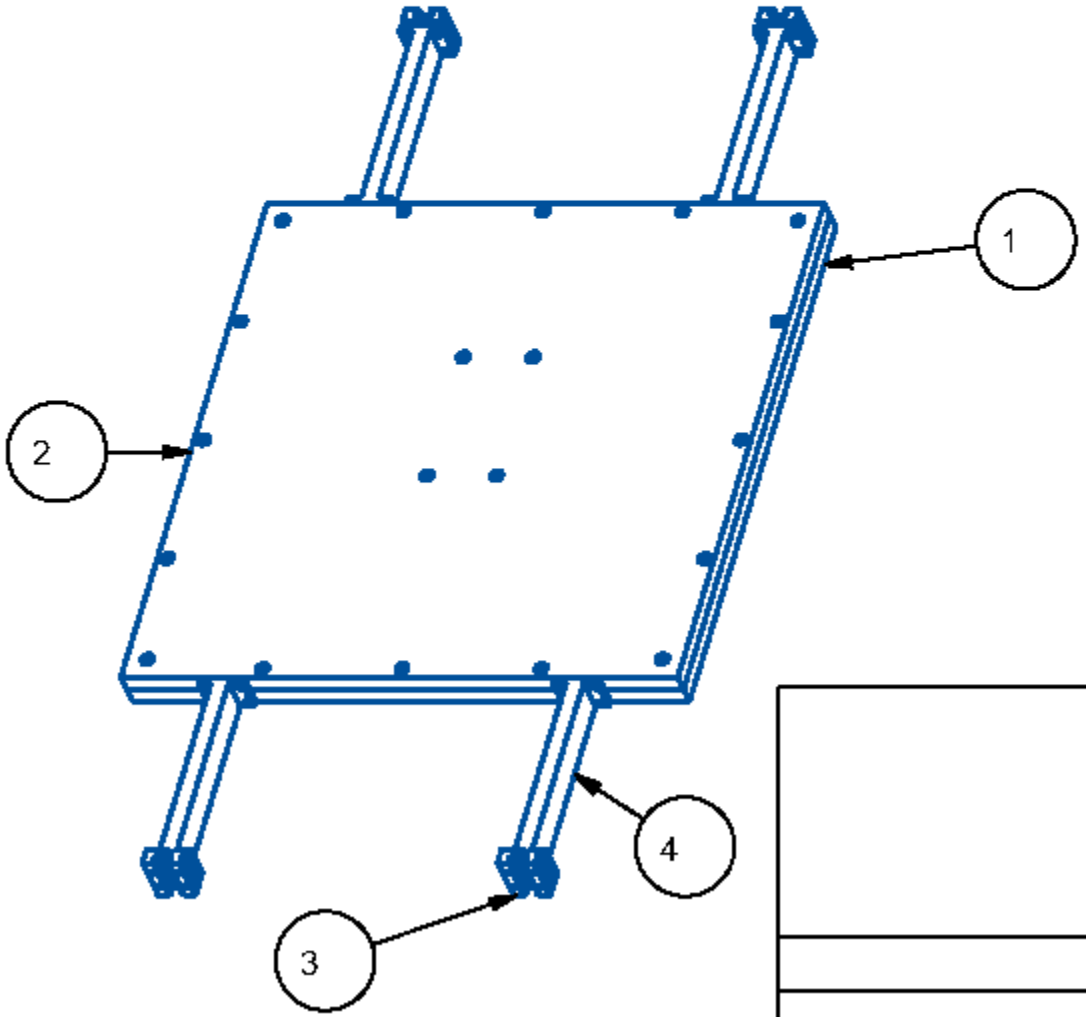

	Cold Plate Free Assembly	
	DRW FILE: COLD_PLATE_FREE	
	MOD FILE: COLD_PLATE_FREE	
	SCALE: 0.2	
	DRW by: A Hayes	SHEET:1 of 1
	DATE: Dec-12-17	TYPE: ASSEM

ITEM NO	PART NUMBER	QTY	DESCRIPTION	NOTES
1	GUARD_RING_BOTTOM	1	guard_ring_bottom.prt	
2	GUARD_RING_TOP	1	guard_ring_top.prt	
3	MC_9880K2	4		McMaster Carr
4	METER_PLATE_BOTTOM	1	meter_plate_bottom.prt	
5	METER_PLATE_SPACER	2	meter_plate_spacer.prt	
6	METER_PLATE_TOP	1	meter_plate_top.prt	
7	SHORT_LEG	4	short_leg.prt	

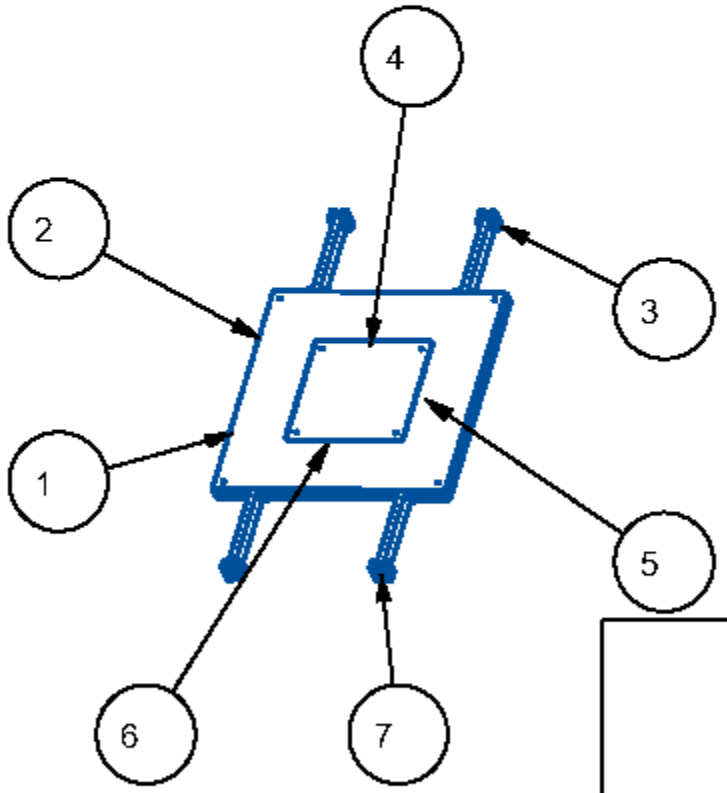

Hot Plate Assembly

	DRW FILE: HOT_PLATE	
	MOD FILE: HOT_PLATE	
	SCALE: 0,083	MATL:
	DRW by: A Hayes	SHEET:1 of 1
	DATE: Nov-08-16	TYPE: ASSEM

ITEM NO	PART NUMBER	QTY	DESCRIPTION	NOTES
1	COLD_PLATE_FIXED	1	cold_plate_fixed.asm	
2	COLD_PLATE_FREE	1	cold_plate_free.asm	
3	HOT_PLATE	1	hot_plate.asm	
4	MC_9880K12	4		McMaster Carr

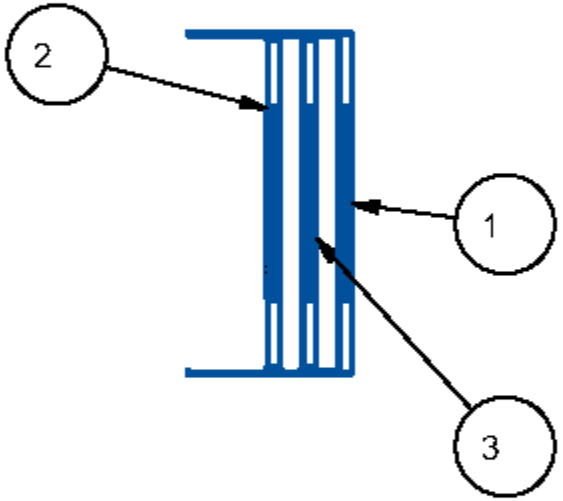

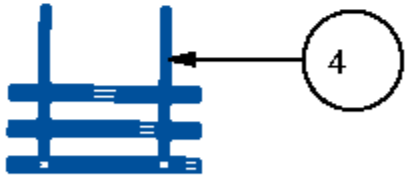

	GHP Assembly	
	DRW FILE: GHP	
	MOD FILE: GHP	
	SCALE: 0,063	MATL:
	DRW by: A Hayes	SHEET:1 of 1
	DATE: Nov-08-16	TYPE: ASSEM

Appendix B Deflection of Cold Plates with Cooling Fluid

To determine if the aluminum plates of the cold plate assembly would separate during testing due to the fluid flowing between the two plates, a process as outlined by Boresi, et al, [42] to calculate the deflection $W_{\max}$ of the aluminum plates was adapted for use in this study. As the cold plates were designed with 16 bolts spread around the outer perimeter of the plates it was decided that the plates could be modeled as a square plate with fixed edges when calculating the deflection at the center of the plates. As the cooling fluid would be spread over the entire face of the plates, the system was modeled as a square plate with fixed edges subjected to a uniformly distributed load represented by Equation B.1.

$$W_{\max} = C(1 - v^2)(pb^4/Eh^3) \quad \textbf{(B.1)}$$

where

$$C = \frac{0.032}{1 + \alpha^4} \quad \textbf{(B.2)}$$

and

$$\alpha = {}^{b}/_{a} \quad \textbf{(B.3)}$$

where a and b are the lengths of the sides of the plate, and in this case $a = b$ = 400 mm and α = 1. In Equation B.1, h is the thickness of the plate at 12.7 mm, E is Young's Modulus, v is Poisson's Ratio and p is the pressure of the system in Pa. As the aluminum used in the machining of the plates was Mic 6 tooling plate, which is a 7000 series aluminum, the material properties could be obtained from material properties tables. Using the values for 7075 T6 Aluminum Alloy from Table A.1 [42], the values E = 72 x 10^6 Pa, v = 0.33 were obtained. The working pressure in the GHP cooling loop was contained to a maximum pressure of 30 pfsi. Using the following conversion in

Equation B.4, the pressure in the system in Pascals can be calculated where p = 206.84 kPa = 20.6 x 10^4 Pa.

$$\text{kPa} = 6.894757\ x\ \text{psi} \tag{B.4}$$

Using Equation B.1, the deflection of the plates could be calculated, where a total defection of 0.5 mm was calculated. As ASTM standards requires a uniformly flat surface to maintain constant contact with the sample being tested a deflection in the cold plate's surface was not desirable. In order to ensure that the plates remained plainer, the addition of bolts at the center of the plates was made. To ensure that the bolts did not shear under the load at the center of the plate the moment M needed to be calculated which can be seen in Equation B.5 which was calculated to be 591 N.

$$M = \frac{\frac{1}{8}pb^2}{3 + 4\alpha^4} \tag{B.5}$$

Looking up the manufactures specifications for the bolts in the center of the plates a tensile strength σ of 70000 pfsi per bolt was obtained [43] which is equal to 4.8 x 10^8 Pa or 4.8 x 10^8 N/m^2. To ensure that the bolts in the center of the plates could withstand the calculated force at the center of the plates, the amount of force a bolt could carry was calculated using the tensile strength and cross sectional area A of the bolt, by rearranging Equation B.6. From the manufacturer the cross sectional area of the bolt was calculated to be 1.96 x 10^{-5} m^2.

$$\sigma = \frac{F}{A} \tag{B.6}$$

Using Equation B.6 each bolt at the center of the plate would be able to withstand 9.42 x 10^3 N of force before shearing which is greater than the moment on the plate.

However as it would be completely undesirable for the plates to move during testing, four bolts were installed at the center of the plates, resulting in a safety factor of 63 which in other applications would be considered too aggressive.

Appendix C Thermal Images of the Hot Plate Assembly

This appendix shows the hot plate assembly of the GHP heating up to a set point temperature of 45℃ in 15 second intervals. The images are arraigned from cold to hot A through E, 1 through 11.

Figure 4-2 and Figure 4-3 show the embedded thermal resistance heaters used to heat the hot plate assembly from the center out. The heating from the center out can be seen as the plates begin to heat in images A2 – E3. As the center of the plates warm, energy starts to flow outwards to the corners and the rest of the meter plate and guard ring begins to climb in temperature as seen in images A4 – E6. The meter plate and guard ring reach their final set point temperature of 45℃ after approximately 12.5 minutes and can be seen with a uniform set point temperature in images A11 – E1.

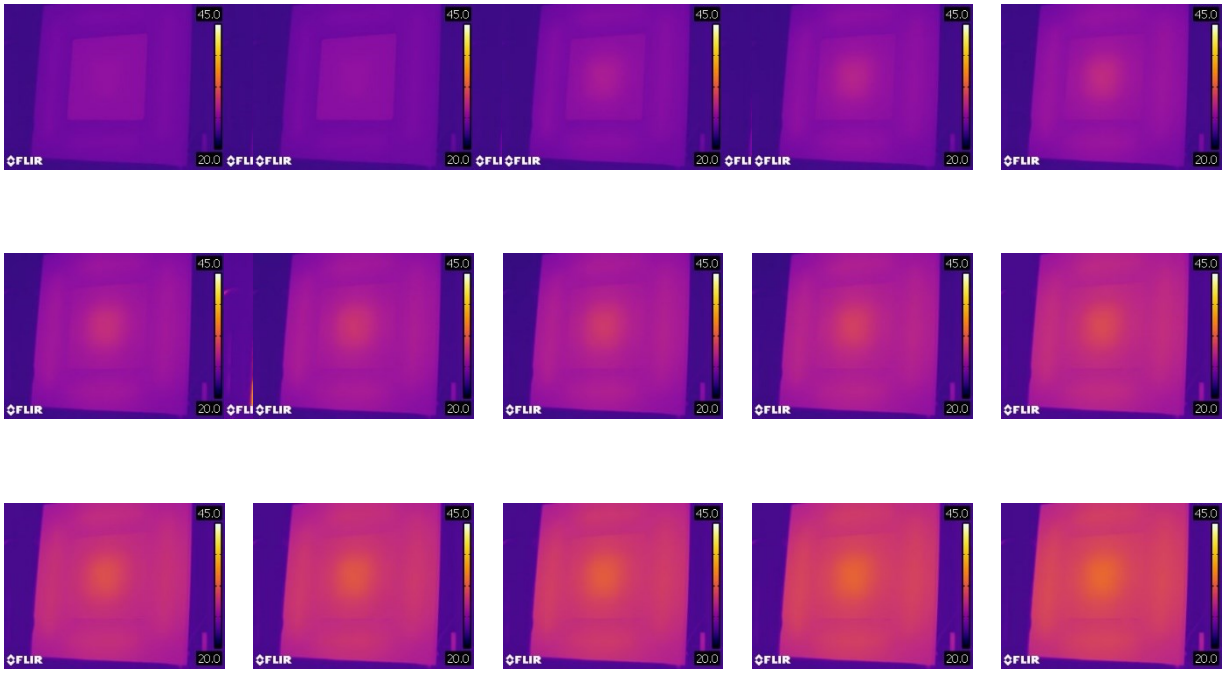

4

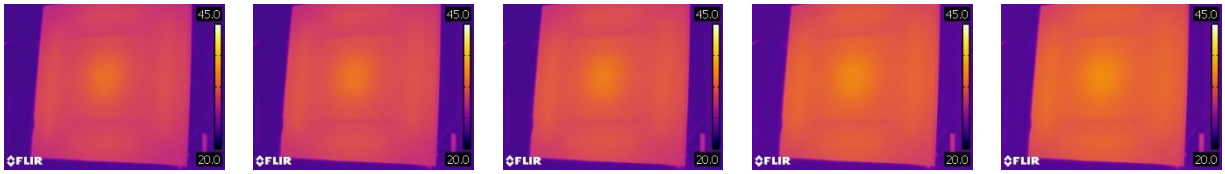
45.0
20.0
FLIR

5

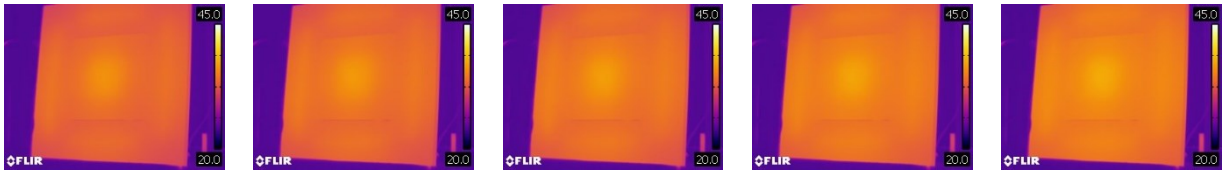
45.0
20.0
FLIR

6

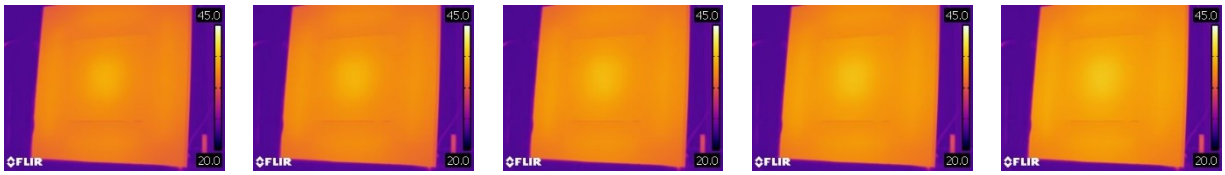
45.0
20.0
FLIR

7

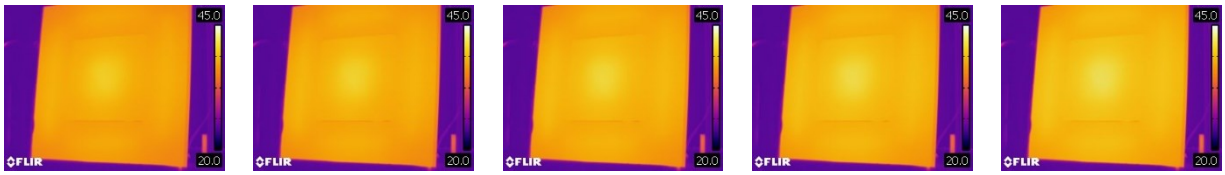
45.0
20.0
FLIR

8

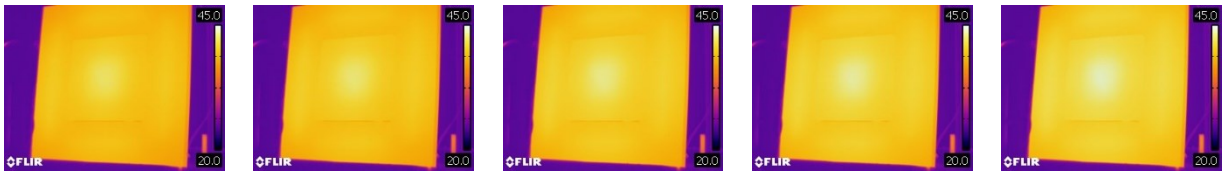
45.0
20.0
FLIR

9

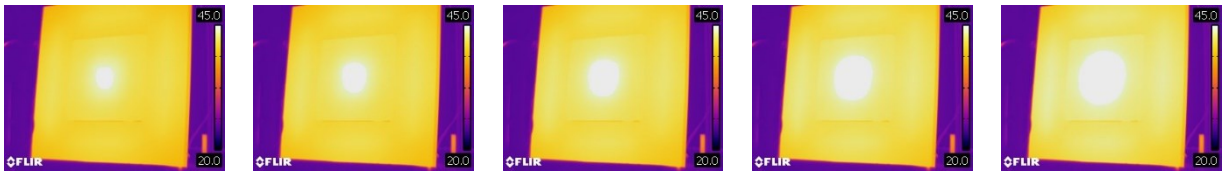
45.0
20.0
FLIR

10

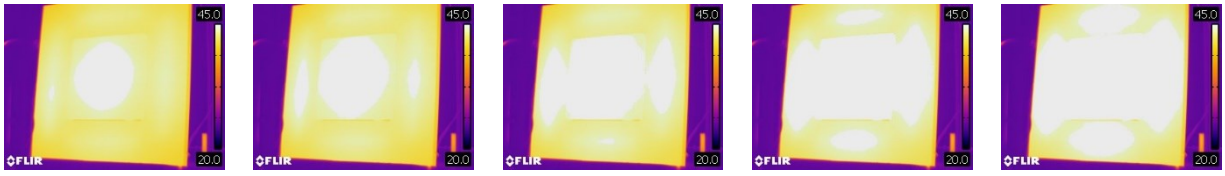

11

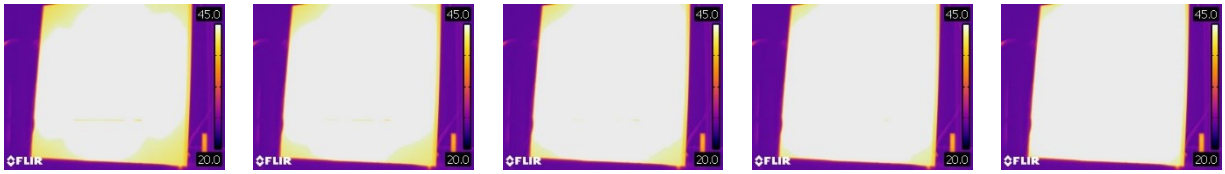

Appendix D Thermal Images of the Cold Plate Assembly

This appendix shows the cold plate assembly of the GHP cooling down to a set point temperature of 0℃ in 15 second intervals. The images are arraigned from warm to cool A through E, 1 through 6.

In the initial cooling of the plates as the cooling fluid begins to circulate within the plates, the thermal images show the cooling fluid following the internal channels within the plates. In images A1 through E2 a defined ring can be seen where the cooling fluid enters the plates at the bottom right of the image and circulates counter clockwise around the perimeter of the plate. The plates reach a uniform temperature around the five minute mark at image E4 and remain at a uniform temperature for the duration of the testing.

	A	B	C	D	E
1		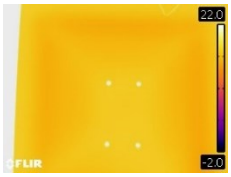		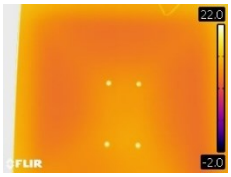	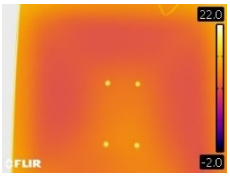
2	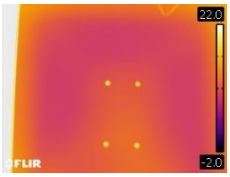	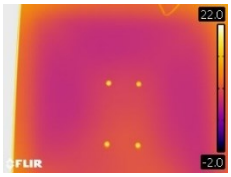	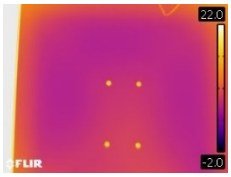	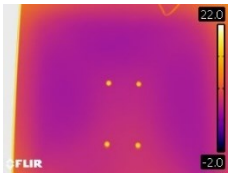	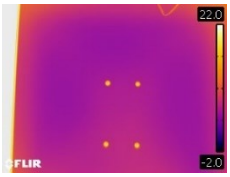
3	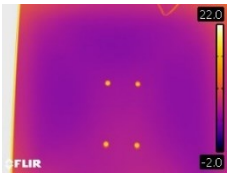	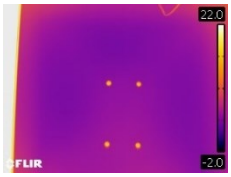	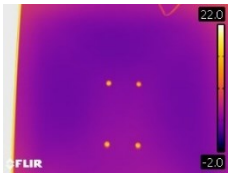	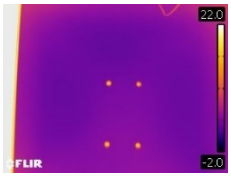	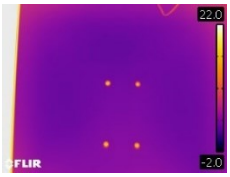

4

5

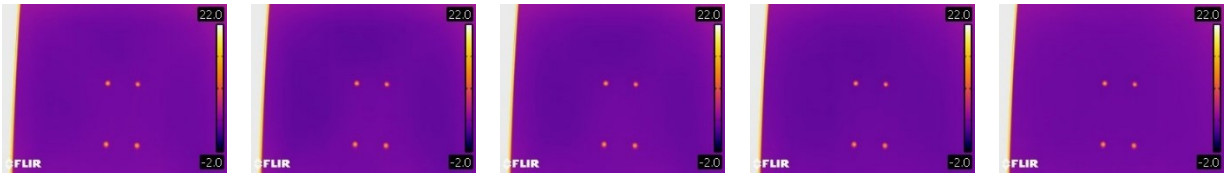

6

Appendix E Uncertainty Analysis

In the analysis of the VIPs within this study, the thermal resistance as well as the mass of the panels will be discussed and as such an uncertainty analysis on the measured and calculated results was conducted and can be seen in detail in Appendix E. In the following section the uncertainty of both the calculated thermal resistance and the measured mass of the panels is presented.

E.1 Uncertainty Analysis on Thermal Resistance Calculations

To calculate the rate at which thermal energy transfers through insulating material, Fourier's Law can be used. Fourier's Law links the rate at which thermal energy q_x, transfers through a material to the cross sectional area A, thickness L, thermal conductivity k and the temperature gradient across the sample between meter plate surface temperature T_1 and the cold plate surface temperature T_2 as seen in Equation E.1.

$$q_x = \frac{kA}{L}(T_1 - T_2) \tag{E.1}$$

Rearranging Equation E.1, the thermal resistance of a sample can be calculated. The thermal resistance of a material is a measure of how well a cross sectional area of material resists the transfer of energy caused by a thermal gradient across the sample as seen in Equation E.2.

$$R_{SI} = \frac{L}{k} = \frac{A \cdot \Delta T}{q_x} = \frac{m^2 \cdot K}{W} \tag{E.2}$$

In order to quantify the experimental error on the thermal resistance of the insulating materials being tested in this study, the error propagation process as outlined in Figliola and Beasley [44] was adapted for use in this thesis. A general formula for the

propagation of uncertainty of the measured variables that are used to calculate a result is given by Equation E.3.

$$u_{\mathrm{Comb}} = \pm\left[\sum_{i=1}^{L}(\theta_{\mathrm{i}} u_{\bar{\mathrm{x}}_{\mathrm{i}}})^2\right]^{1/2} \quad \textbf{(E.3)}$$

In Equation E.3, u_{Comb} is the combination of individual uncertainties $\theta_{\mathrm{i}} u_{\bar{\mathrm{x}}_{\mathrm{i}}}$ and how they contribute to the calculated result with a certain probability level. In this study a 95% confidence interval was used for all uncertainty calculations, as this follows the convention of previous work done in the field. As the meter plate of the GHP was produced using a computer numerical controlled milling machine, the uncertainty on the area of the meter plate was reduced to the point where its contribution to the uncertainty on the thermal resistance calculation was considered negligible. Equation E.3 can then be rewritten as indicated in Equation E.4, where ΔT is the temperature difference across the sample and q is the power used to maintain the sample at steady state conditions.

$$u_{\mathrm{R_{SI}}} = \pm\sqrt{(\theta_{\Delta \mathrm{T}} \cdot u_{\Delta \mathrm{T}})^2 + (\theta_{\mathrm{q}} \cdot u_{\mathrm{q}})^2} \quad \textbf{(E.4)}$$

The sensitivity index for the change in temperature can be calculated by taking the partial derivative of Equation E.2 with respect to ΔT, and can be written as seen in Equation E.5.

$$\theta_{\Delta \mathrm{T}} = \frac{\partial R_{\mathrm{SI}}}{\partial \Delta T} = \frac{A}{q} \quad \textbf{(E.5)}$$

Uncertainty in the temperature difference $u_{\Delta T}$, is given by the root-sum-squared of the uncertainty on both the hot and cold plate thermocouple measurements as outlined in Equation E.1. Both $u_{\mathrm{T_{Cold}}}$ and $u_{\mathrm{T_{Hot}}}$ are comprised of systematic u_{s}, and random u_{r} uncertainties from the measurements taken from the thermocouples.

$$u_{\Delta T} = \sqrt{{u_{T_{Cold}}}^2 + {u_{T_{Hot}}}^2} \quad \textbf{(E.6)}$$

$$u_{T_{Cold}} = \sqrt{{u_s}^2 + {u_r}^2} \quad \textbf{(E.7)}$$

$$u_{T_{Hot}} = \sqrt{{u_s}^2 + {u_r}^2} \quad \textbf{(E.8)}$$

Systematic errors are constant through repeated measurements and can be determined through calibration to a known value. To determine the systematic uncertainty in the temperature readings obtained from the thermocouples in his work Baldwin, [45] performed an uncertainty analysis on calibrated temperature readings obtained from 30 gauge t-type thermocouples calibrated using a constant and uniform temperature bath. It was found that error on the temperature readings of the 30 gauge thermocouples had an uncertainty of ±0.49℃. As the thermocouples used on the GHP were constructed from wire cut from the same spool as the thermocouples, the same uncertainty in temperature reading was used in this thesis. The random error in the thermocouple measurements can be estimated using the sample mean and a confidence interval indicated in Equation E.9.

$$u_{\mathrm{r}} = \pm t_{\mathrm{v,P}} S_{\bar{\mathrm{x}}} \quad \textbf{(E.9)}$$

$S_{\bar{\mathrm{x}}}$ of Equation E.9 can be defined as the standard deviation of the means which is the standard deviation divided by the root of the sample size.

$$S_{\bar{\mathrm{x}}} = \frac{S_{\mathrm{x}}}{\sqrt{N}} \quad \textbf{(E.10)}$$

As mentioned earlier a 95% confidence interval was used, and with a large sample size the value $t_{\mathrm{v,P}} = 1.960$ was obtained from the Student's t-distribution table.

Using Equation E.4, the sensitivity index for the change in power remains to be calculated. θ_{q} can be calculated by taking the partial derivative of Equation E.2 with respect to q, and can be written as seen in Equation E.11.

$$\theta_{\mathrm{q}} = \frac{\partial R_{\mathrm{SI}}}{\partial q} = -\frac{\Delta T \cdot A}{q^2} \quad \textbf{(E.11)}$$

To measure the amount of energy being used by the meter plate, a current transformer was placed around the electrical supply to the heater. When the meter plate was heating, electricity flowed to the meter plate heating element which induced a current in the current transformer which was read by the power meter. As the power meter detected a signal from the current transducer it output a pulse signal that was recorded by LabVIEW. Each pulse from the power meter corresponded to an amount of energy which was calculated from a combination of the size of the current transformer and the model of the power meter. In the case of this study each pulse represented 0.04167 Watt-hours calculated from a 5 amp current transformer [46]. The error on the power u_{Q} meter was 0.5% of the total power recorded plus the equivalent of one pulse as seen in Equation E.12, where t is the time spent at the temperature set point.

$$u_{\mathrm{Q}} = (0.005 \cdot q) + (0.04167/t) \quad \textbf{(E.12)}$$

Substituting Equations E.5 into Equation E.4 the uncertainty on the thermal resistances can be calculated.

$$u_{\mathrm{R_{SI}}} = \pm\sqrt{(\frac{A}{q}\cdot\sqrt{({u_{\mathrm{s}}}^2 + {u_{\mathrm{r}}}^2)_{\mathrm{Cold}} + ({u_{\mathrm{s}}}^2 + {u_{\mathrm{r}}}^2)_{\mathrm{Hot}}})^2 + (-\frac{\Delta T \cdot A}{q^2}\cdot((0.005 \cdot q) + (0.04167/t)))^2} \quad \textbf{(E.13)}$$

E.2 Uncertainty Analysis on Mass of the Panels

In the process of determining whether moisture was accumulating within the core of the VIPs being tested, the panels mass was recorded and as with any measurement an uncertainty in the recorded value was present. To quantify the uncertainty in the measured

mass of the panels, a process from Figliola and Beasley [44] was adapted for use in this thesis.

In taking the mass of the panels, 10 readings were taken in order to increase the sample size and increase the likelihood that the calculated mass was closer to the true value. The first step in calculating the uncertainty on the mass was to calculate the sample mean $\bar{x}$ of the mass readings, which was done using Equation E.14 where N is the number of measurements taken and x_{i} is the mass of the sample.

$$\bar{x} = \frac{1}{N}\sum_{i=1}^{N} x_{\mathrm{i}} \tag{E.14}$$

Upon calculating the sample mean the standard deviation of the values can be calculated using Equation E.15.

$$S_{\mathrm{x}} = \left[\frac{1}{N-1}\sum_{i=1}^{N}(x_{\mathrm{i}} - \bar{x})^2\right]^{1/2} \tag{E.15}$$

After calculating the standard deviation of the values, the standard deviations of the means $S_{\bar{\mathrm{x}}}$ could be calculated from Equation E.16.

$$S_{\bar{\mathrm{x}}}\frac{S_{\mathrm{x}}}{\sqrt{N}} \tag{E.16}$$

To calculate the random error on the measurements the standard deviations of the means was used in Equation E.17 along with the 95% probability from the Student's t-distribution table. As the sample was of finite size the degrees of freedom was used to find the value from the Student's t-distribution table. The degrees of freedom can be calculated by $\mathrm{v} = N - 1$.

$$u_{\mathrm{r}} = \pm t_{\mathrm{v},95} S_{\bar{\mathrm{x}}} \tag{E.17}$$

Figure E-1 shows the Intelligent Weighing Technology model PBX-3200 scale that was used to measure the mass of the VIPs within this thesis. The scale has a maximum capacity of 3200 g with a readability of 0.01 g and a repeatability u_s of ±0.01 g and the linearity of the scale is ±0.02 g [47]. The scale was factory calibrated before use in this thesis.

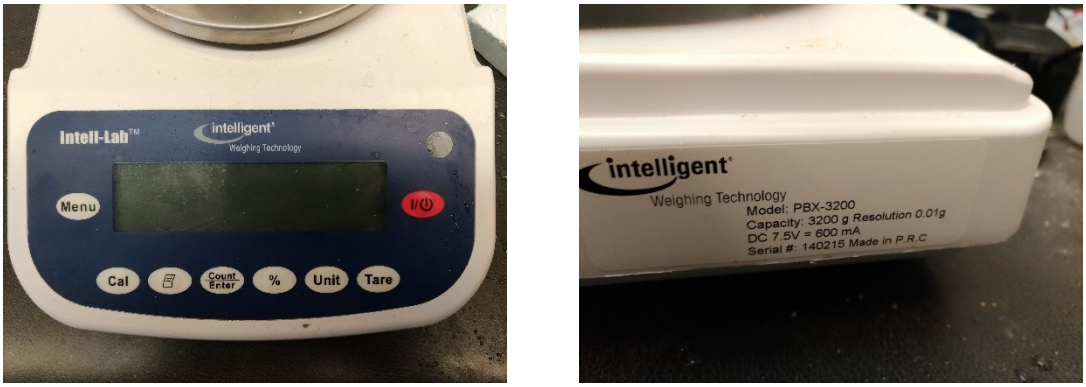

Figure E-1: Scale used to measure the mass of the VIP's

Combining the random and systematic error using the root-sum-squared method the values from Equations E.17 can be used in Equation E.18 where u_M is the total uncertainty on the mass of the sample measured.

$$u_M = \pm\sqrt{(u_r)^2 + (u_s)^2} \quad \textbf{(E.18)}$$